

**Eastern
Economy
Edition**

THEORY AND PRACTICE OF **FOUNDATION DESIGN**

N.N. SOM • S.C. DAS



Theory and Practice of Foundation Design

N.N. SOM

*Professor of Civil Engineering
Jadavpur University, Kolkata*

S.C. DAS

*Professor of Civil Engineering
Jadavpur University, Kolkata*

Prentice-Hall of India Private Limited
New Delhi - 110001
2003

Contents

Preface

xv

1 SOIL AS AN ENGINEERING MATERIAL

1–31

- 1.1 Introduction 1
- 1.2 Nature of Soil 2
- 1.3 Three-phase System 3
 - 1.3.1 Definitions 4
 - 1.3.2 Weight/Volume Relationships 4
- 1.4 Index Properties of Soil 4
 - 1.4.1 Plasticity Chart 6
- 1.5 Soil Classification 7
- 1.6 Relative Density of Granular Soil 8
- 1.7 Some Special Soil Types 9
- 1.8 Groundwater 10
 - 1.8.1 Types of Water-bearing Formations 10
 - 1.8.2 Division of Subsurface Water 11
- 1.9 Engineering Properties of Soil 12
 - 1.9.1 Permeability 12
 - 1.9.2 The Principle of Effective Stress 13
 - 1.9.3 Pore-pressure in Soil due to Applied Load 16
 - 1.9.4 Shear Strength of Soils 17
 - 1.9.5 Consolidation 21
 - 1.9.6 Properties of Soil 26
- 1.10 Soil Deposits of India 29
- References* 30

2 SITE INVESTIGATION

32–53

- 2.1 Introduction 32
- 2.2 Information Extracted from Site Investigation 32
- 2.3 Stages of Site Investigation 33
 - 2.3.1 Reconnaissance Study 33
- 2.4 Boring (Detailed Soil Investigation) 34
 - 2.4.1 Trial Pits 34
 - 2.4.2 Wash Boring 34

2.4.3	Auger Boring	35
2.4.4	Rotary Drilling	36
2.4.5	Percussion Drilling	36
2.4.6	Stabilization of Boreholes	36
2.5	Sampling	37
2.5.1	Sampling from Trial Pits	37
2.5.2	Sampling from Boreholes	37
2.5.3	Preservation of Samples	39
2.6	Testing of Soil	40
2.7	Field Tests	41
2.7.1	Standard Penetration Test (SPT)	41
2.7.2	Dynamic Cone Penetration Test (DCPT)	43
2.7.3	Static Cone Penetration Test (SCPT)	44
2.7.4	Vane Shear Test	46
2.7.5	Direct Shear Test (In-situ)	47
2.7.6	Plate Bearing Test	48
2.7.7	Pressuremeter Test	49
2.8	Laboratory Tests	51
2.9	Ground Water Table	51
2.10	Planning of Exploration Programme	51
2.10.1	Layout and Number of Boreholes	51
2.10.2	Depth of Boreholes	52
<i>References</i>		53

3 SOIL DATA AND DESIGN PARAMETERS 54-64

3.1	Introduction	54
3.2	Soil Investigation	55
3.2.1	Responsibility of Designer	55
3.2.2	Information Required from Soil Investigation	55
3.2.3	Soil Test Report	55

Reference 64

4 FOUNDATIONS: TYPES AND DESIGN CRITERIA 65-75

4.1	Introduction	65
4.2	Types of Foundation	65
4.2.1	Shallow Foundations	66
4.2.2	Deep Foundations	68
4.2.3	Choice of Foundation Type	70
4.3	Design Criteria	70
4.3.1	Bearing Capacity	70
4.3.2	The Settlement Criteria	71

References 75

5 STRESS DISTRIBUTION IN SOILS	76–116
5.1 Introduction	76
5.2 In-situ Stress	76
5.3 Stresses due to Foundation Loading	78
5.3.1 Boussinesq Analysis: Point Load	78
5.4 Vertical Stresses below Uniform Rectangular Load	81
5.5 Vertical Stresses below Uniform Circular Load	83
5.6 Other Common Loading Types	85
5.6.1 Uniform Line Load	85
5.6.2 Uniform Strip Load	85
5.6.3 Triangular Load	86
5.6.4 Embankment Type Loading	87
5.7 Stress at any Point below Rectangular Load	89
5.8 Newmark's Chart	89
5.9 Pressure Bulb	91
5.10 Rigidity of Footings: Contact Pressure	92
5.11 Non-homogeneous Soils	94
5.11.1 Two-layer System	94
5.11.2 Three-layer Systems	97
5.11.3 Multilayer Systems	99
5.11.4 Non-homogeneous Medium	100
5.12 Nonlinear Soil	103
5.13 Approximate Method of Determining Vertical Stress	106
<i>References</i>	113
6 BEARING CAPACITY OF SHALLOW FOUNDATIONS	117–137
6.1 Introduction	117
6.2 Failure Mechanism	118
6.2.1 Prandtl's Analysis	120
6.2.2 Terzaghi's Analysis	122
6.2.3 Skempton Method	125
6.2.4 Meyerhof's Method	125
6.2.5 Hansen's Method	126
6.2.6 Vesic's Method	126
6.3 Local Shear Failure	126
6.4 Square and Circular Footings	127
6.5 Bearing Capacity of Non-homogeneous Soil	127
6.6 Limitations of Theoretical Analysis	129
6.7 Factors Affecting Bearing Capacity	129
6.7.1 Effect of Ground Water Table on Bearing Capacity	130
6.8 Gross and Net Soil Pressure: Safe Bearing Capacity	131
6.9 Bearing Capacity from Field Tests	131
<i>References</i>	136

7 SETTLEMENT ANALYSIS	138–163
7.1 Introduction 138	
7.1.1 Definitions 138	
7.1.2 Methods of Settlement Analysis 139	
7.2 Stress-path 143	
7.2.1 Stresses During Loading and Consolidation in the Field 146	
7.2.2 Influence of Stress-path on the Drained Deformation of Clay 148	
7.2.3 Settlement Analysis by Stress-path Method 149	
7.3 Rate of Settlement 151	
7.4 Foundation on Sand 152	
7.4.1 Elastic Theory 152	
7.4.2 Semi-empirical Method (Buisman, 1948) 152	
7.4.3 Plate Load Test 153	
7.4.4 Static Cone Test 153	
References 161	
8 FOOTINGS AND RAFT DESIGN	164–198
8.1 Introduction 164	
8.2 Design of Footings 165	
8.2.1 Depth of Footing 165	
8.2.2 Allowable Bearing Capacity 166	
8.2.3 Effect of Ground Water Table 168	
8.2.4 Settlement 169	
8.2.5 Dimensioning Footing Foundations 170	
8.2.6 Interference Effect 172	
8.2.7 Design for Equal Settlement 172	
8.2.8 Structural Design of Footings 174	
8.3 Design of Raft Foundation 175	
8.3.1 Types of Raft Foundation 175	
8.3.2 Bearing Capacity 177	
8.3.3 Settlement 177	
8.3.4 Floating Foundation 178	
8.3.5 Basement Raft 181	
8.3.6 Structural Design of Raft Foundation 182	
References 198	
9 PILE FOUNDATIONS	199–265
9.1 Introduction 199	
9.2 Classification 200	
9.2.1 Classification Based on Composition 200	
9.2.2 Classification Based on Method of Installation 201	
9.3 Pile Behaviour Under Axial Load 201	

9.4	Pile Capacity to Resist Axial Forces	203
9.4.1	Structural Capacity of Piles	203
9.4.2	Pile Capacity from Static Analysis	203
9.5	Frictional Resistance	206
9.5.1	Frictional Resistance in Cohesive Soil	207
9.5.2	Frictional Resistance in Cohesionless Soil	210
9.6	End Bearing	213
9.6.1	End Bearing in Cohesive Soil	213
9.6.2	End Bearing in Cohesionless Soil	213
9.7	Critical Depth	215
9.8	Pile Capacity from In-situ Soil Tests	217
9.9	Under-reamed Piles	217
9.10	Allowable Load on Piles from Static Analysis	218
9.11	Dynamics of Pile Driving (Dynamic Analysis)	219
9.11.1	ENR Formula	220
9.11.2	Hiley Formula	220
9.11.3	Simplex Formula	221
9.11.4	Janbu's Formula (Janbu, 1953)	221
9.11.5	Wave Equation	222
9.11.6	Limitations of Dynamic Analysis	222
9.12	Pile Groups	223
9.12.1	Capacity of Pile Group	224
9.12.2	Pile Spacing	225
9.12.3	Pile Group Subjected to Vertical Load and Moment	226
9.13	Settlement of Pile Groups	228
9.13.1	Pile Groups in Cohesive Soil	228
9.13.2	Pile Groups in Cohesionless Soil	230
9.14	Uplift Resistance of Piles	231
9.15	Piles under Horizontal Forces	232
9.15.1	Failure Mechanisms	232
9.15.2	Stiffness Factors and Subgrade Modulus	233
9.15.3	Ultimate Lateral Resistance	234
9.15.4	Deflection, Moment, and Shear under Working Load	237
9.15.5	I.S. Code Method	240
9.16	Negative Skin Friction	242
9.17	Testing of Piles	245
9.17.1	Purpose of Pile Testing	246
9.17.2	Causes of Defect in Piles	246
9.17.3	Integrity Testing	246
9.18	Load Test on Piles	247
9.18.1	Test Procedure	248
9.18.2	Maintained Load Test	248
9.18.3	Constant Rate of Penetration (CRP) Test	249
9.18.4	Pile Driving Analyzer	251
	References	262

10 WELL FOUNDATIONS

- 10.1 Introduction 266
- 10.2 Classification 266
- 10.3 Physical Characteristics—Shape and Size 267
- 10.4 Components of Well Foundation 268
 - 10.4.1 Steinling 269
 - 10.4.2 Well Curb 269
 - 10.4.3 Cutting Edge 269
 - 10.4.4 Bottom Plug 269
 - 10.4.5 Dredge Hole 269
 - 10.4.6 Intermediate/Top Plug 270
 - 10.4.7 Well Cap 270
- 10.5 Sinking of Wells 270
- 10.6 Physical Characteristics—Depth 270
 - 10.6.1 Scour Depth 270
- 10.7 Allowable Bearing Pressure 271
- 10.8 Forces Acting on Well Foundation 272
- 10.9 Lateral Stability 273
 - 10.9.1 Analysis Based on Bulkhead Concept 273
 - 10.9.2 IRC Method 275
 - 10.9.3 Mode of Failure 281
 - 10.9.4 Recommendations of IRC: 78–1983 281
- 10.10 Well Sinking 283
- References* 293

11 FOUNDATIONS ON EXPANSIVE SOILS

- 11.1 Introduction 294
- 11.2 Nature of Expansive Soil 294
 - 11.2.1 Free-swell Test 294
 - 11.2.2 Differential Free Swell 295
 - 11.2.3 Unrestrained Swell Test 295
 - 11.2.4 Swelling Pressure 296
 - 11.2.5 Classification of Swelling Potential 297
- 11.3 Effect of Swelling on Building Foundations 297
- 11.4 Foundation Design in Expansive Soil 298
 - 11.4.1 Isolating the Foundation from the Swelling Zone:
Under-reamed piles 298
 - 11.4.2 Controlling Swelling 300
 - 11.4.3 Measures to Withstand Settlement 302
- References* 302

12 GROUND IMPROVEMENT TECHNIQUES

- 12.1 Introduction 304
- 12.2 Principles of Ground Improvement 304
- 12.3 Ground Treatment in Cohesive Soil 306
 - 12.3.1 Preloading with Vertical Drains 306
 - 12.3.2 Stone Columns 314

12.4	Ground Improvement in Granular Soil	326
12.4.1	Heavy Tamping or Drop Hammer	326
12.4.2	Dynamic Consolidation	328
12.4.3	Vibrocompaction	330
12.4.4	Compaction Piles	332
12.4.5	Control of Field Work	332
	<i>References</i>	344
13	EARTHQUAKE RESPONSE OF SOILS AND FOUNDATIONS	346–370
13.1	Introduction	346
13.2	Earthquake Characteristics	346
13.2.1	Magnitude	346
13.2.2	Energy Release	347
13.2.3	Intensity	347
13.2.4	Ground Acceleration	348
13.2.5	Response Spectrum	348
13.3	Effects of Earthquake	350
13.4	Ground Settlement	350
13.5	Liquefaction	352
13.5.1	Liquefaction Potential	354
13.6	Effect of Earthquake Loading on Behaviour of Fine-grained Soils	358
13.7	Building Damage due to Liquefaction	360
13.8	Measures to Prevent Liquefaction	362
13.9	Effect on Superstructure	362
13.10	Dynamic Properties of Soil	363
	<i>References</i>	369
14	CONSTRUCTION PROBLEMS	371–392
14.1	Introduction	371
14.2	Common Construction Problems	371
14.3	Stability of Excavation	372
14.3.1	Design of Braced Cuts	373
14.4	Dewatering	378
14.4.1	Rate of Seepage	378
14.4.2	Methods of Dewatering	380
14.4.3	Field Control	384
14.5	Land Filling	385
14.5.1	Cohesive Fill	385
14.5.2	Granular Fill	387
14.6	Effect on Adjoining Structures	389
14.6.1	Effect of Vibration	391
	<i>References</i>	392
	<i>Appendix</i>	393–394
	<i>Index</i>	395–399

Preface

Over the long years of our association with the profession of teaching and research in civil and geotechnical engineering, our experiences suggest that foundations are often designed without taking all the essential parameters into consideration particularly those with regard to geology of the site, soil data, ground conditions, type of structure, and land use pattern in the vicinity of the construction area. Though the theoretical aspects of foundation design are well understood, the field situations are usually not given the due importance. As a consequence, the implementation of the proposed design runs into problems necessitating changes in construction methodology or in some cases, even the design.

The book covers the essential features of foundation design through fourteen chapters. The foundation design requires understanding of the soil type, its strength and deformation characteristics, ground water table, and the other details of the site and the structures. We have striven to incorporate all these criteria so as to acquaint the reader with all necessary aspects of foundation design. This treatment begins with Chapter 1 that details the engineering properties of soil as required for the design of sound foundations. Chapter 2 discusses site investigation as the next step towards foundation design. This chapter elaborates on the various methods of soil exploration and testing. The design parameters and the importance of proper interpretation of the data collected from soil investigation are described in Chapter 3 while Chapter 4 introduces different types of foundations and their characteristics.

Chapters 5 through 7 offer detailed study of the mechanical properties of the soil including the stress distribution, the bearing capacity of foundations, and settlement. The effect of non-homogeneity and nonlinearity of the stress-strain relationships on the stress distribution in soils is elucidated and the concept of stress-path method of settlement analysis is introduced in these chapters. The important considerations for obtaining the design parameters from a large amount of soil test data are highlighted. The design procedures for shallow and deep foundations, as also for well foundations are presented in Chapters 8 through 10. The special requirements of expansive soils are covered and the earthquake response of soils and foundations are emphasized in Chapters 11 and 13 respectively. The ground improvement techniques commonly used in practice and the construction problems generally encountered at site are adequately dealt with in Chapter 12. The reader should also find in the book a comprehensive treatment of the design procedures vis-a-vis the construction problems and practices (as discussed in the final chapter). The chapters on analytical aspects are followed by worked-out examples taken from real-life problems which make the reading both topical and interesting. Besides, numerous references have been made to actual cases of foundations for better clarity and understanding of the topics covered.

We have drawn upon our experiences in teaching and consultancy in the same discipline to compile this volume. Almost forty years of teaching and research at Jadavpur University

have given us the opportunity to face many field situations which had to be treated in unconventional ways. The interaction with our students has also been very helpful during all these years. This book is designed to serve undergraduate and postgraduate students of civil engineering with interest in foundations—their design, development, and maintenance. It will be equally useful for practising civil and structural engineers who have to design foundations of structures in difficult subsoil conditions.

We acknowledge the immense help derived out of our association with colleagues in the civil engineering department at Jadavpur University, Kolkata. We are thankful to Prof. R.D. Purkayastha, Prof. P. Bhattacharya, Prof. S.C. Chakraborty, Prof. S.P. Mukherjee, Dr. S. Ghosh, and Dr. R.B. Sahu who participated in many fruitful discussions on the subject and gave their invaluable suggestions. We are also grateful to our staff at the soil mechanics division, particularly Mr. Robin Pal, Ms. Apurba Mukherjee, Mr. Sisir Mondal, Mr. Rantu Jana, and Mr. Bhupesh Ghosh for their skilled help in many ways. The painstaking task of compiling the manuscript was undertaken by Mr. Bivas Roy, Mr. Subhasish Ghosh, and Mr. Hrishikesh Nayak with great interest and patience. We express our sincere thanks to them all.

Last but not the least, we express our sincere gratitude to our spouses Smt. Rita Som and Smt. Sikha Das for bearing with the demand of time that was needed to complete the task often under trying circumstances.

**N.N. SOM
S.C. DAS**

1

Soil as an Engineering Material

1.1 INTRODUCTION

From an engineering viewpoint, soils and soft rocks comprise all the loose and fragmented materials that are found in the earth's crust. They are distinguished from solid rock, i.e., the hard and compact mass in the earth's body, which cannot normally be excavated by manual means. Soils are formed by disintegration or decomposition of a parent rock by weathering or they may be deposited by transportation from some other source.

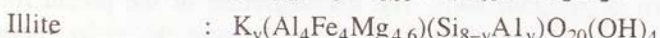
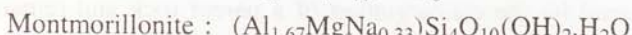
Soils which are formed by the disintegration of a parent rock and remain at their place of formation are known as *residual soils*. The disintegration of the parent rock is caused by physical agents such as temperature changes, freezing, thawing etc. or by chemical agents like oxidation, hydration etc. When the soil is transported from its original bed rock by forces of gravity, wind, water or ice and re-deposited at another location it is known as *transported soil*. Transported soils are generally sorted out according to their grain size as the velocity of the transporting medium gets reduced away from the source. After deposition at a new place, these soils may be subjected to further weathering with the passage of time.

Transported soils are classified into different types according to their mode of transportation. Deposits of soil that are formed by wind are called *Aeolian deposits*. Sand dunes and loess are examples of these deposits. Loose sand is generally swept by wind and transported close to the surface. If the motion is stopped, it is deposited in the form of sand dunes. The common transported soils are, however, those which have been carried by water or ancient glaciers. *Marine soils* which have been carried by sea water and *Alluvial soils* which have been carried by rivers and streams constitute probably the largest group of transported soils on earth. These deposits may also be called *sedimentary* deposits as they have been formed by deposition from either standing or moving water. The deposition is primarily caused by the gradual decrease in velocity of river carrying the sediments. A larger part of the great Indian plains is made up of alluvial deposits. *Glacial* deposits are remnants of the ice age that were carried along by the moving ice. They are generally found as big boulders at places away from their parent rock and are heterogeneous in nature with little or no stratification. Other sedimentary deposits are the *Lacustrine* soils which are deposited on a lake bed and the *Estuarine* soils which are deposited at the mouth of an estuary.

1.2 NATURE OF SOIL

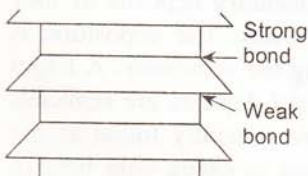
Properties of soil are complex and variable, being primarily influenced by the geological environment under which they have been deposited. An understanding of soil composition is important in appreciating the mechanical behaviour of the soil. Natural soil consists essentially of discrete solid particles which are held together by water and/or gas filling the pore space. These particles are, however, not bonded as strongly as the crystals of a metal are and can, therefore, move freely with respect to one another. The size and shape of grains and the mineralogical composition of soil particles varies widely in nature. However, in coarse-grained soils the most important properties do not depend on the constituent minerals although locally, the minerals may control the frictional characteristics of the individual grains. In these soils, the particles are so large that the forces between the grains other than those due to externally applied forces and gravity are small. The non-clay minerals such as mica, feldspar, and quartz which constitute sand and silt do not render any plasticity and cohesion to the soil. Thus, the influence of the constituent minerals becomes appreciable with the decrease in size.

Clay minerals are hydrated aluminium silicates in crystalline form. These are generally of three different types (Scott 1965):

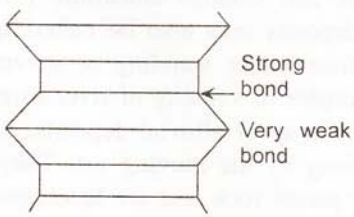


Kaolinite has a very stable structure. It generally resists the ingress of water and consequently, undergoes little volume change when in contact with water. On the other hand, Montmorillonite attracts water and undergoes large swelling and expansion when saturated with water. Most of the black cotton soils of India contain clay minerals of this variety. Illite is less expandable than montmorillonite.

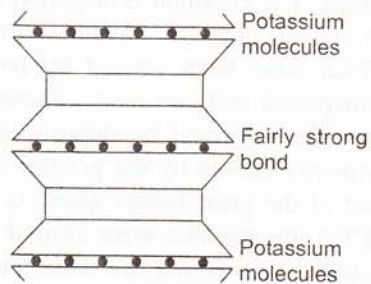
A single particle of clay consists of many sheets of clay minerals piled one on another, as shown in Fig. 1.1. As each sheet has a definite thickness but is large at right angles to its thickness, clay particles are believed to be plate-shaped. The flat surfaces carry residual negative charges, but the edges may carry either positive or negative charges depending upon the environment.



(a) Kaolinite



(b) Montmorillonite



(c) Illite

Fig. 1.1 Structure of clay particles.

Particle orientation has an important bearing on the engineering properties of a soil. Spacing and orientation of particles influence the development of interparticle bonds. For cohesionless soils, individual grains may be approximated as spheres with loose, dense, or honeycombed structure, as shown in Fig. 1.2. A dense structure is more stable than the loose or honeycombed structure. Figure 1.3 shows some simplified structures found in clay. The development of structure is influenced by the origin and nature of deposition of the soil. Thus, the flocculated structure is typical of clay deposits in salt water. This structure may change due to leaching or by external influences, such as loading, drying, freezing, electro-osmotic processes, and so on.

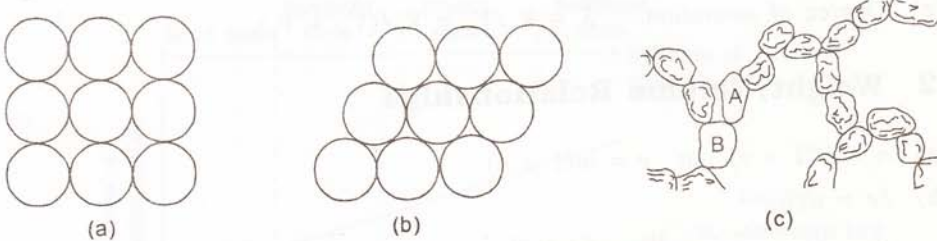


Fig. 1.2 Structure of cohesionless soils.

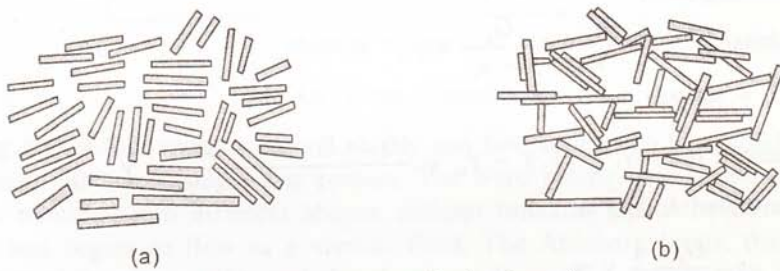


Fig. 1.3 Structure of cohesive soils.

1.3 THREE-PHASE SYSTEM

Figure 1.4 shows a typical soil skeleton consisting of three distinct phases—solid(mineral grains), liquid(usually water), and gas(usually air). These phases have been separated to facilitate the quantitative study of the proportional distribution of different constituents.

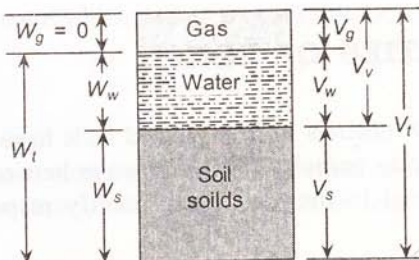


Fig. 1.4 Three-phase system.

1.3.1 Definitions

- (a) Unit weight, Water : $\gamma_w = W_w/V_w$
Solid particles : $\gamma_s = W_s/V_s$
Specific gravity: $G_s = \gamma_s/\gamma_w = W_s/V_s \gamma_w$
- (b) Water content, $W = (W_w/W_s) \times 100\%$
- (c) Void ratio, $e = V_v/V_s = V_w + V_g/V_s$
- (d) Porosity, $n = V_v/V = V_v/(V_v + V_s)$
- (e) Degree of saturation, $S = V_w/V_v = V_w/(V_w + V_g)$

1.3.2 Weight/Volume Relationships

- (a) $n = e/(1 + e)$ or $e = n/(1 - n)$
- (b) $Se = wG_s$
- (c) Bulk density, $\gamma = \frac{W}{V} = \frac{Se + G_s}{1 + e} \times \gamma_w$
- (d) Dry density, $\gamma_d = \frac{W_s}{V} = \frac{G_s}{1 + e_o} \times \gamma_w$
- (e) $\gamma = (1 + w) \gamma_d$
- (f) Submerged density, $\gamma' = \gamma - \gamma_w = \frac{(G_s - 1) - (1 - S)e}{1 + e} \times \gamma_w$
For saturated soil, $S = 1.0$,

$$\therefore \gamma' = \frac{G_s - 1}{1 + e} \times \gamma_w$$

The range over which the typical values of the above parameters vary are as follows:

- (i) $G_s = 2.60-2.75$
- (ii) $\gamma = 1.60-2.25 \text{ g/cc}$
- (iii) $\gamma_s = 1.30-2.00 \text{ g/cc}$
- (iv) $n = 0.25-0.45$ (for sand)
- (v) $S = 0$ (for dry soil)-100% (for fully saturated)

1.4 INDEX PROPERTIES OF SOIL

As already mentioned, the clay minerals in fine-grained soils have sufficient surface forces to attract water molecules to the clay particles. The interaction between the clay minerals, water, and various chemicals dissolved in the water is primarily responsible for developing the consistency of these particles.

Pure water mainly consists of molecules of H_2O but a few of them get dissociated into hydrogen ions, H^+ and Hydroxyl ions, OH^- . If impurities such as acids and bases are present,

they also dissociate into cations and anions. Salt, for example, breaks up into Na^+ and Cl^- . Since plane surfaces of the clay minerals carry negative charges, cations including H^+ from water are attracted towards the surface of these particles. The water molecules closest to the clay particles, called the adsorbed water, are tightly held to the clay and exhibit properties which are somewhat different from those of ordinary water. This adsorbed water is believed to lead cohesive and plastic properties to clayey soils. It is obvious, therefore, that the amount of water present in a clay will determine its plasticity characteristics and, in turn, its engineering properties. The Atterberg limits are designed to serve as an index of the plasticity for clayey soils, refer Fig. 1.5.

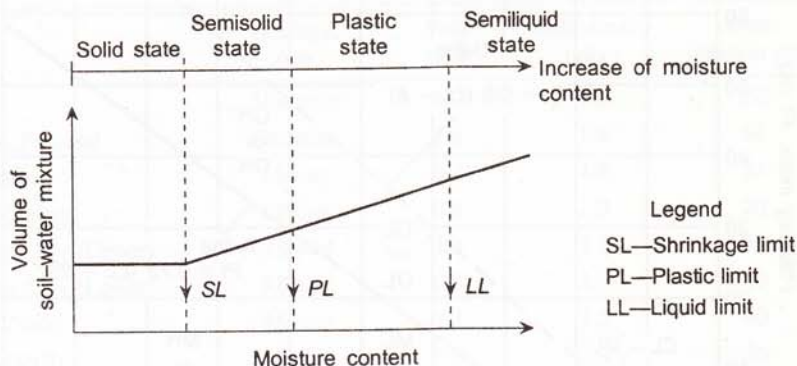


Fig. 1.5 Limits of consistency.

Starting with a low water content a clayey soil first appears to be a solid and moves to the plastic state with increasing water content. The word *plastic* here refers to the ability of a soil to be moulded into different shapes without breaking up. At even a higher water content, the soil begins to flow as a viscous fluid. The Atterberg limits, that is, the liquid limit (LL), the plastic limit (PL), and the shrinkage limit (SL) indicate the limits of water content at which the consistency of clayey soil changes from one state to another.

The Atterberg limits along with the natural water content give useful indication of the nature of the clayey soil. A natural water content close to the liquid limit indicates a soft compressible soil while a natural water content close to the plastic limit is characteristic of a stiff and less compressible clay.

Plasticity index, PI

The range of water content over which a soil remains plastic is called the plastic limit.

i.e.

$$PI = LL - PL(\%) \quad (1.1)$$

Liquidity index, LI

It is the ratio of natural water content, w of a soil in excess of its plastic limit to its plasticity index and is indicative of the state of the water content in relation to the liquid limit and the plastic limit of the soil.

$$LI = \frac{w - PL}{LL - PL} \times 100\% \quad (1.2)$$

1.4.1 Plasticity Chart

It has been observed that properties of clay and silt can be correlated at least qualitatively with the Atterberg limits by means of the *Plasticity Chart*, as shown in Fig. 1.6. The liquid limit and the *plastic limit* of a soil are plotted on the plasticity chart and the soil is classified according to the region in which it falls, the A-line being an arbitrary boundary between inorganic clays and inorganic silt/organic clays. Table 1.1 gives the liquid limit of some cohesive soils.

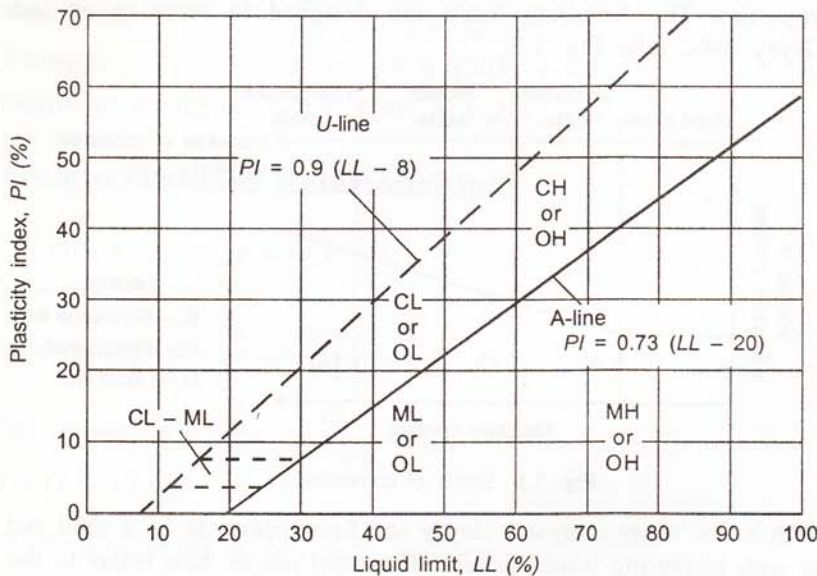


Fig. 1.6 Plasticity chart.

Table 1.1 Consistency limits of some soils

Soil	Liquid Limit (%)	Plastic Limit (%)
Alluvial Deposits		
Boston Blue Clay	41	20
Chicago Clay	58	21
Normal Calcutta Soil	55	28
Marine/Estuarine		
London Clay	75	29
Norwegian Quick Clay	40	17
Bombay Marine Clay	90	40
Cochin Marine Clay	90	45
Shellhaven Clay	97	32
Clay Minerals		
Illite	100	45
Kaolinite	50	25
Montmorillonite	500	50

1.5 SOIL CLASSIFICATION

Density, void ratio, and water content are fundamental soil parameters which help to identify and assess—at least qualitatively, the nature of the soil deposit. For example, a high void ratio of a sandy soil would indicate a loose state of compaction while a clayey soil with high water content is likely to be more compressible than one with low water content. Table 1.2 gives the density, void ratio, and the water content of some common soil deposits.

Table 1.2 Density, void ratio, and water content of some soils

<i>Soil</i>	<i>Geologic type</i>	<i>Void ratio</i>	<i>Bulk density (g/cc)</i>	<i>Water content (%)</i>
Mexico City	Volcanic	9.0	1.0	350
Shellhaven clay, England	Estuarine	1.6	1.8	60
London Clay, Selset	Marine	0.7	1.9	35
Boulder Clay, England	Glacial	0.4	2.0	20
Normal Calcutta Clay (Upper)	Alluvial	1.3	1.7	50
Normal Calcutta Clay (Lower)	Alluvial	0.8	2.0	30
Bangkok Clay (Soft)	Marine	2.1	1.5	80
Bangkok Clay (Stiff)	Marine	0.8	2.0	30
Norwegian Quick Clay	Marine	1.0	1.9	38

Soil consists of solid grains that have various sizes ranging from coarse grained particles such as boulder, gravel and sand down to the fine grained particles like, silt and clay. The grains are classified according to their sizes. The most common system of classification is the M.I.T. system as illustrated in Fig. 1.7.

2.0	0.6	0.2	0.06	0.02	0.006	0.002	0.0006	0.0002	
Coarse	Medium	Fine	Coarse	Medium	Fine	Coarse	Medium	Fine (colloidal)	
Sand			Silt			Clay			

Fig. 1.7 M.I.T. classification system.

Natural soil generally consists of mixture of several groups and the soil, in such cases, is named after the principal constituent present. For example, a soil that is predominantly clay but also contains some silt is called silty clay.

The grain-size distribution of a soil is best represented by the grain-size distribution curves, refer Fig. 1.8. The shape of the curve indicates whether the soil is uniform or poorly graded, or well-graded.

The uniformity coefficient of the soil is defined as

$$c_u = \frac{D_{60}}{D_{10}} \quad (1.3)$$

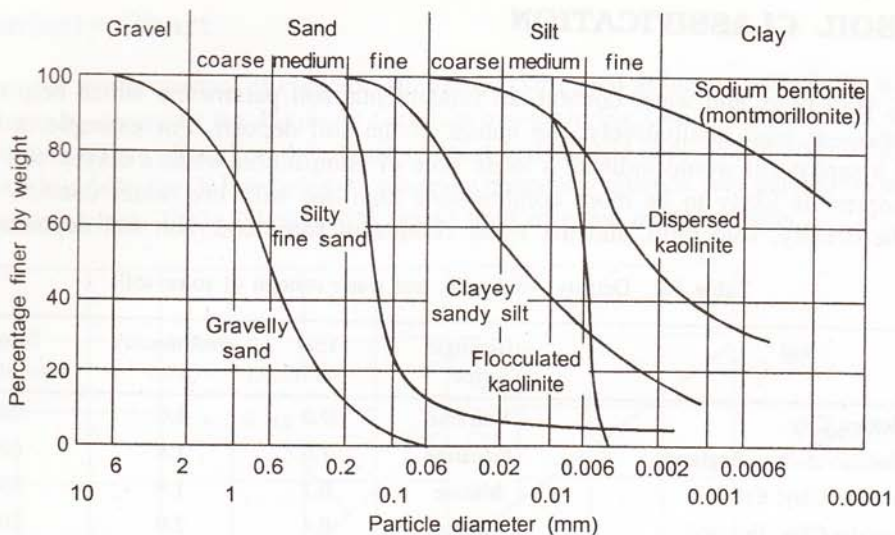


Fig. 1.8 Grain-size distribution curve.

where D_{60} is the diameter of particles corresponding to 60% finer and D_{10} is the diameter of the particle corresponding to 10% finer. The gradation of soil is determined by the following criteria:

$$\text{Uniform soil} : c_u = 1$$

$$\text{Poorly-graded soil} : 1 < c_u < 4$$

$$\text{Well-graded soil} : c_u > 4$$

It must be considered, however, that the particle size alone is not an adequate criterion for the classification of a soil, as the shape of grains and clay fraction may vary widely depending upon the constituent minerals. More elaborate soil classification systems, making use of the Atterberg limits, in addition to the particle size distribution, have since been evolved.

The most comprehensive of these systems are the Unified Soil classification system and the Indian Standard Classification System. The *Unified Soil Classification System* divides the soil into coarse-grained soil (having more than 50% retained on number 200 sieve) and fine grained soil (more than 50% passing through number 200 sieve). Further subdivisions are made according to gradation for coarse-grained soils and plasticity for fine-grained soils and each soil type is given a group symbol (Table 1.3). The *Indian Standard Classification System* (IS 1498) is similar in some respects except that the fine-grained soils are divided into three ranges of liquid limit as opposed to only two in the unified soil classification system.

1.6 RELATIVE DENSITY OF GRANULAR SOIL

The engineering properties of granular soil primarily depend upon its relative density, grain-size distribution, and shape of grains. The relative density determines the compactness to which the solid grains are assembled in a soil skeleton and is expressed as

$$R_D\% = \frac{e_{\max} - e}{e_{\max} - e_{\min}} \times 100 \quad (1.4)$$

Table 1.3 Unified soil classification system

Field identification procedures (excluding particles larger than 3 sq. inches and basing fractions on estimated weights)										Information required for describing soils		Laboratory classification criteria	
		Group symbols ¹		Typical names									
Sands													
More than half of coarse fraction is smaller than 4.75 mm										Gravels More than half of coarse fraction is larger than 4.75 mm			
(For visual classifications, the 1/4" size may be used as equivalent to the number 4 sieve size)													
Clean gravels (little or no fines)													
Gravels with fines (Appreciable amount of fines)													
Wide range in grain size and substantial amounts of all intermediate particle sizes.	GW	Well-graded gravels, gravels, gravel-sand mixtures, little or no fines.											
Predominantly one size or a range of sizes with some intermediate sizes missing.	GP	Poorly-graded gravels, gravel-sand mixtures, little or no fines.											
Non-plastic fines (For identification procedures, see ML below).	GM	Silty gravels, poorly-graded gravel-sand-silt mixtures.											
Plastic fines (For identification procedures, see CL below).	GC	Clayey gravel, poorly-graded gravel-sand-clay mixtures.											
Wide range in grain-sizes and substantial amounts of all intermediate particle sizes.	SW	Well-graded sands, gravelly little or no fines.											
Predominantly one size or a range of sizes with some intermediate sizes missing.	SP	Poorly-graded sands, gravelly sands, little or no fines.											
Non-plastic fines (For identification procedures, see ML below).	SM	Silty sands, poorly-graded sand-silt mixtures.											
Plastic fines (For identification procedures, see CL below).	SC	Clayey sands, poorly-graded sand-clay mixtures.											
Identification procedures of Fraction Smaller than 0.425 mm													
Dry strength (Crushing characteristics)		Dilatancy (Retention to plastic limit)	Toughness (Consistency near plastic limit)										
None to slight	Quick to slow	None	ML	Inorganic silts and very fine sands, rock flour, silty or clayey fine sands with slight plasticity.									
Medium to high	None to very slow	Medium	CL	Inorganic clays of low to medium plasticity, clays, sandy clays, silty clays, lean clays.									
Slight to medium	Slow	Slight	OL	Organic silt sand, organic silt-clays of low plasticity									
Slight to medium	Slow to none	Slight to medium	MH	Inorganic silts, naticaceous or diatomaceous fine sandy or silty soils, elastic silts.									
High to very high	None	High	CH	Inorganic clay of plasticity, fat clays.									
Medium to high	None to very slow	Slight to medium	OH	Organic clays of medium to high plasticity.									
High organic soils			Pt	Peat and other highly organic soils.									
Example. Clayey silt, brown, slightly plastic, small percentage of fine sand; numerous vertical root holes; firm and dry in place (ML.)													
Use grain-size curve in identifying the fractions as given under field identification.													
Plasticity index													
60													
50													
40													
30													
20													
10													
$\text{CL} - \text{ML} \rightarrow$													
0	10	20	30	40	50	60	70	80	90	100			
Liquid limit													
Plasticity chart for laboratory classification of fine soils													

1. Applications: Soils possessing characteristics of two groups are designated by combinations of group symbols for example, GW-GC, well-graded gravel-sand mixture with clay binder.

Table 1.3 Unified soil classification system

where e_{\max} = void ratio in loosest state
 e_{\min} = void ratio in densest state
 e = in-situ void ratio

The properties of granular soil are also dependent on their particle size distribution, that is, whether the soil is well-graded or poorly-graded. In well-graded soils, the smaller grains tend to fill the voids between the larger grains and thus, make the soil more compact. The shape of grains (angular sub-rounded or rounded) may also have some effect on the properties of granular soil.

1.7 SOME SPECIAL SOIL TYPES

Apart from the common soil types that may be identified by the different soil classification systems, certain natural soils are characterized by the properties of their chemical and mineral constituents. Such soils exhibit characteristic features with regard to their strength and compressibility and need particular care when used to support a foundation.

Organic soils are those which contain large quantity of organic/vegetable matter in various stages of decomposition. Natural soils may contain varied percentages of organic matter and only a small percentage may be sufficient to affect its properties. In *organic clay*, vegetable matter is intermixed with the predominant clay mineral while *peat* consists almost wholly of vegetable matter. Peat is characterized by high liquid limit and spongy structure with low specific gravity. The top 10–12 m of the normal Calcutta deposit is a common organic clay of the Bengal basin. A thin layer of peat is often encountered in this deposit at many locations as shown in Fig. 1.9.

Description of strata	Soil properties (average)					
	N blows /30cm	w (%)	LL (%)	PL (%)	C _u (t/m ²)	m _v m ² /t
I Light brown/brownish grey silty clay/clayey silt with occasional lenses of fine sand	5–8	30	54	24	4.0	0.002
II Grey/dark grey silty clay, clayey silt with semi-decomposed timber pieces	2–4	55	12	28	2.5	0.007
III Bluish grey silty clay with calcareous modules	10	30	60	25	6.0	0.002
IV Brown/yellowish brown sandy silt/silty fine sand with occasional lenses of brown and grey silty clay	20	38	20	30	4.5	—
V Mottled brown/grey silty clay with laminations often with rusty brown spots	20–30	25	65	25	10.0	0.001
VI Brown/light brown silty fine to medium sand	40	$\phi' >> 40^\circ$				

Fig. 1.9 Normal Calcutta deposit.

Expansive soils are found in many parts of India, Africa, and the middle-east. The black cotton soils of India and Africa are the most common types of expansive clays. These soils have high expansive potential because of the predominant presence of montmorillonite minerals. They are apparently stiff when dry but undergo swelling when saturated with water, e.g., due to seasonal fluctuation of ground water table. The Atterberg limits along with the percentage of solid particles less than 0.001 mm is taken as criteria for identification and classification of the expansive soils. Table 1.4 gives the classification of expansive clays.

Table 1.4 Classification of expansive clays

% of Particles finer than 0.001 mm	Index Test Data			Probable expansion under pressure of 0.07 kg/cm ² (Dry to saturated condition)	Degree of expansion
	Plasticity index (%)	Shrinkage limit (%)			
28	35	11		30	Very high
20-31	25-41	7-12		20-30	High
13-23	15-41	10-16		10-20	Low
15	18	15		10	Low

1.8 GROUNDWATER

The water which is available below the ground surface is termed as *groundwater* or *subsurface water*. Practically all ground water originates from the surface water. The process by which the surface water infiltrates into the ground surface and percolates deep into the ground is termed as *natural recharge* and *artificial recharge*. Main sources of natural recharge of groundwater include precipitation, rivers, lakes, and other natural water bodies. Artificial recharge of groundwater occurs from excess irrigation, seepage from canals, leakage from reservoirs or tanks, or from water purposely applied on the ground surface to augment groundwater storage. Water from any of these sources infiltrates into the ground and percolates downwards under the action of gravity through soil pores and, rock crevices until further movement is prevented by an impermeable stratum. It is then stored as groundwater. The groundwater exposed to atmospheric pressure beneath the ground surface constitutes the *water table*. Water table rises and falls based on the amount of precipitation, the rate of withdrawal or recharge, and climatic conditions. Groundwater held by the geological formation is, however, not static but moves slowly in the lateral direction towards some point of escape and appear as springs, infiltration galleries or wells, or reappears to join the river, or lake, or the sea.

1.8.1 Types of Water-bearing Formations

Groundwater occurs in most geological formations, of which the most important ones are aquifers. An *aquifer* is defined as a geological formation that permits storage as well as transmission of water through it. Thus, an aquifer contains saturated soil which yields significant quantity of water to wells and springs. Sands and gravels are typical examples of formations which serve as aquifers.

Other geological formations include aquiclude, aquitard, and aquifuge. An *aquiclude* may be defined as a geological formation of relatively impermeable material which permits storage of water but is not capable of transmitting it easily. Thus, an aquiclude contains saturated soil which does not yield appreciable quantities of water to wells. Clay is an example of such a formation.

An *aquitard* is defined as a geologic formation of poorly permeable or semipervious material which permits storage of water but does not yield water freely to wells. However, it may transmit appreciable quantity of water to or from adjacent aquifers. A sufficiently thick aquitard may constitute an important groundwater storage zone. A formation of sandy clay belongs to this category.

An *aquifuge* is a geological formation of relatively impermeable material which neither contains nor transmits water, for example, solid rocks.

1.8.2 Division of Subsurface Water

As shown in Fig. 1.10, subsurface water can be divided into the following zones:

- (a) Soil–water zone
- (b) Intermediate zone
- (c) Capillary zone, and
- (d) Zone of saturation

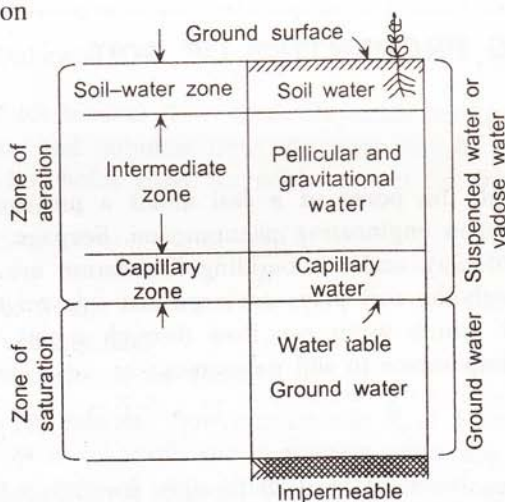


Fig. 1.10 Zones of subsurface water.

Soil–water zone

The soil–water zone extends from the ground surface to the major root zone. The soil in this zone becomes saturated either during irrigation or rainfall. The water in the soil–water zone is gradually depleted by evaporation from within the soil and by transpiration by vegetal growth on the ground surface and if it is not replenished, the water content may be reduced to such an extent that only thin film of moisture known as *hygroscopic water* remains adsorbed on the surface of the soil particles.

Intermediate zone

The intermediate zone occupies the space between the lower edge of soil–water zone and upper limit of the capillary zone. This zone usually contains static water which is held by molecular and surface tension forces in the form of hygroscopic and capillary water. Temporarily, though, this zone may also contain some excess water which moves downward as gravitational water. The thickness of this zone may vary from zero when the water table is high to more than 100 m under deep water table conditions.

Capillary zone

The capillary zone extends from the water table upto the limit of capillary rise of water. In this case, the pore space may be considered to represent a capillary and hence, just above the water table almost all pores contain capillary water.

Zone of saturation

In the zone of saturation, all the interstices are filled with water under hydrostatic pressure. The zone of saturation is bounded at the top either by the ground water table or an overlying impermeable stratum, and stretches upto underlying impermeable strata (or bed rock). Generally, all soils below ground water table are fully saturated.

1.9 ENGINEERING PROPERTIES OF SOIL

1.9.1 Permeability

The flow of water through the pores of a soil under a pressure gradient or under a differential head is a common engineering phenomenon. Seepage of water through earth dams and consolidation of clay under a building foundation are some instances where percolation of water through the soil plays an important role on the performance of the foundation. The ease with which water can flow through a soil, called *permeability*, is therefore, of fundamental importance in soil mechanics.

Darcy's law

Darcy's law which governs the flow of fluid through porous media is also found to be applicable to soils when flow is due to a combination of pressure and positional gradient. With the exception of flow through coarse gravels, the flow of water through soils is streamlined, and can be expressed as:

$$v = ki \quad (1.5)$$

where,

v = average rate of flow of water in unit time.

i = hydraulic gradient, i.e., head loss per unit length of soil measured in the direction of flow, and

k = coefficient of permeability of the soil.

For any given soil, k depends on the porosity of the soil, the structural arrangement of particles, the size of particles, the properties of pore fluid (e.g. density and viscosity) etc. (Taylor 1948). The temperature of the pore fluid should theoretically have some effect but for practical purposes, the variation of k with the range of temperature normally encountered in the soil is small.

The coefficient of permeability of a soil can be measured from the laboratory constant head test, variable head test, or the field pumping test. In view of the heterogeneity and non-homogeneity of natural soil, field pumping tests give a better measure of the permeability of the soil in the field. Typical values of permeability for different types of soil are given in Table 1.5.

Table 1.5 Permeability of different types of soil

Soil type	Coeff. of permeability	Drainage quality
Gravel	1	
Coarse sand	$1-10^{-1}$	
Medium sand	$10^{-1}-10^{-2}$	
Fine sand	$10^{-2}-10^{-3}$	Good
Silty sand	$10^{-3}-10^{-4}$	Poor
Silt/weathered clays	$10^{-4}-10^{-7}$	
Intact clays	$10^{-7}-10^{-9}$	Very poor

Range of validity of Darcy's law

Darcy's law is valid only for laminar flow. Since Reynolds number serves as a criterion to distinguish between laminar and turbulent flow, the same may be employed to establish the limit upto which Darcy's law holds good. Reynolds number for this case is expressed as

$$R_e = \frac{pvd}{\mu} \quad (1.6)$$

where p is mass density of fluid,

v is the discharge velocity, and

μ is the dynamic viscosity of the fluid.

Most of the natural groundwater flow occurs with $R_e < 1$ and hence, Darcy's law is valid. However, Darcy's law is not applicable in aquifers containing coarse gravels, rockfills, and also in the immediate vicinity of wells where the flow may not be laminar due to steep hydraulic gradients.

1.9.2 The Principle of Effective Stress

In a multi-phase system composed of solids and voids, the behaviour of the material under applied stresses depends on how total stress is distributed amongst several components in the soil aggregate, namely the intergranular pressure that acts between the soil grains at their points of contact and the pore pressure which acts in the pore fluid. The normal stress on any plane is, in general, the sum of two components, namely the stress carried by the solid particles and the pressure in the fluid in the void space. The principle of effective stress

provides a satisfactory basis for understanding the deformation and strength characteristics of a soil under an applied load. This can be simply be stated as:

- The volume change of a soil is controlled not by the total normal stress applied on the soil, but by the difference between the total normal stress and the pressure in the fluid in the void space, termed the pore pressure. For an all-round pressure increase, this can be expressed by the relationship.

$$-\frac{\Delta V}{V} = C_c(\Delta\sigma_n - \Delta u) \quad (1.7)$$

where,

$\Delta V/V$ = volume change per unit volume of soil

$\Delta\sigma_n$ = total normal stress/pressure

Δu = pore pressure

C_c = compressibility of soil skeleton

This relationship can be illustrated by a simple test where a saturated soil sample is subjected to undrained loading followed by drained compression as shown in Fig. 1.11. Not until there is a change of effective stress, is there a change of volume of the soil. This is the primary cause of long term consolidation settlement of foundation on clay. This also explains the settlement of an area due to ground water table lowering, either for construction work or for water supply.

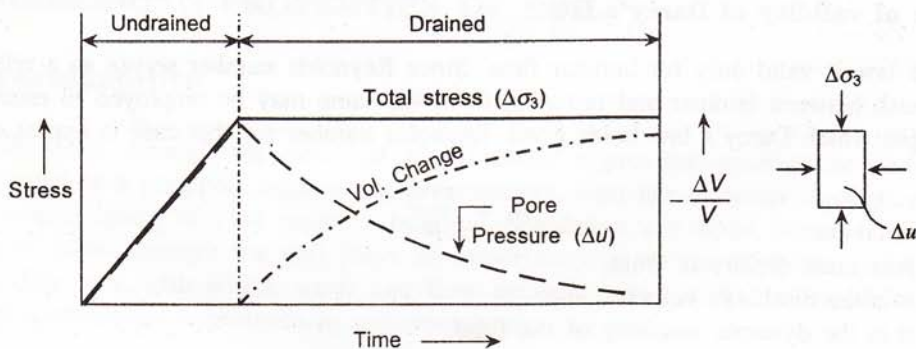


Fig. 1.11 Principle of effective stress.

- The shear strength of a soil is determined by the frictional forces between the solid particles. These are clearly a function of the component of normal stress that is carried by the solid grains rather than the total normal stress on the plane considered. This may be expressed by the equation.

$$\tau = c' + (\sigma_n - u) \tan \phi' \quad (1.8)$$

where,

c' = apparent cohesion

ϕ' = angle of shearing resistance

σ_n = total normal pressure

u = pore-pressure.

In Eqs. (1.7) and (1.8), the term $(\sigma_n - u)$ is termed the effective stress and is denoted by the symbol σ' , that is,

$$\sigma' = \sigma - u \quad (1.9)$$

In most engineering problems, the magnitude of total normal stress can be estimated from considerations of statics while the magnitude of pore pressure depends on the hydraulic boundary conditions. Bishop (1955) has shown that the effective stress in a soil can be related to the intergranular pressure at the points of contact.

For a unit area perpendicular to the plane X-X through a soil mass, the total stress, σ acting on the plane of contact can be divided into two components, (refer Fig. 1.12)

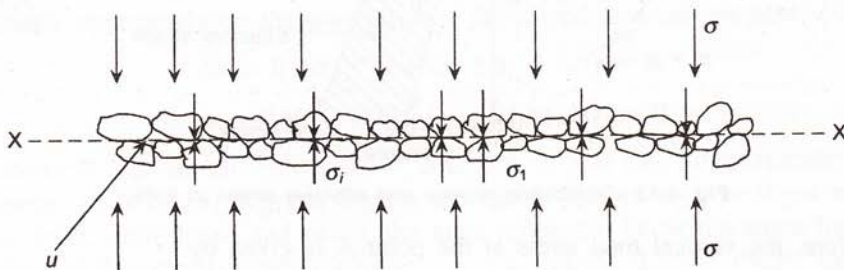


Fig. 1.12 Effective stress and intergranular pressure.

$$\sigma = \sigma' + u \quad (1.10)$$

where,

u = Pore water pressure and

σ' = Effective stress

If a = effective contact area per unit area of the plane and σ_i = average intergranular pressure, then, for a unit area

$$\sigma \times 1 = \sigma_i \times 1 + (1 - a)u$$

or

$$\sigma_i = (\sigma - u) + au \quad (1.11)$$

But a is small (though not equal to 0) and hence,

$$\sigma_i = (\sigma - u) \quad (1.12)$$

From Eqs. (1.11) and (1.12)

$$\sigma_i = \sigma' \quad (1.13)$$

Thus, for practical purposes, effective stress may be considered equal to the intergranular pressure, the average pressure between the solid gains.

In a natural soil deposit, (refer Fig. 1.13), the total stress at any depth is given by the overburden pressure at that depth while the pore pressure, in the absence of any artesian condition, is given by the hydrostatic head of water at that depth. The distribution of total and effective stress in the soil is shown in Fig. 1.13.

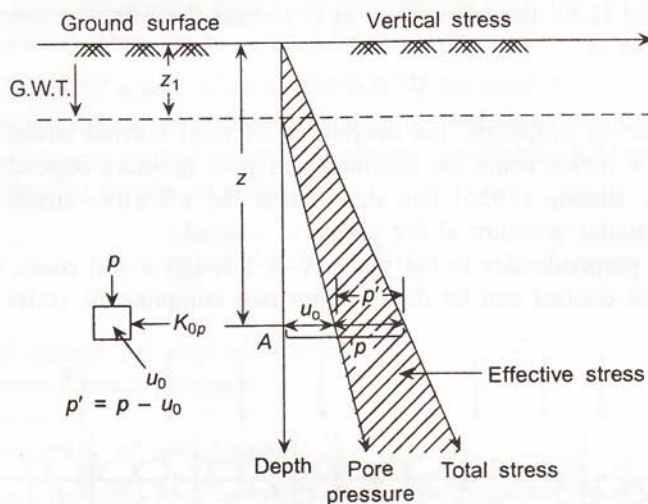


Fig. 1.13 Distribution of total and effective stress in soils.

Therefore, the vertical total stress at the point A is given by

$$\sigma_v = \gamma_1 z_1 + \gamma(z - z_1) \quad (1.14)$$

where,

γ_1 = unit weight of soil within depth z_1

γ = unit weight of soil below depth z_1

The pore water pressure

$$u = \gamma_w(z - z_1) \quad (1.15)$$

where γ_w = unit weight of water.

Hence, the effective stress at A is given by

$$\begin{aligned} \sigma'_v &= \gamma_1 z_1 + \gamma(z - z_1) - \gamma_w(z - z_1) \\ &= \gamma_1 z_1 + \gamma'(z - z_1) \end{aligned} \quad (1.16)$$

where γ' = submerged density of soil below water table

1.9.3 Pore-pressure in Soil due to Applied Load

The application of structural load causes an increase in the total stresses in the ground, the magnitudes of which can be determined from the theory of elasticity. If the subsoil consists of clay of low permeability and construction is sufficiently rapid, these changes in total stress occur under conditions of no volume change and are associated with simultaneous development of excess pore water pressure.

The concept of pore pressure coefficient is utilized to obtain a clear picture of how the pore-pressure in a soil responds to different combinations of applied stress (Skempton 1954). This concept not only explains the relationship between different types of triaxial test, but also provides a basis for estimating the magnitude of pore-pressure to be encountered in practical problems.

Skempton (1954) expressed the change of pore-pressure in a soil under axi-symmetric stress changes in terms of two empirical parameters A and B where

$$\Delta u = B[\Delta\sigma_3 + A(\Delta\sigma_1 - \Delta\sigma_3)] \quad (1.17)$$

where,

Δu = change in pore-pressure

$\Delta\sigma_1$ = change in total vertical pressure

$\Delta\sigma_3$ = change in total lateral pressure

A and B = pore-pressure parameters

By putting $\Delta\sigma_3$ and $(\Delta\sigma_1 - \Delta\sigma_3)$ equal to zero successively, it can be shown that the parameters B and A represent the effect of the allround stress increase and the deviatoric stress increase respectively on the pore-pressure developed in a soil element. Accordingly,

$$\Delta u = B \cdot \Delta\sigma_3 \quad \text{when } \Delta\sigma_1 - \Delta\sigma_3 = 0$$

$$\text{and} \quad \Delta u = A[\Delta\sigma_1 - \Delta\sigma_3] \quad \text{when } \Delta\sigma_3 = 0 \quad (1.18)$$

The parameter B depends on the degree of saturation of soil (for fully saturated soil $B = 1$). The parameter A , however, depends upon a number of factors such as stress history of the soil, stress level, strain level, and so on, the most influential being the stress history, that is, whether the soil is normally consolidated or overconsolidated (Lambe 1962). Table 1.6 gives typical values of pore-pressure parameter A for different stress history of the soil.

Table 1.6 Pore-pressure parameter A of different soil types

Soil type	Value of A at failure
Sensitive clay	1.2–2.5
Normally consolidated clay	0.7–1.2
Overconsolidated clay	0.3–0.7
Heavily overconsolidated clay	-0.5–0.0

Data from Winterkorn and Fang (1975).

1.9.4 Shear Strength of Soils

The shear strength of a soil under any given condition of drainage is defined as the maximum shear stress which the soil can withstand. When a structure is erected on a soil, the soil elements beneath the foundation are subjected to increased shear stresses. The capacity of the foundation to bear load is a function of the shear strength of the soil. The maximum shear stress a soil can withstand depends to an appreciable extent on the manner of loading and the boundary conditions. A soil specimen does not, therefore, have a unique shear strength and it depends on factors such as rate of strain, drainage condition, and size of sample.

The failure criterion most commonly used for defining the shear strength of a soil along a plane is expressed by the Mohr–Coulomb equation, as illustrated in Fig. 1.14,

$$\tau = c + \sigma_n \tan \phi \quad (1.19)$$

where

c is the cohesion intercept,

σ_n is the normal pressure on the plane considered, and

ϕ is the angle of shearing resistance

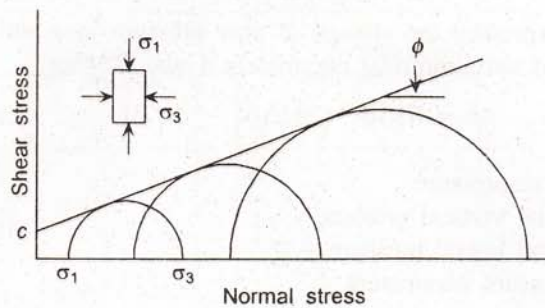


Fig. 1.14 Mohr-Coulomb failure criterion.

In Eq. (1.19), the shear strength parameters c and ϕ for any particular soil depend on several factors, the most important being the condition of drainage. Therefore, Eq. (1.19) expressed in terms of the total normal stress on the plane considered may be used to study the shear behaviour of soil under undrained condition. A more general expression may be written in terms of effective stress (Bishop 1955) as:

$$\tau = c' + (\sigma_n - u) \tan \phi'$$

or

$$\tau' = c' + \sigma' \tan \phi' \quad (1.20)$$

where c' and ϕ' are the shear strength parameters in terms of effective stress.

Measurement of shear strength

While the Vane shear test (Cadling and Odenstad 1950) or the Pressuremeter test (Menard 1956, 1969) may be used to determine the undrained shear strength of soils in the field, the shear behaviour of soils is best understood from the laboratory triaxial test. Figure 1.15

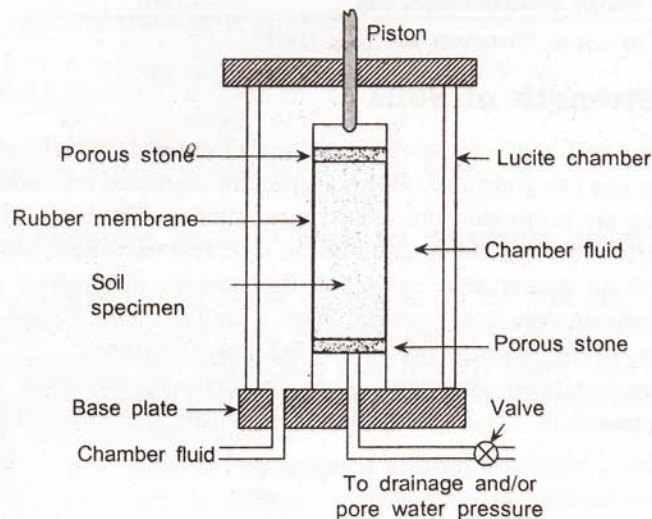


Fig. 1.15 Triaxial test set-up.

shows triaxial test set-up. Here, a cylindrical soil specimen is enclosed in a thin rubber membrane with rigid caps at top and bottom. The soil is placed inside a triaxial cell which is then filled with water. Pressure is applied to the specimen through water and deviator stress is applied through the end caps until the specimen fails in compression. Drainage of water from the pores of the soil may be controlled through suitable valves at the base of the triaxial cell. If required, volume change and/or pore water pressure can be measured. The details of the triaxial apparatus and various tests that can be performed with it have been described by Bishop and Henkel (1962).

Types of triaxial test

There are, in general, three conditions of drainage under which the triaxial test is performed, namely unconsolidated undrained (UU), consolidated undrained (CU), and consolidated drained (CD).

In the unconsolidated undrained (UU) test, the sample is first subjected to an all round pressure σ_3 and then to a deviator stress ($\sigma_1 - \sigma_3$) under undrained condition. The deviator stress is applied rapidly—usually at a rate of strain of 1–2% per minute, and failure is achieved in 10–20 minutes. For saturated soil, the Mohr envelope remains horizontal giving $\phi_u = 0$. The shear strength obtained from the UU test is called the *undrained shear strength* of the soil c_u , see Fig. 1.16. The shear strength obtained from the UU test is used in the study of bearing capacity of foundations on clay or in the rapid construction of embankments on clay. The unconfined compression test is a special case of UU test, where no confining pressure is applied to the specimen prior to shear.

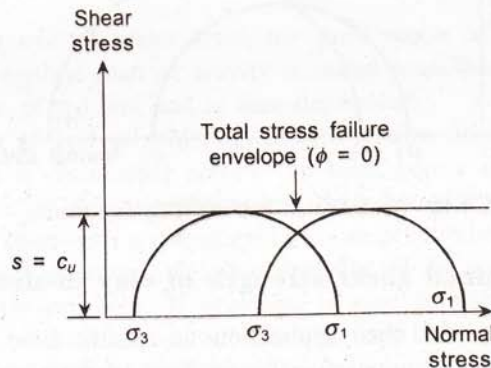


Fig. 1.16 Unconsolidated undrained (UU) test on saturated clay.

In the consolidated undrained (CU) test, the sample is allowed to consolidate under an all round pressure σ_3 but no drainage is allowed during shear. If pore pressure is measured during the test, both the pore pressure parameter A and B , and the shear strength parameters c' and ϕ' can be determined. Figure 1.17 depicts consolidated undrained (CU) test on saturated clay. The data from CU test may be used in the analysis of stability for stage construction of embankments on clay.

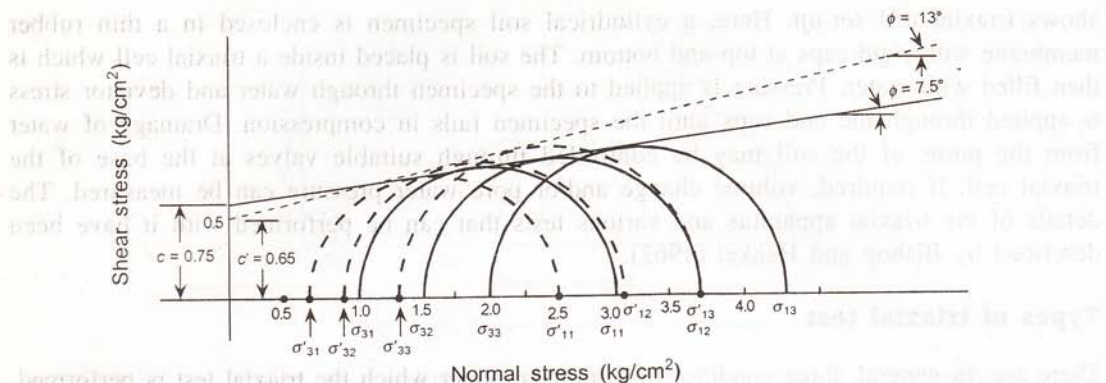


Fig. 1.17 Consolidated undrained (CU) test on saturated clay.

The consolidated drained (CD) test differs from the consolidated undrained test in the way that both, the initial all round pressure and the subsequent shear stresses are applied under fully drained condition. The test, therefore, gives the shear strength parameters of a soil in terms of effective stress, as given by Fig. 1.18. The results of this test can be used in the study of long term stability problems.

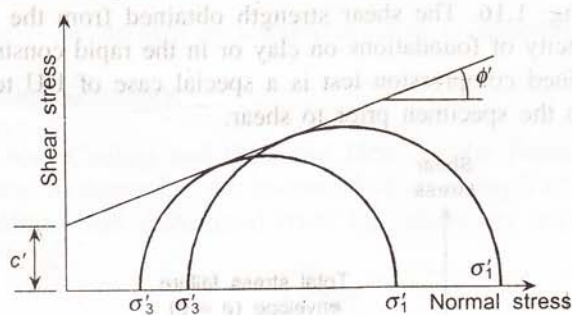


Fig. 1.18 Consolidated drained (CD) test results.

Factors affecting undrained shear strength of clay in-situ

Different types of triaxial test find their applications in specific field problems but, the most important strength parameters required for the analysis of foundations on clay are those obtained from the quick unconsolidated undrained (UU) triaxial test. For saturated clays, this shear strength is expressed by the undrained cohesion $c_u \cdot \phi_u$ should theoretically be zero, if the soil is fully saturated (Skempton 1948). Therefore, the shear strength of the clay in this condition may be expressed as

$$(1.21)$$

Although the UU test is easy to perform in the laboratory, application of the test data to field problem has to be done with care. Factors such as anisotropy, rate of shear, sample size, and so on affect the test results significantly (Skempton and L. Rochelle 1955). For stiff-fissured clays, in particular, the shear strength of the clay mass in the field may be

considerably less than the strength obtained from conventional laboratory tests on small size samples (Bishop 1966).

Sensitivity

Most clays have been found to lose a part of their strength when remoulded. This remoulding may be caused by physical or mechanical means such as pile driving. However, with time, the clay may regain this strength either wholly or partly, by a phenomenon known as *thixotropic hardening* (Skempton and Northey 1952). From the point of view of sensitivity towards remoulding, clays may be classified as follows (Table 1.7):

Table 1.7 Sensitivity of clays
(Skempton and Northey 1952)

<i>Sensitivity</i>	<i>Classification</i>
Less than 2	Ininsensitive
2–4	Moderately sensitive
4–8	Sensitive
8–16	Very sensitive
16	Quick clays

Sensitivity, in this context, is defined as the ratio of the undrained shear strength of the undisturbed soil to that of the fully remoulded soil.

1.9.5 Consolidation

The gradual squeezing out of water from the pore space of a soil skeleton under the influence of externally applied load or gravity is called *consolidation*. The process results in a net change in volume of the soil and is time-dependent.

When an element of soil is subjected to an increase of total stress under undrained condition, the pressure is distributed among the solid grains and water depending on the relative compressibilities of the two phases and their boundary conditions. For a confined saturated clay–water system with no drainage, the compressibility of the mineral skeleton is so large compared to that of water alone that virtually all the applied pressure is transmitted as an excess pore water pressure. If drainage is now permitted, the resulting hydraulic gradient initiates a flow of water out of the clay and the soil consolidates. There is a consequent transfer of the applied load from the water to the mineral skeleton.

The mechanism of consolidation and the factors that govern the process of consolidation of clayey soils are studied experimentally in the laboratory in the consolidation test or the oedometer test. The arrangement for oedometer test is shown in Fig. 1.19. A sample, usually 76 mm dia × 20 mm thick, is enclosed in a metal ring and sandwiched between two porous stones placed at top and bottom. A load is applied to the sample through the porous stones using a lever arrangement. As the sample consolidates, thickness of the sample decreases. Being laterally confined within the metal ring, the sample is prevented from expanding laterally and the entire volume change takes place in the vertical direction. The flow is, therefore, one dimensional and the rate of consolidation is governed by the permeability of

the soil in the vertical direction only. However, consolidation is not always one-dimensional in the field and the consolidation test as performed in the laboratory represents the field condition only under certain boundary conditions.

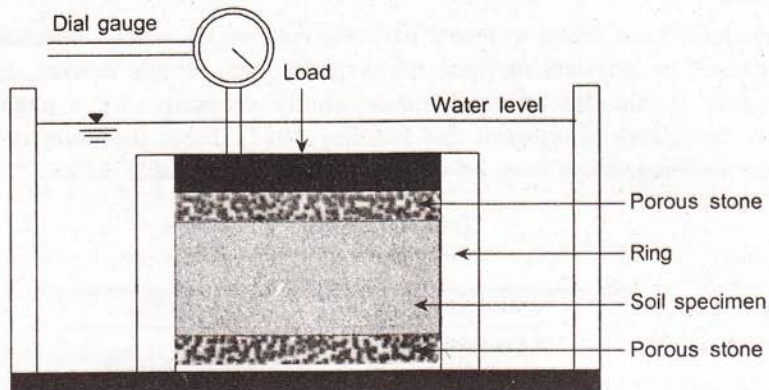


Fig. 1.19 Oedometer test apparatus.

Pressure–void ratio relationships

The change of volume of a sample as measured in the consolidation test is a function of increment in applied stress and is generally expressed in terms of the pressure–void ratio relationship of the type shown in Fig. 1.20. For a normally consolidated soil, this relationship is found to be linear on a semi-log plot.

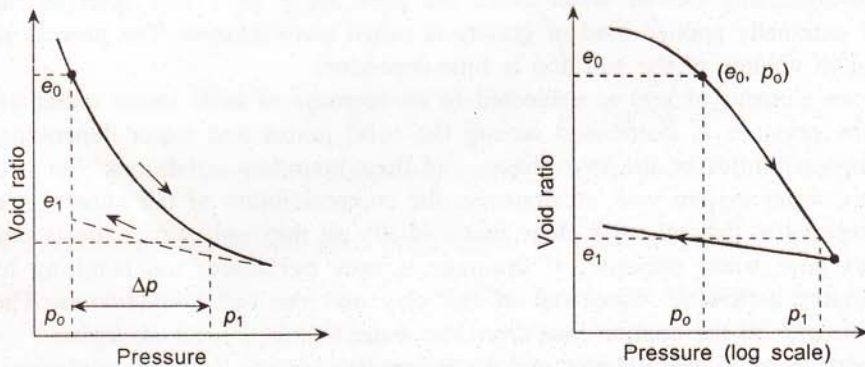


Fig. 1.20 Pressure–void ratio relationship.

The coefficient of volume decrease is defined as the volumetric strain per unit increase of effective pressure and this can be expressed, in terms of void ratio, as

$$m_v = -\frac{de}{dp} \frac{1}{1 + e_0} \quad (1.22)$$

where,

e_0 = initial void ratio for the stress increment considered.

For the linear void ratio versus effective stress relationship on the semi-log plot, the compressibility of the soil is given by the compression index, C_c defined as,

$$C_c = \frac{de}{d(\log p)} \quad (1.23)$$

and

$$\frac{\Delta V}{V} = \frac{C_c}{1 + e_0} \log(p_1 p_o) \quad (1.24)$$

The compressibility of a soil is a measure of its consistency. Greater the compressibility, softer is the soil and vice versa. Again, compressibility of a soil is not a constant property. It decreases with increasing effective stress, as is evident from the decreasing slope of the pressure–void ratio relationship with increasing pressure. But for the range of stresses usually encountered in practice, Table 1.8 gives one dimensional compressibility of some representative clays.

Table 1.8 One-dimensional compressibility of some clays

Stress History	Clay	m_v (cm^2/kg)	$C_c/(1 + e_0)$
Normally Consolidated	Gosport Clay, England	0.15	—
	Shellhaven Clay	0.25	—
	Normal Calcutta Clay	0.05	0.15–0.20
	Cochin Marine Clay	0.06	0.20
Over Consolidated	Brown London Clay	0.017	—
	Blue London Clay	0.010	—
	Normal Calcutta Clay (desiccated)	—	0.05

(Data from Skempton and Bishop (1954), Chummer (1976) and Author's files)

Normally consolidated and overconsolidated clays

Let us consider an element of soil during deposition under water, Fig. 1.21. As more and more soil is deposited on the element, the overburden pressure on the element increases and its void ratio decreases along the curve AB. When the maximum height of deposition, H_c is reached, the pressure increases to P_c and the void ratio decreases to e_c . The soil anywhere on the curve AB is called *normally consolidated*, to indicate that it has never in its past, been subjected to a pressure greater than that corresponding to the curve AB. Marine clays and alluvial soils of India are typical examples of normally consolidated clays.

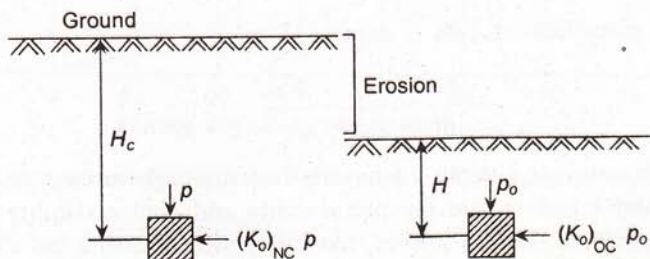


Fig. 1.21 Stresses in an element of soil below ground surface.

Now, if some part of the overburden is removed by, say, erosion and the remaining height of deposition is only H , corresponding to which the pressure is p_0 , the element of soil will undergo swelling and the void ratio will increase to e . This means that the soil in its past has been subjected to a pressure greater than that exists now. Many clays and clay shales, for example, London clay and Bearpaw shale, are heavily overconsolidated in nature. The strength and deformation characteristics of a soil depend to a large extent on it being normally consolidated or overconsolidated. Soft clays are normally consolidated and their behaviour differs from overconsolidated clays and clay shales. Structures founded on normally consolidated clays, in general, experience much more settlement than those founded on overconsolidated clays.

Although erosion of overburden has been identified as one of the causes of overconsolidation, many residual and alluvial soils near the ground surface are rendered overconsolidated by desiccation. Alternate wetting and drying due to seasonal fluctuation of water table and changes of temperature introduce capillary forces in the soil and the latter develops a pseudo overconsolidation effect. This results in increased strength and decreased compressibility of the soil. Depending on the severity of changes during desiccation, the over consolidation effect may be quite appreciable. Most residual soils of India and occasionally the alluvial soils near the ground surface appear overconsolidated due to desiccation.

Rate of consolidation

The rate of consolidation of clayey soils is governed by the theory of one-dimensional consolidation (Terzaghi 1923), as shown in Fig. 1.22:

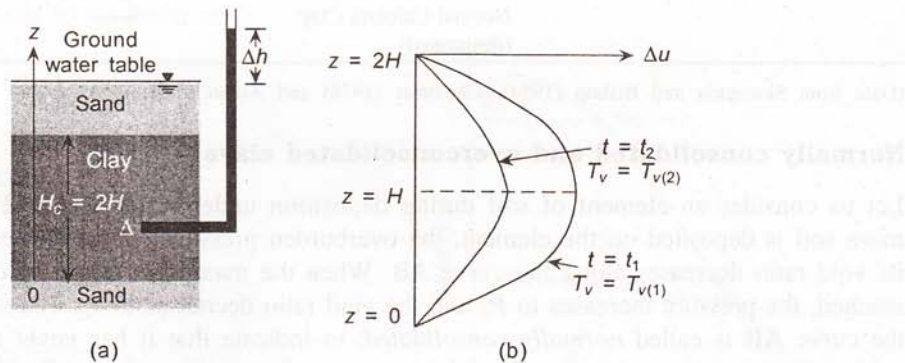


Fig. 1.22 One-dimensional consolidation.

The one-dimensional consolidation rate is expressed as

$$\frac{\delta u}{\delta t} = \frac{k}{\gamma_w m_v} \frac{\delta^2 u}{\delta z^2} \quad (1.25)$$

where u is the pore pressure at a depth z from the free drainage surface, at a time t after the pressure increment; and k and m_v are the permeability and compressibility of the soil for a particular pressure increment. Both k and m_v may vary with pressure but their ratio remains

approximately constant (Skempton and Bishop 1954). Consequently, Eq. (1.25) may be written as,

$$\frac{\delta u}{\delta t} = C_v \frac{\delta^2 u}{\delta z^2} \quad (1.26)$$

where C_v is defined as the coefficient of consolidation.

Solving Eq. (1.26) for the appropriate boundary conditions, we get the distribution of excess pore pressure with depth at a given time t as shown in Fig. 1.22(b). Then, integrating the area of the pore pressure dissipation diagram at a given time and expressing it as a ratio of the initial pore pressure diagram, we get the average degree of consolidation, U of the soil as a function of the time factor T_v . Thus, the degree of consolidation, U can be conveniently expressed as,

$$U = f(T_v) \quad (1.27)$$

where,

$$T_v = \frac{C_v t}{H^2} \quad (1.28)$$

and H = length of the drainage path, to be taken as full depth of clay when drainage is from one end and half the depth of clay when drainage is from both ends.

The coefficient of consolidation is governed primarily by the size and nature of particles as reflected by the water content or whether the soil is normally consolidated or overconsolidated. C_v is determined from laboratory consolidation test by curve fitting methods (Taylor 1948). The relationship between the U and T_v for the most common boundary conditions of single or two-way drainage is plotted in Fig. 1.23.

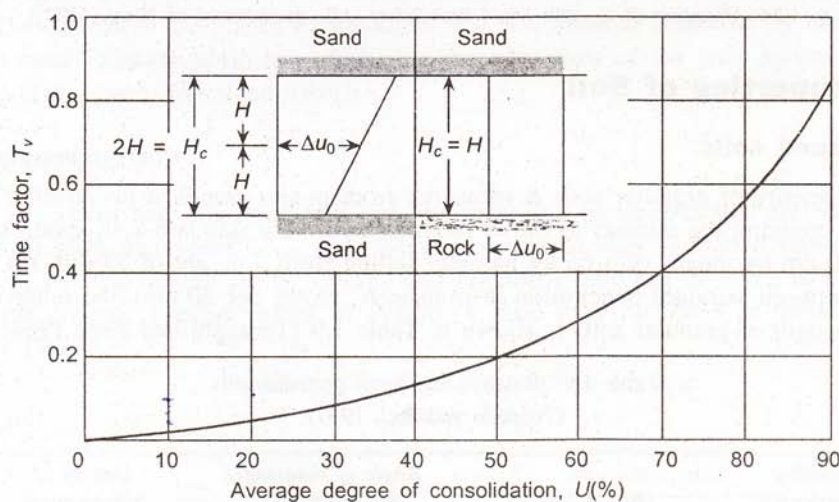
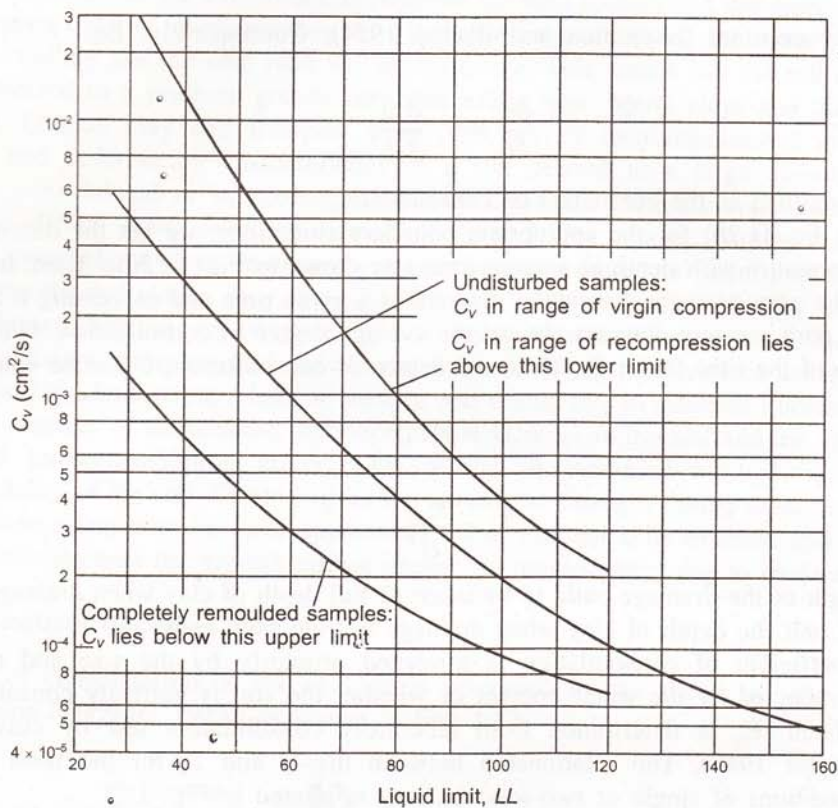


Fig. 1.23 Degree of consolidation versus time factor plot for one-dimensional consolidation.

This gives the C_v value for one-dimensional consolidation of small size specimens. U.S. Department of Navy (1971) proposed an empirical relationship between C_v and liquid limit for determining the field C_v for practical use and this is shown in Fig. 1.24.

Fig. 1.24 Variation of C_v with liquid limit (after U.S. department of Navy (1971)).

1.9.6 Properties of Soil

Coarse-grained soils

The relative density of granular soils is measured from in-situ *standard penetration test*. This test involves counting the number of blows required to drive a standard split-spoon sampler to a depth of 30 cm by means of a 65 kg hammer falling from a height of 75 cm. An empirical correlation between standard penetration resistance, N (blows per 30 cm), the relative density, and shear strength of granular soils is shown in Table 1.9 (Terzaghi and Peck 1967).

Table 1.9 Relative density of granular soils
(Terzaghi and Peck 1967)

Relative density (%)	N (Blows/30 cm)	Angle of shearing resistance (ϕ)	Degree of compactness
0–15	0–4	28°	Very Loose
15–35	4–10	28–30°	Loose
35–65	10–30	30–36°	Medium
65–85	30–50	36–41°	Dense
7–85	50	41°	Very Dense

Note: ϕ values are to be increased by 5° for soils containing less than 5% silt.

Fine-grained soils

Soils containing clay-size particles and large proportion of silt have low permeability and their properties vary with the rate of load application. Under undrained condition, their strength is derived almost exclusively from cohesion. These soils often possess low shear strength and high compressibility, thus making them poor foundation material.

A cohesive soil is described as very soft, soft, medium, stiff, and so on according to its shear strength as determined from the unconfined compression test or from the undrained triaxial test. Attempts have also been made to correlate the standard penetration resistance (as above) with the shear strength of cohesive soils. Table 1.10 gives the classification of cohesive soils on the basis of their shear strength (Terzaghi and Peck 1967).

Table 1.10 Shear strength of cohesive soils
(Terzaghi and Peck 1967)

Consistency	Undrained shear strength, c_u (t/m^2)	N (Blows per 30 cm)
Very Soft	0–1.25	0–2
Soft	1.25–2.50	2–4
Medium	2.50–5.00	4–8
Stiff	5.00–10.00	8–16
Very Stiff	10.00–20.00	16–32
Hard	> 20.00	32

Stiff clay often possesses cracks and fissures which affect the shear strength of the clay mass. These fissures are planes of weakness and are prone to softening by water. Laboratory tests on small specimens do not often give the properties of the soils in-situ (Bishop 1966, Burland et al. 1966, Marsland 1971).

Elastic parameters

Young's modulus and Poisson's ratio are important soil parameters that are required to study the deformation behaviour of a soil. When a saturated clay is loaded rapidly, no volume change of the clay occurs during loading and Poisson's ratio can be taken as 0.5. When there is volume change, typical values of Poisson's ratio may be taken as those in Table 1.11 (Barkan 1962).

Table 1.11 Poisson's ratio of different soils
(Barkan 1962)

Soil type	Poisson's ratio
Saturated clay (undrained)	0.50
Clay with sand and silt	0.30–0.42
Unsaturated clay	0.35–0.40
Loess	0.44
Sand	0.30–0.35

Young's modulus of a soil can be determined from the stress-strain relationship obtained from laboratory triaxial tests. However, these relationships are highly susceptible to sampling disturbances and the E value thus obtained is generally much lower than the in-situ modulus. In case of homogeneous deposits, determination of E by back calculation from field plate load test gives reliable data. Indirect estimate of E can also be made from empirical relation with the shear strength measured from the unconsolidated undrained triaxial test. Bjerrum (1964), and Bozuzuk and Leonards (1972) suggest the following approximate correlation:

$$E = (500 - 1000)c_u \quad (1.29)$$

where c_u is the undrained shear strength of the clay.

In-situ compressibility

The pressure versus void ratio relationships of natural clays are very sensitive to sampling disturbances and the linear e versus $\log p$ relationship is not always obtained even for a normally consolidated clay. Also, there is a pseudo overconsolidation effect on the sample because of the removal of in-situ stresses by sampling. Consequently, e versus $\log p$ relationship obtained from laboratory consolidation tests on undisturbed samples generally takes the shapes as shown in Fig. 1.25. The curves move downwards as the sampling disturbances are increased. Schmertman (1953) observed that, irrespective of sampling disturbances, the straight line portions of all the curves meet at a void ratio equal to $0.42 e_0$, where e_0 is the in-situ void ratio of the sample. Then joining this point with that corresponding to e_0 and p_0 (where p_0 = in-situ effective overburden pressure) would give the virgin consolidation curve. For normally consolidated soil, the e_0-p_0 point lies to the right of the extension of the straight line in the laboratory e versus $\log p$ curve while for overconsolidated samples, the point would lie to the left. The field e versus $\log p$ relationship for the overconsolidated range is obtained by drawing a line parallel to the laboratory rebound curve and the point of intersection of this line with extended straight line of the laboratory curve would give the pre-consolidation pressure (Fig. 1.25).

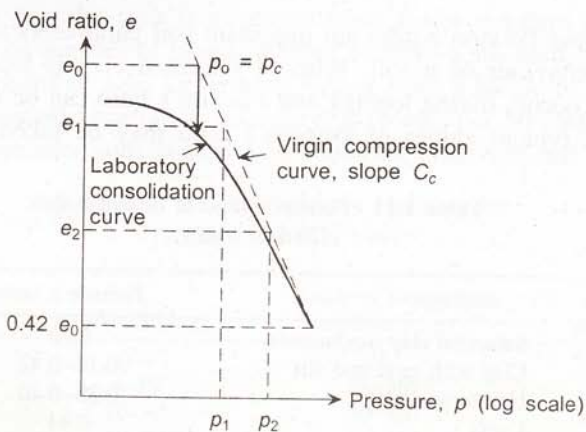


Fig. 1.25 Laboratory e versus $\log p$ relationship.

1.10 SOIL DEPOSITS OF INDIA

The soil deposits of India may be classified under most of the predominant geological formations (described earlier), namely

- | | | |
|--------------------|---------------------|-----------------------|
| (a) Alluvial soils | (b) Marine deposits | (c) Black cotton soil |
| (d) Laterite soil | (e) Desert soil | (f) Boulder deposits |

Figure 1.26 shows the distribution of predominant soil deposits in India (Ranjan and Rao 2000).

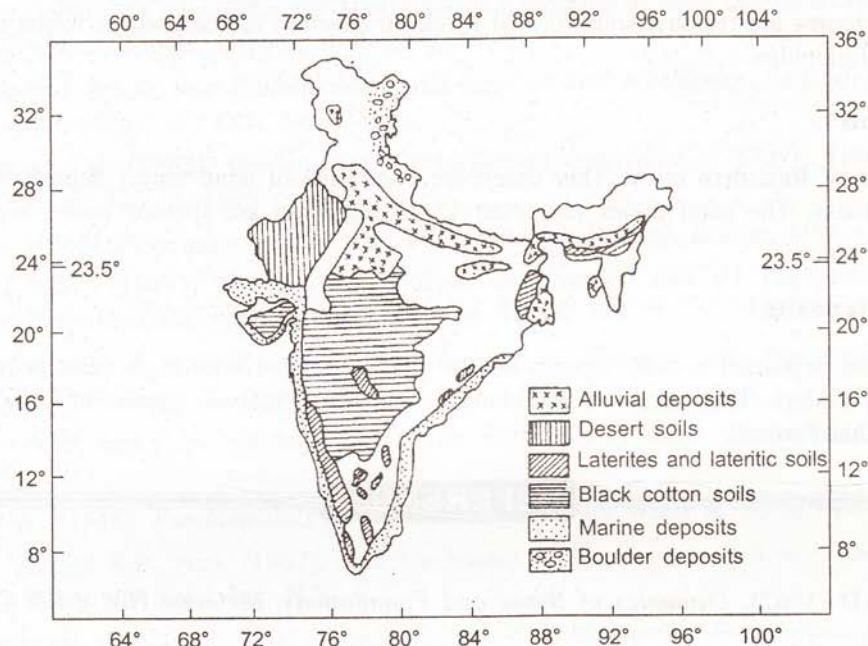


Fig. 1.26 Soil deposits of India.

Alluvial soils

Large parts of northern and eastern India lying in the Indo-ganggetic plains and the Brahmaputra valley are covered by the sedimentary deposits of the rivers and their tributaries. They often have thickness greater than 100 m above the bed rock. The deposits mostly constitute layers of sand, silt, and clay depending on the position of the river away from the source.

Marine deposits

India has a long coast line extending along the Arabian sea, Indian ocean, and the Bay of Bengal. The deposits along the coast are mostly laid down by the sea. These marine clays of India are generally soft and often contain organic matter. They possess low shear strength and high compressibility.

Black cotton soil

The central part of India has extensive deposits of the expansive soil known as black cotton soil. This covers wide areas of Maharashtra, Madhya Pradesh, Karnataka, Andhra Pradesh, Tamil Nadu, and Uttar Pradesh. The soil contains montmorillonite clay mineral which has high swelling potential.

Laterite soil

This soil covers wide areas of Kerala, Karnataka, Maharashtra, Orissa, and parts of West Bengal. Laterites are residual soils formed by decomposition of rock which forms oxides of iron and aluminium.

Desert soil

Large areas of Rajasthan in the Thar desert are composed of wind blown deposits of desert soil, like loess. The sand dunes are often 15 m high and are formed under highly arid conditions.

Boulder deposits

Boulders are deposited in hilly terrains where the rivers flow with high velocity and carry large size boulders. These deposits are found in the sub-Himalayan regions of Uttar Pradesh and Himachal Pradesh.

REFERENCES

- Barkan, D.D (1962), *Dynamics of Bases and Foundations*, McGraw Hill Book Co., New York.
- Bishop, A.W. (1959), The Principle of Effective Stress, *Teknisk Ukeblad*, Vol. 106, No. 39, pp. 859–863.
- Bishop, A.W. (1966), Strength of Soils as Engineering Materials, *Geotechnique*, Vol. 16, pp. 89–130.
- Bishop, A.W. and D.J. Henkel (1964), *The Measurement of Soil Properties in the Triaxial Test*, Edward Arnold, London.
- Bjerrum, L. (1964), *Relasjon Melom Malte og Berengnede Setninger av Byggverk pa Leire og Sand*, Norwegian Geotechnical Institute, Oslo, Norway.
- Bozuzuk and G.A. Leonards (1972), *The Gloucester Test Fill*, Proceedings ASCE Speciality Conference on performance of earth and earth retaining Structures, Lafayette, Indiana, USA.
- Burland, L., F.G. Butler, and P. Duncan (1966), *The Behaviour and Design of Large Diameter Bored Piles in Stiff Clay*, Proceedings Symposium on Large Bored Piles, The Institution of Civil Engineers, London, pp. 51–71.

- Chummar, A.V. (1976), *Foundation Problems in Cochin*, Proceedings Symposium in Foundations and Excavations in Weak Soil, Calcutta, Vol. 1, Paper No. C 4.
- IS 1498 (1970), *Classification and Identification of Soils*, Bureau of Indian Standards, New Delhi.
- Lambe, T.W. (1962), *Pore-pressures in a Foundation Clay 1962*, Proceedings ASCE, Soil Mechanics and Foundation Division, Vol. 88, pp. 19-47.
- Marsland, A. (1971), *The Shear Strengths of Stiff Fissured Clays*, Proceedings Roscoe Memorial Symposium, Cambridge, U.K., pp. 59-68.
- Menard, L. (1956), *An Apparatus for Measuring the Strength of Soils in Place*, MS. Thesis, University of Illinois, Urbana, Illinois, USA.
- Ranjan, G. and A.S.R. Rao (2000), *Basic and Applied Soil Mechanics*, 2nd edition, New Age International (P) Ltd., New Delhi.
- Schmertmann, J.H. (1953), *Undisturbed Consolidation Behaviour of Clays*, Transactions, ASCE, Vol. 120, p. 1201.
- Scott, R.F. (1965), *Principles of Soil Mechanics*, Addison Wesley, Boston, USA.
- Skempton, A.W. (1948), *The $\phi = 0$ Analysis of Stability and its Theoretical Basis*, Proceedings 2nd International Conference on SMFE, Vol. 2.
- Skempton, A.W. and A.W. Bishop (1954), *Soils, their Elasticity and Inelasticity*, North Holland Publishing Co, Amsterdam.
- Skempton, A.W. and R.D. Northey (1952), *The Sensitivity of Clays*, Geotechnique, Vol 3, pp. 30-54.
- Taylor, D.W. (1948), *Fundamentals of Soil Mechanics*, John Wiley & Sons, New York.
- Terzaghi, K. and R.B. Peck (1967), *Soil Mechanics in Engineering Practice*, 2nd edition, John Wiley and Sons, Inc, N.Y.
- U.S. Department of Navy (1971), *Design Manual—Soil Mechanics, Foundations and Earth Structures*, NAVFAC, DM-7, U.S. Government Printing Office, Washington, D.C.

2

Site Investigation

2.1 INTRODUCTION

It is essential to carry out site investigation before preparing the design of civil engineering works. The investigation may range in scope from simple examination of the surface soils, with or without a few shallow trial pits, to a detailed study of the soil and ground water conditions for a considerable depth below the ground surface by means of boreholes and in-situ and/or laboratory tests on the soils encountered. The extent of the investigation depends on the importance of the structure, the complexity of the soil conditions, and the information already available on the behaviour of existing foundations on similar soils. Thus, it is not the normal practice to sink boreholes and carry out soil tests for single or two-storey dwelling houses since normally, there is adequate knowledge of the safe bearing pressure of the soil in any particular locality. Only in troublesome soils such as peat or loose fill would it be necessary to sink deep boreholes, possibly supplemented by soil tests. More extensive investigation for light structures is needed when structures are built on filled-up soil or in ground conditions where there is no information available on foundation behaviour of similar structures. A detailed site investigation involving deep boreholes and laboratory testing of soils is always a necessity for heavy structures, such as bridges, multi-storeyed buildings or industrial plants.

Thus, the major objectives of site investigation are:

- (a) Knowing the general suitability of the site for proposed works.
- (b) Assessing local conditions and problems likely to be encountered in foundation construction.
- (c) Acquiring data for adequate and economic design of foundation.

2.2 INFORMATION EXTRACTED FROM SITE INVESTIGATION

A lot of information is extracted from site investigation to facilitate foundation design. This includes

1. General topography of the site which affects foundation design and construction, e.g., surface configuration, adjacent property, presence of water courses, and so on.

2. Location of buried services such as power lines, telephone cables, water mains, sewers pipes and so on.
3. General geology of the area with particular reference to the principal geological formations underlying the site.
4. Previous history and use of the site including information of any defects and failures of structures built on the site.
5. Any special features such as possibility of earthquake, flooding, seasonal swelling etc.
6. Availability and quality of local construction materials.
7. A detailed record of soil or rock strata, ground water conditions within the zone affected by foundation loading and of any deeper strata affecting the site conditions in any way.
8. Design data which comprises strength and compressibility characteristics of the different strata.
9. Results of chemical analysis on soil or ground water to determine possible deleterious effects on foundation structures.

2.3 STAGES OF SITE INVESTIGATION

Different stages of site investigation for a major civil engineering project may be summarised as shown in Table 2.1.

Table 2.1 Stages of site investigation

<i>Reconnaissance Study</i>	(a) Geological data (b) Pedological data (c) Areal photographs (d) Geophysical investigation
<i>Detailed Investigation</i>	(a) Boring (b) Sampling (c) Testing (i) Lab test (ii) Field test (d) Aerial photographs (e) Geophysical methods
<i>Performance Study</i>	(a) Further testing (b) Instrumentation (c) Performance evaluation

2.3.1 Reconnaissance Study

Reconnaissance study involves the preliminary feasibility study that is undertaken before any detailed planning is done—mainly for the purpose of selection of site. This is to be done at minimum cost and no large scale exploratory work is usually undertaken at this stage. The required data may be obtained from:

Geological survey reports and maps

Geological interpretation of land forms and underlying strata give the sequence of events leading to the formation of subsoil deposits. They help to define the properties of the material in a general way.

Pedological data

Many areas have been surveyed for agricultural purposes—usually to depths of 2 or 3 m. Materials are often classified according to colour, texture, chemical composition, and so on.

Aerial photographs/satellite images

Photographic representation of a portion of earth's surface taken from the air or space.

Geophysical methods

Application of the methods and principles of physics to determine the properties of subsurface materials. These methods are particularly useful for identifying bed rock. Seismic refraction method or electrical resistivity tests are usually done for this purpose.

2.4 BORING (DETAILED SOIL INVESTIGATION)

Detailed soil investigation is done through a series of boring, sampling, and testing to obtain the engineering properties of soil. The following subsections are devoted to boring which discuss different methods of boring in detail.

2.4.1 Trial Pits

Trial pits are the cheapest way of site exploration and do not require any specialized equipment. A pit is manually excavated to get an indication of the soil stratification and obtain undisturbed and disturbed samples. Trial pits allow visual inspection of any change of strata and facilitate in-situ testing. They are, however, suitable for exploration of shallow depth only. Figure 2.1 is a diagrammatic representation of trial pits.

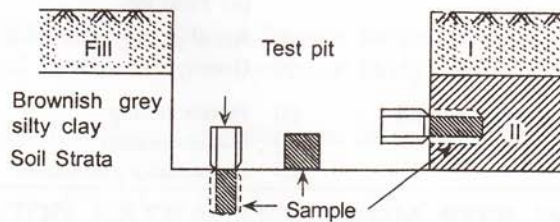


Fig. 2.1 Trial pit.

2.4.2 Wash Boring

A hole, usually 150–200 mm diameter, is advanced into the soil through a suitable cutter at the bottom of a drill rod. The soil is loosened and removed from the borehole by a stream of water or drilling mud, issuing from the lower end of the wash pipe which is worked up and

down or rotated by hand in the borehole. Water or mud flow carries the soil up the annular space between the wash pipe and the casing, and it overflows at ground level where the soil in suspension is allowed to settle in a tank and the fluid is re-circulated or discharged to waste as required. Samples of the settled soil can be retained for identification purposes. Figure 2.2 shows the arrangement for wash boring.

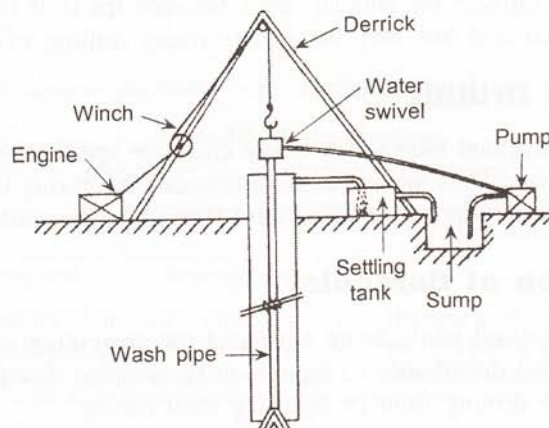


Fig. 2.2 Wash boring.

The method is simple and cheap. The structure of the soil below the boring apparatus is not disturbed and thus, both disturbed and undisturbed samples can be obtained.

2.4.3 Auger Boring

In this method, the borehole is advanced by turning an auger into the soil, withdrawing it and removing the soil for examination and test. The auger is re-inserted for further boring.

The auger may be manually or mechanically operated. Extensions are added to reach the desired depth. Disturbed samples may be obtained from the soil brought up by the auger while undisturbed samples are obtained by pushing sampling tubes at suitable intervals in the borehole. The apparatus for auger boring is shown in Fig. 2.3.

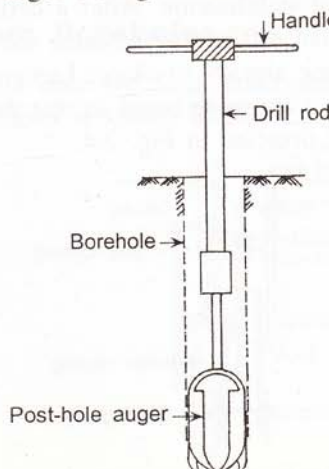


Fig. 2.3 Auger boring.

2.4.4 Rotary Drilling

Rotary drilling is done by rapidly rotating drilling bits attached to the bottom of the drill rod to cut and advance the borehole. Rotary drilling can be used in sand, clay or intact rocks with water or drilling mud being circulated through the drill rod to remove the cuttings as the mud returns upwards through the annular space between the drill rod and the side of the hole. Core barrels with diamond bits may be used in rotary drilling to obtain rock cores.

2.4.5 Percussion Drilling

The soil is loosened by repeated blows of a heavy chisel or spud and the resulting slurry is removed by circulating water. This method is recommended for boring in rocks and hard soil. The hole is advanced with a cutting edge using steel shots, tungsten carbide, or diamond bits.

2.4.6 Stabilization of Boreholes

Boreholes need to be stabilized while being advanced for preventing caving in of sides and bottom of hole and to avoid disturbance to the soil to be sampled. Stabilization may be done by circulation of water or drilling fluid or by using steel casing.

Stabilization by water: Stabilization by water is not suitable in partly-saturated soils above G.W.T. because free water destroys the capillary forces and causes increase in water content. It is generally used in rock and stiff clays.

Stabilization by drilling fluid: Borehole is filled with drilling fluid or mud which, when circulated, removes the loose material from the bottom of the hole. Drilling mud is obtained by mixing locally available fat clays with water or by using commercially available bentonite.

Stabilizing effect of drilling mud is improved by higher specific gravity of the mud in comparison with water. Also, there is formation of a relatively impermeable layer on the side of the borehole which gets liquefied again by resuming the agitation.

Stabilization by casing: Casing or lining a borehole with steel pipes provides the safest, though relatively expensive method of stabilization. After a certain depth or when difficult ground condition is reached, it is often difficult to advance the original casing. A smaller casing is then inserted through the one already in place. Lower end of casing is generally protected by a shoe or hardened steel with inside bevel so that the soil enters the casing and can be removed. This arrangement is depicted in Fig. 2.4.

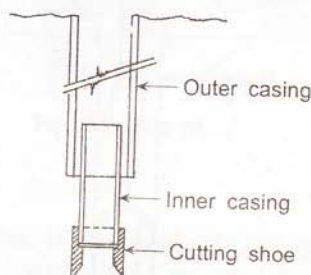


Fig. 2.4 Stabilization of borehole by casing.

Except when undisturbed samples are required in sensitive clays, the casing is generally driven by repeated blows of a drop hammer. Casing prevents side caving, but not always bottom caving. This can be achieved by filling the casing with water or drilling fluid. However, casing should not be filled with water if bottom of casing is above ground water table and undisturbed samples are required.

2.5 SAMPLING

The different types of sample obtained from boreholes are shown in Table 2.2.

Table 2.2 Types of sample

		Samples	
		Disturbed	Undisturbed
Remoulded	Representative		
	(The structure of the soil is disturbed to a considerable degree by the action of boring tools and excavation equipment.)	(Retains as closely as practicable, the true in-situ structure and water content of the soil.)	

2.5.1 Sampling from Trial Pits

Block samples (refer Fig. 2.5) are hand cut from trial pits or open excavations. A block of clay is carefully trimmed with a sharp knife, taking care that no water comes into contact with the sample. Good quality samples can be obtained by this method, but if the soil does not possess any cohesion, it may be difficult, if not impossible, to obtain block samples.

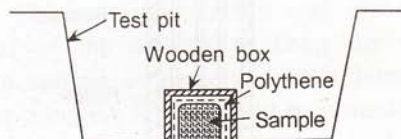


Fig. 2.5 Block sample of clay.

2.5.2 Sampling from Boreholes

Undisturbed samples may be obtained from boreholes by open drive samplers or piston samplers. An open drive sampler is shown in Fig. 2.6.

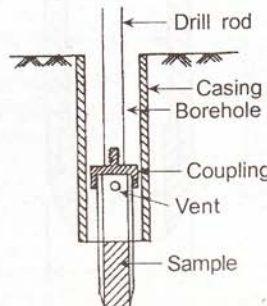


Fig. 2.6 Open drive sampler.

Open drive samplers consist of thin-walled tubes which are pushed or driven into the soil at the bottom of the hole and then rotated to detach the lower end of the sample from the soil as shown in Fig. 2.6. Most soft or moderately stiff cohesive soil can be sampled without extensive disturbance in thin-walled seamless steel tubes having diameter not less than 50 mm. The lower end of the tube is sharpened to form a cutting edge and the other end is machined for attachment to drill rods. The entire tube is pushed or driven into the soil at the bottom of the hole and is removed with the sample inside. The two ends of the tube are then sealed and the sample shipped to the laboratory.

Good quality undisturbed samples are obtained from piston samplers which use thin-walled sampling tubes with a piston inside. While the tube is being lowered to the bottom of the drill hole, the piston rods and the piston are held at the bottom of the sampler by means of a drill rod which rises to the top of the borehole. A piston sampler is shown in Fig. 2.7. The presence of the piston prevents excess soil from squeezing into the tube and thus, maintains the integrity of the sample.

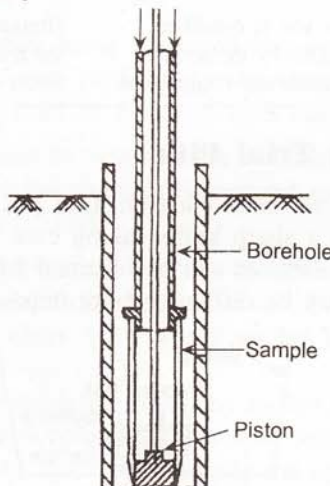


Fig. 2.7 Piston sampler.

Table 2.3 lists the requirements of a good sampling tube (refer Fig. 2.8) as follows:

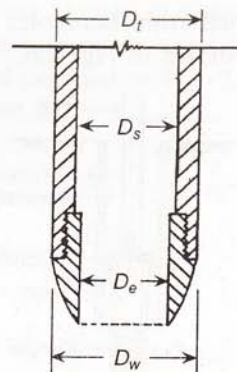


Fig. 2.8 Sampling tube.

Table 2.3 Requirements of sampling tube

$$(a) \text{ Area ratio, } C_a = \frac{D_w^2 - D_e^2}{D_e^2}$$

This represents the amount of soil that is displaced when the sampler is forced into the ground. Thicker the tube, more is the disturbance. The area ratio of a good sampling tube should not exceed 15%.

$$(b) \text{ Inside clearance ratio, } C_i = \frac{D_s - D_e}{D_e}$$

For long samples, $0.75\% < C_i < 1.5\%$

For short samples, $0 < C_i < 0.5\%$

The diameter of the sampling tube is kept slightly larger than the diameter of the cutting edge to minimise friction on the sample as it enters the sampling tube.

$$(c) \text{ Outside clearance ratio, } C_o = \frac{D_w - D_t}{D_t}$$

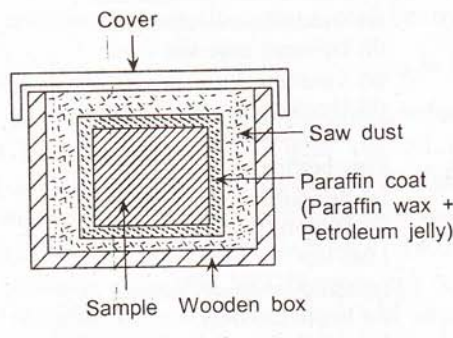
$\approx 2-3\%$

This clearance is provided to reduce the driving force required to penetrate the sampler into the soil. Diameter of samples should not be less than 38 mm. In general, 50–150 mm diameter undisturbed samples are obtained from boreholes.

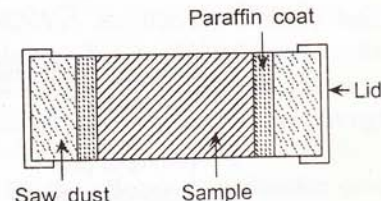
2.5.3 Preservation of Samples

Undisturbed samples which are to be tested after some time should be maintained in such a way that the natural water content is retained and no evaporation is allowed.

Usually, two coats of 12 mm thick paraffin wax and petroleum jelly are applied in molten state on either end of the sample to keep the water content unchanged for considerable time when the sample is preserved in a humidity controlled room. In the absence of such facilities, the sampling tubes should be covered by hessian bags and sprinkled with water from time to time. Block samples may be coated with 6 mm thick paraffin wax and kept in air-tight box with saw dust filling the annular space between the box and the sample. Figure 2.9 shows some typical arrangements for preservation of samples.



(a) Block sample



(b) Tube sample

Fig. 2.9 Preservation of samples.

2.6 TESTING OF SOIL

Soil properties are determined from appropriate laboratory and field tests. The specifications regarding laboratory tests and field tests for routine soil investigation are given in Tables 2.4 and 2.5.

Table 2.4 Laboratory testing of soils

<i>Property of soil</i>	<i>Type of test</i>	<i>Quality of sample</i>
<i>Classification</i>		
1. Identification	Visual soil classification	R/D
2. Grain size distribution	(a) Sieve analysis (b) Wet analysis }	D
3. Consistency limits of cohesive soils	(a) Liquid limit (b) Plastic limit (c) Shrinkage limit }	R/D
4. Moisture content	Moisture content	UD
5. Unit weight	Specific gravity	D
<i>Engineering properties</i>		
1. Shear strength	(a) Unconfined compression (b) Direct shear (c) Triaxial (UU/CU/CD) }	UD
2. Compressibility	(a) Oedometer test (b) Triaxial test }	UD
3. Permeability	(a) Constant head permeability test (b) Variable head permeability test }	UD
4. Compaction characteristics	(a) Proctor test (b) CBR test }	R/D
5. Chemical and mineralogical composition	(a) X-Ray diffraction (b) D.T.A. (c) Chemical test }	R/D

R—Representative

D—Disturbed

UD—Undisturbed

Table 2.5 Field testing of soils

<i>Purpose of test</i>	<i>Type of test</i>
1. Relative density (granular soils)	(a) Standard penetration test (b) Dynamic cone test
2. Shear strength (cohesive soil)	(a) Vane test (b) Direct shear test (c) Static cone test
3. Bearing capacity and settlement	Plate bearing test
4. Permeability	(a) Borehole/pumping test (b) Piezometer test
5. Testing of piles	Load test
6. Compaction control	(a) Moisture-density relation (b) In-place density (c) C.B.R. test
7. In-situ strength and deformation characteristics of soil	(a) Pressuremeter test (b) Dilatometer test

2.7 FIELD TESTS

2.7.1 Standard Penetration Test (SPT)

It is extremely difficult to obtain undisturbed samples of granular soils, so in-situ SPT is performed at frequent intervals along the depth of a borehole. A standard split spoon sampler (Fig. 2.10) is driven 45 cm into the ground by means of a 65 kg hammer falling freely from a height of 75 cm. The total number of blows required to drive the second and third depth of 15 cm (i.e. total 30 cm) is called the standard penetration resistance (N blows per 30 cm). After the blow counts are recorded, the spoon is withdrawn and a representative sample is obtained for identification tests.

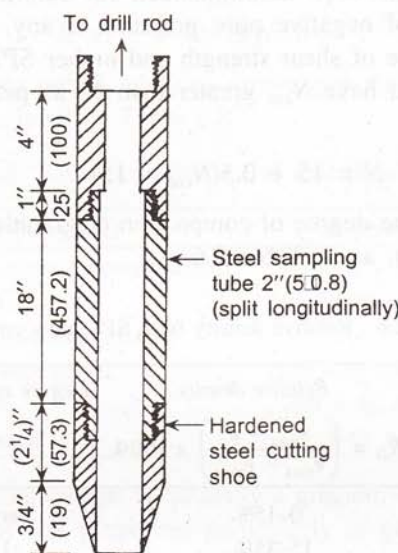


Fig. 2.10 SPT sampler.

For cohesive soils, a simple correlation between the standard penetration resistance (N) and the undrained shear strength, c_u has been proposed by Stroud (1974),

$$c_u = kN \quad (2.0)$$

where k is a constant having an average value of 4.5 kN/m^2 . Similar relationship has been obtained by Sengupta (1984) who studied the correlation for some cohesive soils and obtained a value of 4.2 for the constant k . Terzaghi and Peck's relationship has been widely used to obtain the consistency of cohesive soils in terms of the undrained shear strength, as shown in Table 1.9 (Terzaghi and Peck, 1967).

In granular soils, the SPT blow count is affected by the effective overburden pressure, σ_v' . So, N value obtained from the field should be corrected to correspond to a standard value of σ_v' . Accordingly,

$$N_{\text{cor}} = C_n N_F \quad (2.1)$$

where

N_{cor} = corrected N value for a standard value of σ'_v (100 kN/m²)

C_n = correction factor

N_F = N value obtained from field

The correction factor C_n may be taken from the empirical relationship given by Skempton (1986),

$$C_n = \frac{2}{1 + 0.01\sigma'_v} \quad (2.2)$$

where σ'_v = vertical overburden pressure in kN/m²

A dilatancy correction has been recommended for saturated fine sands and silts to account for the development of negative pore pressure, if any, during driving of the SPT sampler and consequent increase of shear strength and higher SPT blow count (Terzaghi and Peck, 1967). For such soils that have N_{cor} greater than 15 as per Eq. (2.1), a correction for dilatancy may be made as,

$$N = 15 + 0.5(N_{\text{cor}} - 15) \quad (2.2a)$$

The relative density and the degree of compaction of granular soil can be obtained from Terzaghi's empirical correlation, as in Table 2.6.

Table 2.6 Relative density from SPT blow count

No. of blows ($N/30$ cm)	Relative density $R_D = \left(\frac{e_{\max} - e}{e_{\max} - e_{\min}} \right) \times 100\%$	Degree of compaction
0–4	0–15%	Very loose
4–10	15–35%	Loose
10–30	25–65%	Medium
30–50	65–85%	Dense
> 50	> 85	Very Dense

Many attempts have been made to obtain empirical correlation between N_{cor} and the angle of shearing resistance of sand. The most recent attempt by Halanakar and Uchida (1996) appears to agree well with laboratory test data, which gives

$$\phi = \sqrt{20N_{\text{cor}}} + 17 \text{ degrees} \quad (2.3)$$

The modulus of elasticity is obtained by the relationship given by Mezenbach (1961) as

$$E = C_1 + C_2 N \text{ kg/cm}^2 \quad (2.4)$$

where C_1 and C_2 are functions typical of the type of sand. Some C_1 and C_2 values corresponding to different soil types are given in Table 2.7.

Table 2.7 Modulus of elasticity of sand

<i>Soil type</i>	C_1 (kg/cm ²)	C_2 (kg/cm ² /blow)
1. Fine sand (above G.W.T)	52	3.3
2. Fine sand (below G.W.T)	71	4.9
3. Sand (Medium)	39	4.5
4. Coarse sand	38	10.5
5. Sand + gravel	43	11.8
6. Silty sand	24	5.3
7. Silt	12	5.8

A similar correlation between the compression modulus E and the SPT blow count N has been obtained by Papadopoulos (1992). This is given by

$$E = 75 + 8N \text{ (kg/cm}^2\text{)} \quad (2.4a)$$

Bowles (1988) also gives useful relations to evaluate the stress-strain modulus of sand from SPT blow count, as depicted in Table 2.8.

Table 2.8 Stress-strain modulus of sand (Bowles, 1988)

<i>Type of sand</i>	E (kg/cm ²)
Sand (normally consolidated)	$5(N + 15)$
Sand (saturated)	$2.5(N + 15)$
Sand (overconsolidated)	$7.5(N + 24)$
Sand with gravel	$12(N + 6)$ for $N > 15$ $6(N + 6)$, $N \leq 15$
Silty sand	$3(N + 6)$

Although standard penetration test is basically a qualitative test, correct interpretation of data gives good evaluation of soil properties particularly in granular soil. The main sources of error include inadequate cleaning of borehole, eccentric hammer blow, and presence of large boulders and gravels which give erratic results.

2.7.2 Dynamic Cone Penetration Test (DCPT)

Dynamic cone penetration test is done by driving a standard 60° cone attached to a drill rod into the soil by blows of 65 kg hammer falling from a height of 750 mm. The blow count for every 30 cm penetration is made to get a continuous record of the variation of soil consistency with depth. The test does not need a borehole. It can be done quickly to cover a large area economically. The test helps to identify variability of subsoil profile and to locate soft pockets, such as filled up ponds. When DCPT is carried out close to a few boreholes, suitable correlations may be obtained for a particular site and the number of boreholes can be reduced.

The dynamic cone penetration test is done either by using a 50 cm diameter cone or a 65 mm diameter cone with circulation of bentonite slurry to eliminate friction on the drill rod. One of the proposed correlations between N_{cd} obtained from DCPT and N_{cor} obtained from SPT is

$$N_{cd} = (1.5 - 2) N_{cor} \quad (2.5)$$

These correlations can be used to obtain the SPT blow count, N from DCPT data.

2.7.3 Static Cone Penetration Test (SCPT)

The static cone penetration test (SCPT) is a direct sounding test which is done to obtain a continuous record of soil characteristics with depth and to estimate their engineering properties. The test does not need any borehole. A 60° cone having an apex angle of 60° and a base area of 10 cm^2 with a friction jacket above, is pushed into the ground at a steady rate of 20 mm/s . Modern static cone penetrometers have electrical measuring devices with wires from the transducers attached to the cone and the friction jacket giving continuous record of the cone and friction resistances as illustrated in Fig. 2.11.

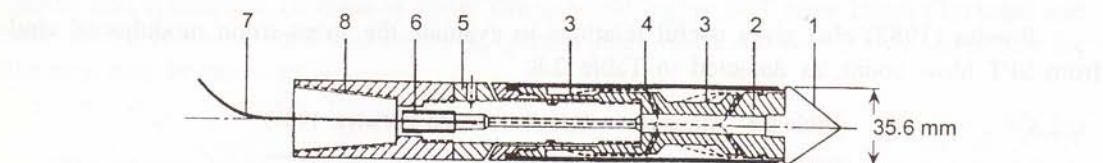


Fig. 2.11 Static cone penetrometer (electrical). 1. Conical point (10 cm^2); 2. Load cell; 3. Strain gauges; 4. Friction sleeve (150 cm^2); 5. Adjustment ring; 6. Waterproof bushing; 7. Cable; 8. connection with rods

The test measures the cone resistance, q_c , developed against the penetration of the cone and the frictional resistance, f_c developed between the sleeve and the surrounding soil as in Fig. 2.12.

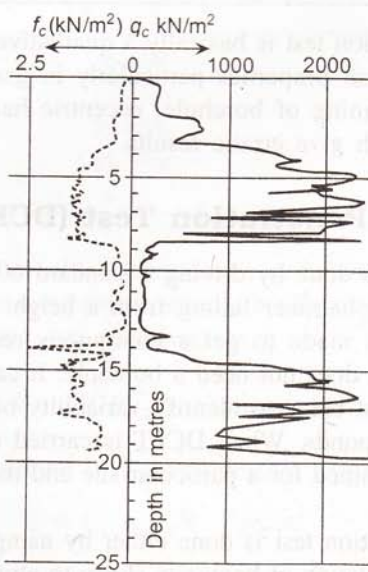


Fig. 2.12 Static cone penetrometer data.

Typical penetrometer test data give a continuous variation of the cone resistance and the frictional resistance with depth. In recent years, the static cone penetrometer has been modified to incorporate an electrical piezo-cone to give simultaneous measurement of tip resistance, side friction and the pore pressure as the cone is advanced in the soil. The development of pore pressure makes the interpretation of soil type more accurate in terms of permeability of the soil.

Lancellotta (1983) and Jamilkowski et al. (1985) proposed an empirical correlation between the relative density of normally consolidated sand, D_r and q_c ,

$$D_r(\%) = -98 + 66 \log_{10} \left(\frac{q_c}{\sqrt{\sigma'}} \right) \quad (2.6)$$

where σ' = vertical effective stress at depth considered and both q_c and σ' are in units of tonnes per sq.m.

This relationship is based on the correlation obtained from several sands as depicted in Fig. 2.13.

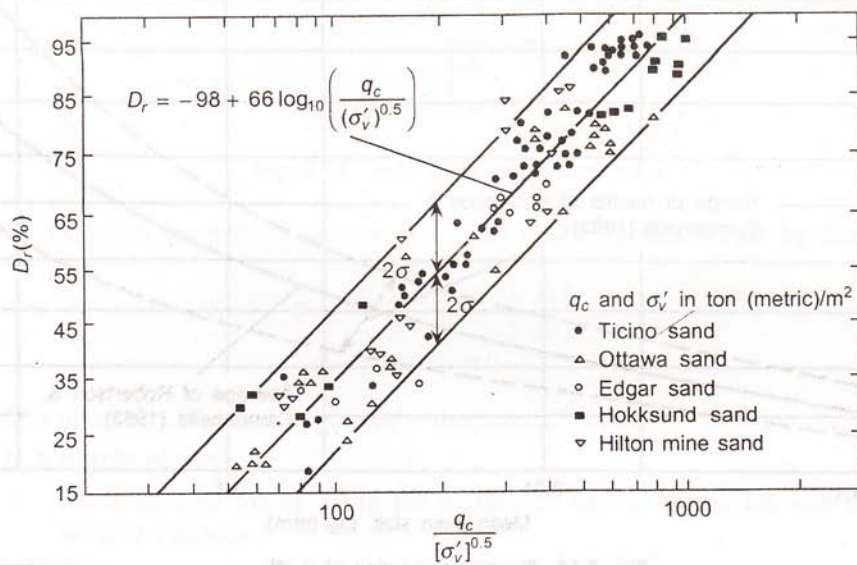


Fig. 2.13 Relationship between cone penetration resistance and relative density (after Jamilkowski et al., 1985).

The peak friction angle ϕ' of normally consolidated sand may be obtained from the expression, (Kulhawy and Mayne 1990),

$$\phi' = \tan^{-1} \left(0.1 + 0.38 \log \frac{q_c}{\sigma'_v} \right) \quad (2.7)$$

For cohesive soil, Mayne and Kemper (1988) gave the following relations for the undrained shear strength c_u , preconsolidation pressure p_c , and the overconsolidation ratio, OCR as

$$c_u = \frac{q_c - \sigma_v}{20}$$

$$p_c = 0.243 (q_c)^{0.96} \quad (2.8)$$

$$OCR = 0.37 \left(\frac{q_c - \sigma_v}{\sigma'_v} \right)^{1.01}$$

where σ_v and σ'_v are the total and effective vertical stresses at the level of test respectively.

Some useful relationship between q_c and the SPT blow count have also been obtained by Robertson and Campanella (1983). The range of variation of q_c/N_F with mean grain size D_{50} is illustrated in Fig. 2.14.

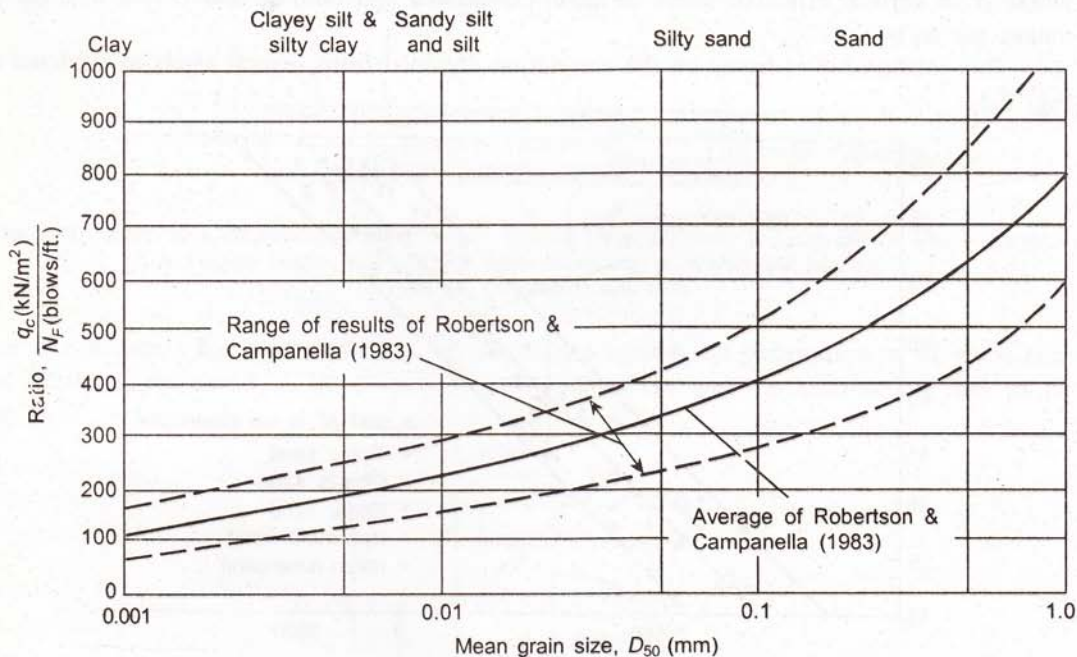


Fig. 2.14 Range of variation of q_c/N_F .

Meyerhof's (1965) simple correlation between q_c and N for fine to medium dense sand is also extensively used. This relation is expressed as

$$q_c = 4N \quad (2.9)$$

where q_c is in kg/cm^2 .

2.7.4 Vane Shear Test

Vane shear test in cohesive soils obviates the difficulty of obtaining un-disturbed samples and are particularly suitable for sensitive clays. This test facilitates "averaging" the mass characteristics of soil in-situ.

A four bladed vane at the bottom of a drill rod is pushed into the soil and a torque is applied by turning a handle at the top to create a cylindrical shear surface, as depicted in Fig. 2.15.

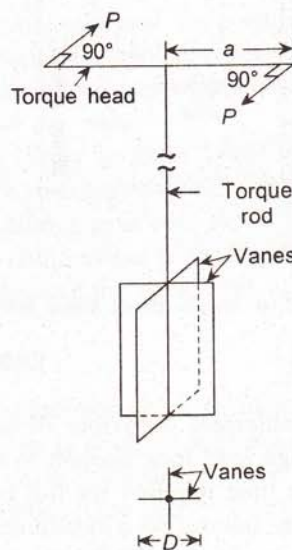


Fig. 2.15 Vane shear test arrangement.

At failure, the shear strength of the soil is related to the applied torque by the relationship

$$T = \frac{\pi D^2 H}{2} \left(1 + \frac{1}{3} \frac{D}{H} \right) \tau \quad (2.10)$$

where,

D = diameter of sheared cylinder \approx diameter of vane

H = Height of vane

τ = Shear strength acting along the surface as well as at the top and bottom of the sheared cylinder.

The assumption that the shear stress is uniformly distributed across the top and bottom is questionable but the variation due to any other assumed distribution is not great. Normally, 50 mm diameter \times 100 mm long four bladed vane is used and the vane is rotated at the rate of 0.1 degree/s. Both undisturbed and remoulded strengths can be determined by first finding the undisturbed strength and then rotating the vane fully to obtain the remoulded strength.

2.7.5 Direct Shear Test (In-Situ)

In-situ direct shear test, depicted through Fig. 2.16, is particularly suitable where tests on small specimens are not representative of the performance of the in-situ soil, e.g. fissured clays. The test has been done extensively on London clay (Bishop 1966).

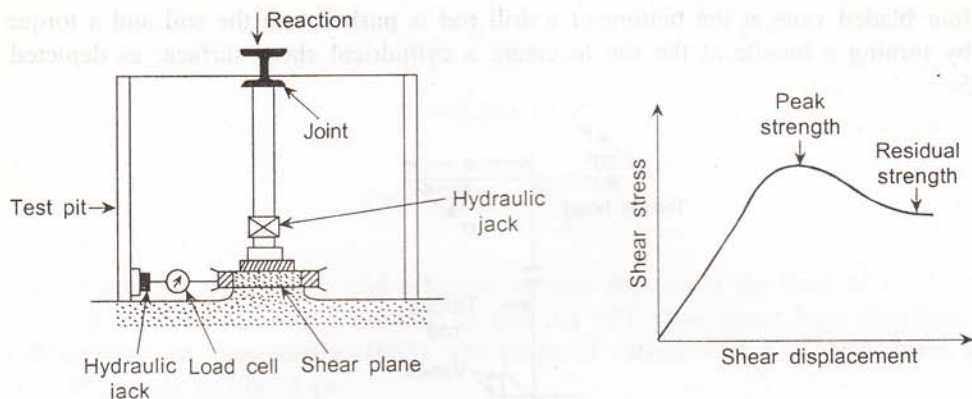


Fig. 2.16 In-situ direct shear test.

2.7.6 Plate Bearing Test

To study the bearing capacity and settlement behaviour of soils, a suitable method is to test a full scale foundation under its design load long enough to observe all settlement. However, this is rarely possible because of the time required for full consolidation and the heavy load required to produce a bearing capacity failure. As a substitute, small scale plate load tests are performed. The load can be applied by dead weight or by jacking against a reaction.

The test is carried out in a pit with either circular or square plates of width/diameter 300–750 mm. The size of the plate should be as large as possible and consistent with the capacity of the loading device. The load is increased in increments of about 1/10th of the estimated failure load or 1/5th of the proposed design load until complete bearing capacity failure or twice the design load is reached. A plot of settlement versus load intensity is then obtained as in Fig. 2.17.

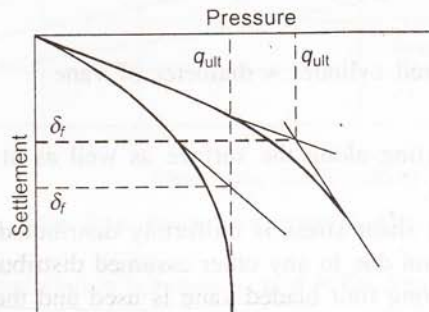


Fig. 2.17 Plate load test data.

The failure load is given by the intersection of initial and final tangent. If no well defined failure point is reached, the data are plotted on $\log \delta$ versus $\log p$ scale to obtain the point of intersection. Failure may also be taken to be the point corresponding to an arbitrarily chosen limit of settlement, depending on the requirement of the structure. Knowing the failure load and deformation characteristics from plate load test, the shear strength and modulus of elasticity of the soil may be obtained from correlation with bearing capacity and settlement equations of shallow foundations.

Limitations of load tests

The limitations of plate load test arise out of

- Extrapolation on the basis of theory of elasticity and/or empirical relation is only approximate due to non-homogeneity of the soil. Some agencies recommend the use of plates of different sizes and extrapolation for the actual foundation.
- Load test data reflect the characteristics of a soil only within a depth approximately equal to twice the width of the plate.
- Plate loading test is essentially a short term test (run in a few hours), so no indication of the long term consolidation behaviour is obtained.
- The load test data alone do not give full indication of the properties of a subsoil. But, used judiciously in conjunction with other test data, it has valuable use in design, particularly in estimating the settlement of cohesionless soil.

2.7.7 Pressuremeter Test

Menard (1956) developed the pressuremeter test to measure the strength and deformation characteristics of soil in-situ. The test is done at different depths in a borehole with the help of a pressuremeter which consists of an expandable probe with a measuring cell at the centre and two guard cells at top and bottom. One such arrangement is shown in Fig. 2.18.

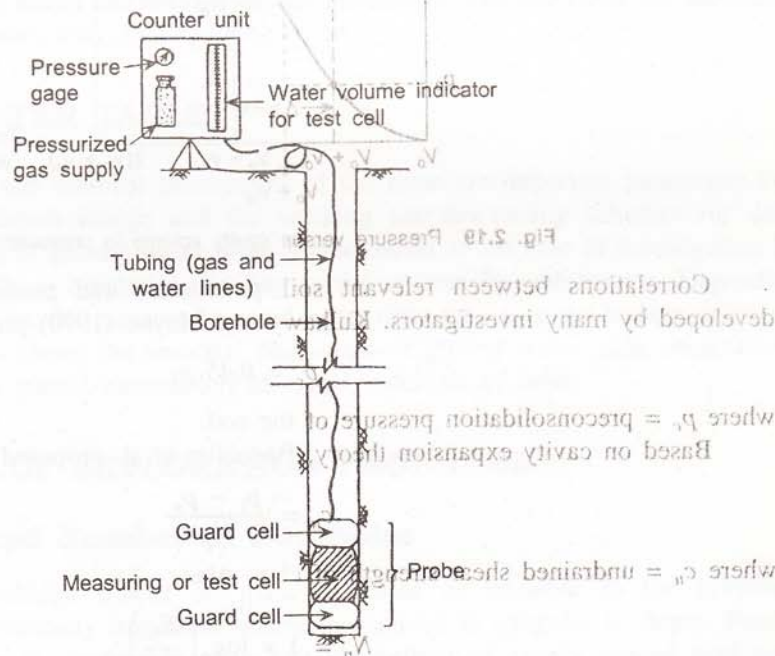


Fig. 2.18 Menard pressuremeter.

The probe is inserted in a pre-bored hole and is expanded in volume either by liquid or air pressure until the soil fails or the expanded volume of the measuring cell reaches twice the original volume of the cavity. The guard cells are used to minimise the end effect on the measuring cell. Table 2.9 gives the typical dimensions of the probe and borehole.

Table 2.9 Dimensions of pressuremeter probe and borehole

Hole designation	Diameter of probe (mm)	L_o (m)	L (m)	Borehole dia (mm)	
				Nominal	Maximum
Ax	44	36	66	46	52
Bx	58	21	42	60	66
Nx	70	25	50	72	48

Figure 2.19 shows typical results of a pressuremeter test. The expanded volume of the measuring probe is plotted against the applied pressure. The curve is divided into three zones. Zone I represents reloading of the soil during which the soil is pushed back into the initial state of stress. The pressure p_o represents the in-situ overburden pressure. Zone II represents the pseudoelastic condition when the cell volume increases linearly with the pressure and p_f defines the yield stress. Zone III gives the plastic zone, p_l representing the limit pressure which is obtained by extrapolation.

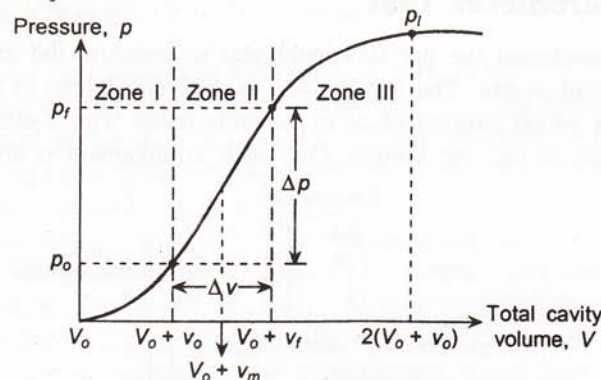


Fig. 2.19 Pressure versus cavity volume in pressuremeter test.

Correlations between relevant soil parameters and pressuremeter data have been developed by many investigators. Kulhawy and Mayne (1990) proposed the relationship,

$$p_c = 0.45 p_l \quad (2.11)$$

where p_c = preconsolidation pressure of the soil.

Based on cavity expansion theory, Baguëlim et al. proposed the relationship

$$c_u = \frac{p_l - p_o}{N_p} \quad (2.12)$$

where c_u = undrained shear strength of clay. Also,

$$N_p = 1 + \log_e \left(\frac{E_p}{c_u} \right)$$

$$\text{Here, } E_p = 2.66 \left(V_o + \frac{V_o + v_f}{2} \right) \left(\frac{p_f - p_o}{v_f - V_o} \right)$$

E_p is pressuremeter modulus (generally lies between 5 and 12).

Further innovations in in-situ testing have been achieved through the flat-plate dilatometer test (Marchetti 1980, Schmertmann 1986). This is a further development of the pressuremeter test. But these tests are rather expensive and are yet to be adopted as a part of routine soil investigation.

The remaining field tests indicated in Table 2.5 are not directly relevant to foundation design. Field pumping tests are done to obtain the in-situ permeability of the soil which is required for working out a dewatering scheme. Compaction control tests are done to control the field compaction of soil in land reclamation and embankment construction. Load test on piles, which are required to check the safe load capacity of piles will be discussed in the chapter on pile foundations.

2.8 LABORATORY TESTS

A set of routine laboratory tests are required to be done to obtain the soil parameters for foundation design. These tests are indicated in Table 2.4. Care needs to be taken in choosing the appropriate tests for a particular soil type. Classification and identification tests are normally done on representative or disturbed samples while engineering properties are to be determined from tests on undisturbed samples. Sufficient number of tests should be done for each identified stratum to assess the relevant design parameters. The procedure for laboratory tests are given in I.S. Codes and other building codes.

2.9 GROUND WATER TABLE

The ground water table and seasonal fluctuations of the same are important parameters that are necessary for foundation design and for working out dewatering schemes for deep excavations. The position of ground water table is determined at the time of investigation by observations in open wells or boreholes allowing sufficient time for stabilization. Depending on the time of investigation, the measured ground water table may give the highest or lowest position of the same. To obtain the seasonal fluctuation of ground water table observations may be made in suitably placed piezometers at regular intervals of time.

2.10 PLANNING OF EXPLORATION PROGRAMME

2.10.1 Layout and Number of Boreholes

Whenever possible boreholes should be made as close as possible to the proposed foundations. This is particularly important where the subsoil is irregular in depth. First a preliminary layout is made, preferably on a suitable pattern of evenly spaced grid with supplementary boreholes as necessary. The number of boreholes depend on local conditions and the amount of fund allotted for site investigation. One may start with the minimum number, then go for supplementary boreholes if the subsoil conditions prove irregular. A minimum of two boreholes would be required for a foundation design. Some typical layout of boreholes are shown in Fig. 2.20.

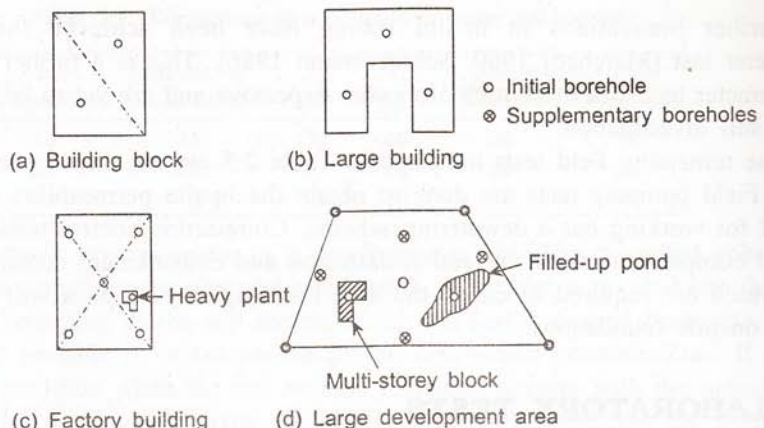
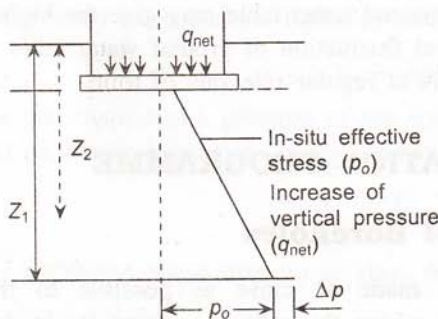


Fig. 2.20 Layout of boreholes.

2.10.2 Depth of Boreholes

Depth of boreholes is governed by the depth of soil affected by the foundation loading. It should be at least one and a half times the width of the loaded area. In case of narrow and widely spaced strip foundations, the borings may be comparatively shallow. But for large raft foundations or pile foundations, the borings have to be deep. Where foundations are extended to rock, it is necessary to prove that rock is, in fact, present at the assumed depth, so boreholes should be taken down to establish the depth to the rock surface. In general, unless hard soil bed rock is encountered at shallow depth the boring should be done to such depth that the net increase in soil pressure due to the foundation loading is less than 10% of the average foundation pressure or 10% of the vertical effective overburden pressure, as shown in Fig 2.21.



Depth of boreholes

1. Obtain depth Z_1 such that $\Delta p/p_o = 0.10$
2. Obtain depth Z_2 such that $\Delta p/q_{net} = 0.1$
3. Depth of borehole should be Z_1 or Z_2 whichever is less

Fig. 2.21 Depth of boreholes.

As a rough indication, it is worthwhile to investigate the subsoil to a depth of at least twice the width of the anticipated largest size of foundation. If pile foundation is to be considered, the depth of boring should extend well into the bearing stratum so as to obtain the soil data necessary for evaluating the tip resistance of the piles.

REFERENCES

- Bishop, A.W. (1966), Strength of Soils as Engineering Materials, *Geotechnique*, Vol. 16, pp. 89–130.
- Hatanaka, M. and A. Uchida (1996), Empirical Correlation Between Penetration Resistance and Internal Friction Angle of Sandy Soils, *Soils and Foundations*, Vol. 36, No. 4, pp. 1–10.
- Jamilkowski, M., C.C. Ladd, J.T. Germaine, and R. Lancellotta (1985), *New Developments in Field and Laboratory Testing of Soils*, Proceedings, 11th International conference on Soil Mechanics and Foundation Engineering, San Francisco, Vol. 1, pp. 57–153.
- Kulhawy, F.H. and P.W. Mayne (1990), Manual on *Estimating Soil Properties for Foundation Design*, Electric Power Research Institute, Palo Alto, California.
- Lancellotta, R. (1983), *Analisi Di Affidabilità in Ingegneria Geotecnica*, Atti Instituto Scienze Costruzioni, No. 625, Politecnico di Torino.
- Marchetti, S. (1980), *In-situ Test by Flat Dilatometer*, *Journal of Geotechnical Engineering Division*, ASCE, Vol. 106, GT3, pp. 299–321.
- Mayne, P.W. and J.B. Kemper (1988), Profiling OCR in Stiff Clays by CPT and SPT, *Geotechnical Testing Journal*, ASTM, Vol. 11, No. 2, pp. 139–147.
- Menard, L. (1956), *An Apparatus for Measuring the Strength of Soils in Place*, M.S. Thesis, University of Illinois, Urbana, Illinois, USA.
- Meyerhof, G.G. (1965), Shallow Foundations, *Journal of Soil Mechanics & Foundation Division*, ASCE, Vol. 91, No. SM 2, pp. 21–31.
- Robertson, P.K. and R.G. Campanella (1983), Interpretation of Cone Penetration Tests. Part I: Sand, *Canadian Geotechnical Journal*, Vol. 20, No. 4, pp. 718–733.
- Schmertmann, J.H. (1986), Suggested Method for Performing the Flat Dilatometer Test, *Geotechnical Testing Journal*, ASTM, Vol. 9, No. 2, pp. 93–101.
- Skempton, A.W. (1986), Standard Penetration Test Procedures and the Effect in Sands of Overburden Pressure, Relative Density, Particle-size, Aging and Over consolidation, *Geotechnique*, Vol. 36, No. 3, pp. 425–447.

3

Soil Data and Design Parameters

3.1 INTRODUCTION

The purpose of soil investigation is to provide the engineer with knowledge of the subsurface conditions at a given site for

- Safe and economic design of foundation and substructure.
- Overcoming construction problems that may be encountered at site.
- Investigation of failure/distress of engineering structures.

The extent and nature of investigation depends on the importance and type of the structure.

There should be a desired degree of interaction between the designer, the investigation agency, and the construction agency so that problems of design and construction may be identified in time and measures taken to tackle them before things get out of hand. Figure 3.1 is a schematic representation of interaction of various agencies involved in construction work.

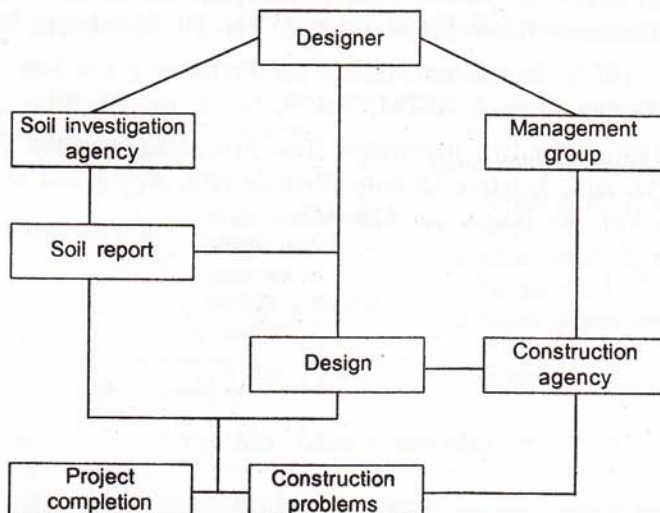


Fig. 3.1 Interaction of various agencies in construction work.

3.2 SOIL INVESTIGATION

3.2.1 Responsibility of Designer

The designer has major responsibility in ensuring proper execution of a soil investigation work. If adequate know-how is not available with the designer, he/she may engage the services of a consultant to advise him/her on all problems related to soil investigation and design.

The responsibilities of the designer in this respect may be summarized as follows:

- (a) Draw up a comprehensive programme and specification of soil exploration work relevant to the project.
- (b) Select a competent investigation agency.
- (c) Ensure that field and laboratory tests are appropriate and done with care and thoroughness.
- (d) Evaluate/interpret the soil report and select design parameters.
- (e) Make the design.
- (f) Interact with the contractor to overcome construction problems, if any.

3.2.2 Information Required from Soil Investigation

The objective of soil investigation is to obtain the following data pertaining to a given site:

- (a) Engineering geology of the area
- (b) General topography
- (c) Past history and land use pattern, if any
- (d) Soil stratification
- (e) Depth to rock, if any
- (f) Ground water and drainage
- (g) Engineering properties of different strata
- (h) Design recommendations, if the scope permits

3.2.3 Soil Test Report

A good soil test report should contain data regarding the following information:

- (a) Project and site description
- (b) Regional and site geology
- (c) Dates of field and laboratory work
- (d) Layout of structures and location of boreholes/field tests
- (e) Method of investigation
 - Field work
 - Laboratory tests
- (f) Details of field and laboratory work
- (g) Ground water characteristics
- (h) Field test data

- (i) Laboratory test data
- (j) Soil profile and stratification
- (k) Interpretation of data
- (l) Design parameters
- (m) Design recommendations, if included in the scope of work

Some of these parameters are discussed in the remaining part of this section.

Project and site description

A soil report should give some background information pertaining to the project site for the designer to work out an economic design. Such information relates to

- General level of the site with respect to adjacent area
- Problems of water logging/drainage
- Surface configuration
- Pond, rock outcrop etc.
- Adjacent buildings
- Layout and type of structure, and
- Location of borehole and field tests

A layout plan of the site showing location of proposed constructions, old structures to be demolished, if any, adjacent buildings/facilities and so on, should form an integral part of the soil report. This reveals, at a glance, the test locations in relation to the proposed structures and the problems to be encountered in making a deep excavation, close to an existing structure, for example. Such a plan also gives the information about possible weak spots in the site which may require special attention in design. A typical layout plan for a building project is shown in Fig. 3.2.

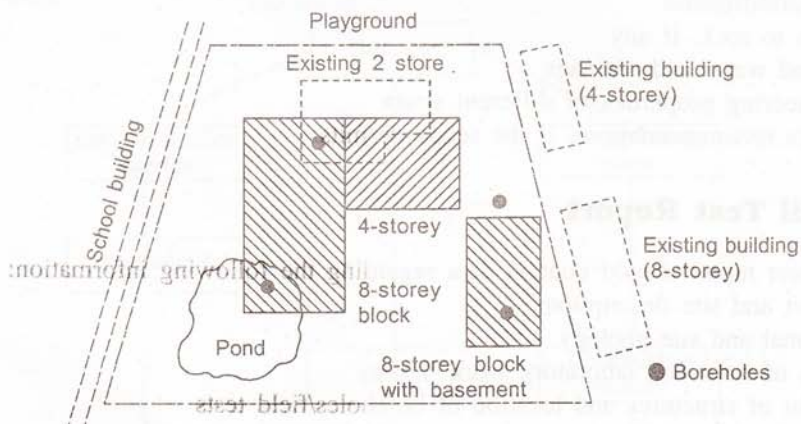


Fig. 3.2 Layout plan showing location of boreholes.

Method of investigation

Routine soil exploration is carried out through boreholes, in-situ standard penetration test within boreholes, and field tests such as static and dynamic cone penetration tests. Laboratory

tests are carried out on disturbed/undisturbed samples collected from the boreholes. For a big project, a limited number of boreholes may be supplemented by dynamic cone penetration tests which are particularly useful for determining the depth of fill, if any, through appropriate correlation with borehole data. It is, however, necessary to do at least one dynamic cone test adjacent to each borehole. The location of a filled-up pond in the HUDCO project area in Ultadanga, Calcutta was demarcated in this manner with the help of dynamic cone test, as shown in Fig. 3.3.

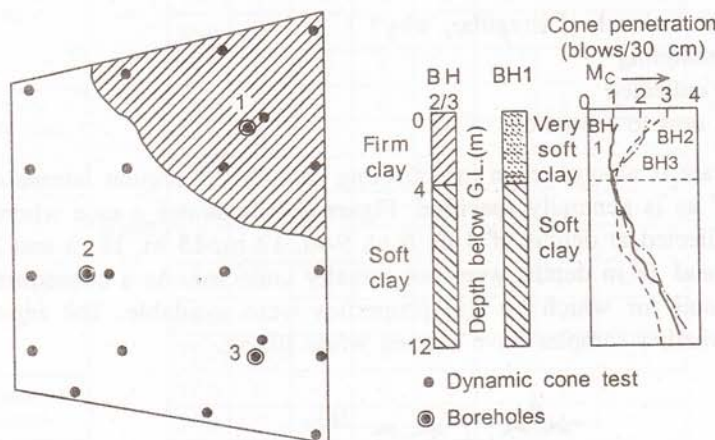


Fig. 3.3 Location of filled-up pond in HUDCO project site, Calcutta.

Date of investigation

The date of investigation is important in evaluating the fluctuation of ground water table (G.W.T.) at a given site. If there is seasonal fluctuation in water table, measurement at the time of investigation does not necessarily give the highest or lowest position of G.W.T. In case investigation is done in the dry season, local enquiry should be made about seasonal fluctuation for proper evaluation of G.W.T. The date of investigation becomes important in such an evaluation.

Boring and sampling

The method of boring adopted at a given site should be given due importance in evaluating the soil data. The report should clearly specify the technique—shell and auger, wash boring, or bentonite mud drilling—that has been used to make the boreholes. Also, the use of casing or chiselling done, should be clearly indicated in the report.

Sampling is an important aspect of soil investigation. The quality of samples determine the reliability or otherwise of the laboratory test data. The relevant data on sample and sample collection are:

- (i) Type of sampler used
 - open drive sampler/piston sampler

- (ii) *Size of samplers*
 - length and diameter
 - area ratio
- (iii) *Method of advancing sampler*
 - pushing or driving
- (iv) *Schedule of sampling*
 - disturbed
 - undisturbed
 - regular interval; if irregular, why?
- (v) *Date of sampling*
 - when collected
 - when sent to laboratory

Not much care is always taken in collecting samples 'at regular intervals of depth or at changes of strata' as is generally specified. Figure 3.4 illustrates a case where samples were required to be collected at depths of 3 m, 6 m, 9 m, 12 m, 15 m, 18 m and 21 m but those from 6 m, 15 m and 18 m depths were not actually collected. As a consequence, there were some depths of soil for which no soil properties were available. The report should also clearly indicate whether samples have slipped while lifting.

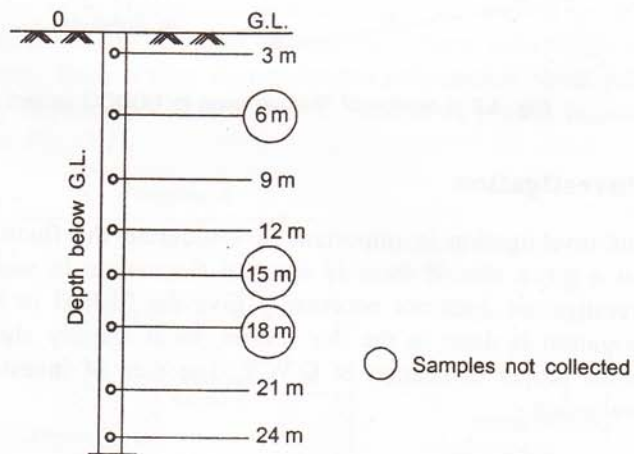


Fig. 3.4 Collection of undisturbed samples.

Testing

Laboratory tests on disturbed/undisturbed samples are done for the purpose of classification of strata and also for determination of their engineering properties. The schedule of tests should be drawn up with care, reflecting the soil type, and the nature of problem to be solved. This should better be done in consultation with the designer to avoid a random choice of the type of test from the schedule of tests given in the bill of quantities. Figure 3.5 gives a schedule of tests on samples from different strata of normal Calcutta deposit. The types of

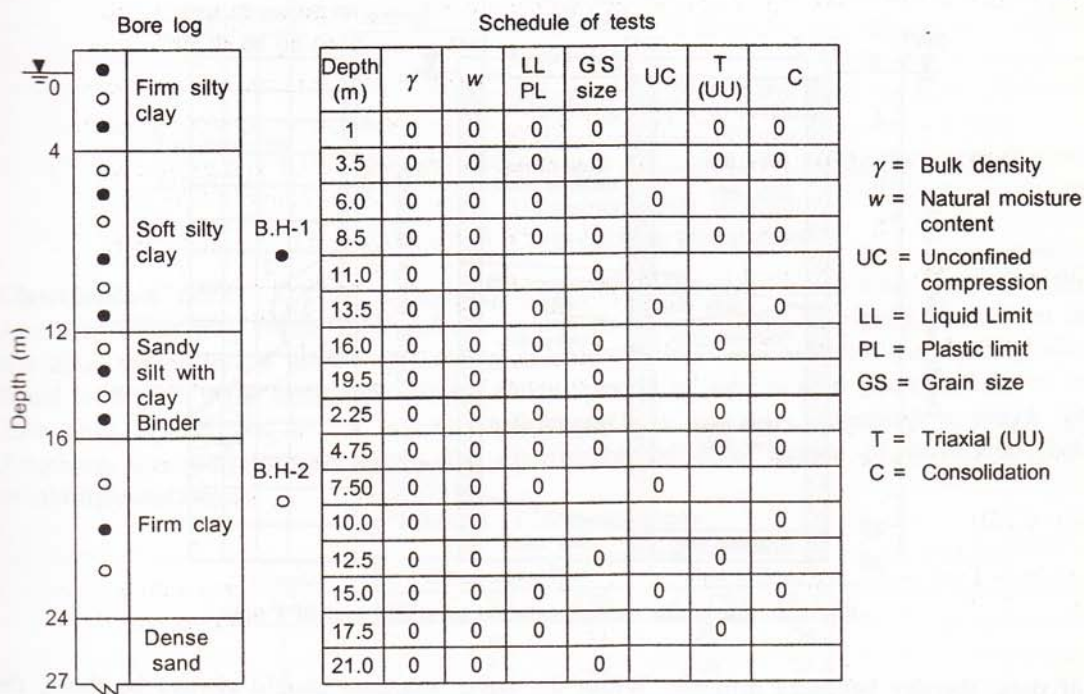


Fig. 3.5 Schedule of laboratory tests.

tests should be so chosen as to give the properties of all the strata relevant for design. One should avoid going for unconfined compression test in a predominantly silty soil.

Similarly, consolidation tests are required for cohesive strata only. For sandy strata, one has to rely more on field tests, such as SPT. Even undisturbed samples in sand do not provide much help.

Soil profile

Soil profiles should be drawn through a number of boreholes, if not through all of them, to give the subsoil stratification along a chosen alignment. Such soil profiles drawn for a number of carefully chosen alignments give a comprehensive picture of the variation of soil strata, throughout the site. Plotting separately for individual boreholes does not give the true picture at a glance. Therefore, the best way is to plot the soil profile on a desired alignment with respect to the variation of N value with depth. The relative consistency of different strata emerges clearly from such a diagram, as depicted through Fig. 3.6.

The position of ground water table at the time of investigation should be clearly indicated in the soil profile. Design of foundations should take appropriate note of any seasonal fluctuation in ground water table.

Laboratory test data

The laboratory test data are given in different forms in the soil test report. The interpretation

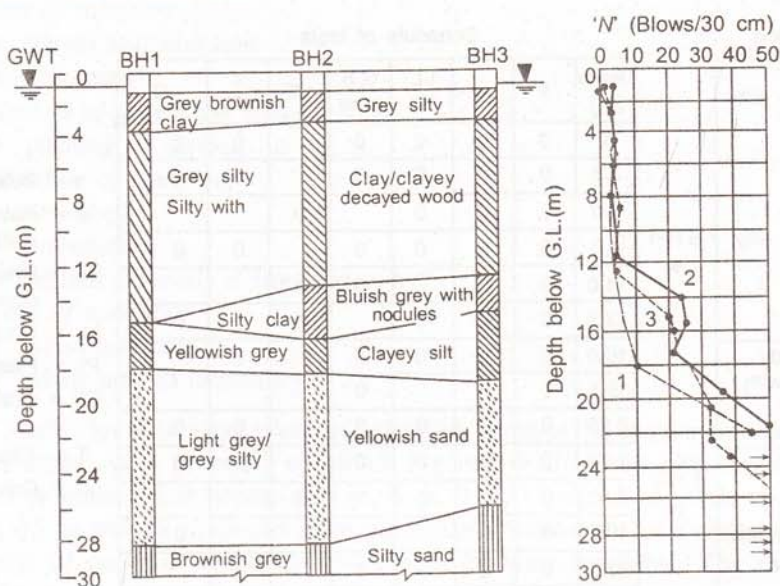


Fig. 3.6 Soil profile through selected boreholes and SPT data.

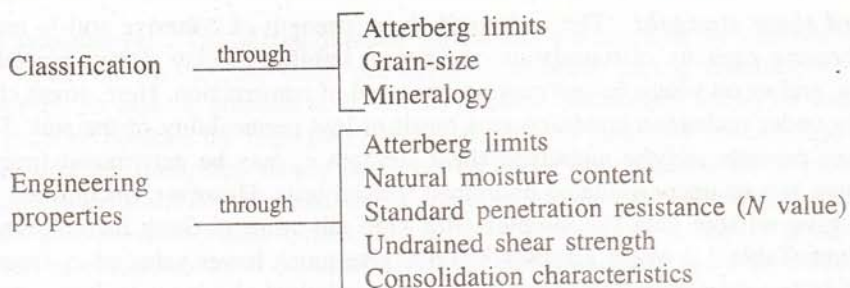
of data, thereby becomes difficult. While the basic test data should always be there, the engineer should be in a position to make proper assessment of the engineering properties of different strata to be used for design.

The basic test data may be summarized under the following categories for each major stratum of a subsoil deposit:

- Classification data*
 - Bulk density
 - Natural moisture content
 - Atterberg limits
 - Grain-size distribution
- Engineering properties*
 - Shear strength parameters
 - Permeability
 - Consolidation test data: m_v , C_c , C_v
 - Compaction characteristics
- Chemical and mineralogical data*
- Chemical test on water samples*

Data interpretation

The consistency data should be established before choosing the design parameters for a given problem. Further, the reliability of data and their consistency may be studied qualitatively from the results of individual tests. For example,



Classification tests: A close examination of the grain-size distribution data and the Atterberg limits may reveal inconsistency in test results. In Table 3.1 which gives a set of test data, sample no. 4 with clay fraction of only 8% indicates a highly plastic clay with liquid limit 62% while sample no. 5 with a clay fraction as high as 48% has a liquid limit of 35% only. These data do not inspire confidence. It is necessary, therefore to check the Atterberg limits against the grain-size distribution of each sample to determine their reliability/consistency.

Table 3.1 Classification tests

Sample no.	Grain-size (%)			Atterberg limits	
	Sand	Silt	Clay	LL (%)	PL (%)
1	7	60	33	58	26.4
2	2	53	45	76	28.2
3	16	65	19	39	24.0
4	20	72	8	62	30.2
5	6	46	48	35	25.0

Consistency: The variation of Atterberg limits and natural moisture content with depth gives a clear indication of the relative consistency of different strata. A natural moisture content close to the plastic limit and a high bulk density confirms a firm to stiff clay whereas a natural moisture content approaching liquid limit should generally give a lower unit weight and thus, indicates a soft normally consolidated soil, Fig. 3.7.

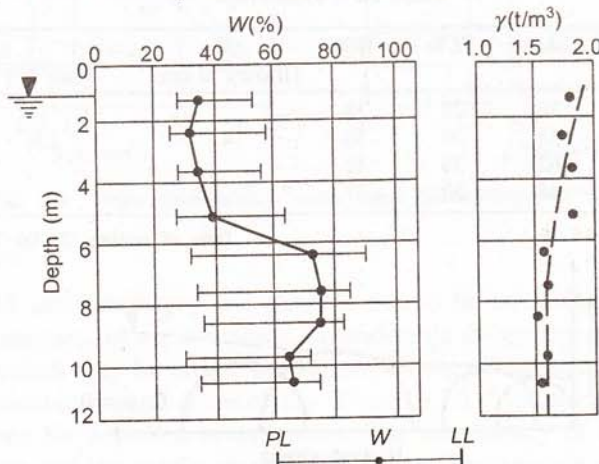


Fig. 3.7 Variation of natural moisture content and Atterberg limits with depth.

Undrained shear strength: The undrained shear strength of cohesive soil is required for to analyze bearing capacity of foundation, short-term stability of clay slopes, braced excavation, tunnelling, and so on where failure may occur at end of construction. Here, stress changes occur essentially under undrained condition as a result of low permeability of the soil. The condition $\phi_u = 0$ then prevails and the undrained shear strength c_u may be determined from unconfined compression test or unconsolidated undrained triaxial tests. However, unconfined compression does not give reliable data for samples with high silt content. Such inconsistent results are evident from Table 3.2 where samples 3 and 4 give much lower value of c_u from unconfined compression test than from UU triaxial test due to relatively high sand/silt content.

Table 3.2 Undrained shear strength

Sample no.	Grain-size (%)			c_u (t/m ²)	
	Sand	Silt	Clay	UC test	UU test
1	7	60	33	3.2	4.6
2	2	53	45	2.3	2.5
3	16	65	19	3.4	7.3
4	20	72	8	2.8	5.6

Time effect is an important parameter in evaluating the undrained shear strength of cohesive soils. Samples not preserved properly after sampling lose moisture content by evaporation and give higher strength from laboratory tests. Table 3.3 gives the typical data for samples tested after $2\frac{1}{2}$ months without proper preservation. The c_u values obtained from laboratory tests give much higher strength than in-situ vane shear test carried out during boring and sampling. Also, the Mohr envelopes obtained from UU triaxial tests are often shown to give a ϕ value for saturated cohesive soil. This is not theoretically permissible. If such results are obtained, the degree of saturation of the samples should be checked. Also, the friction in the loading piston if not eliminated properly may give misleading results. Figure 3.8 shows typical Mohr's circles from UU triaxial tests. In such situation it would be more appropriate to obtain an average c_u value for the sample (with $\phi = 0$) rather than trying to draw an envelope giving both C and ϕ .

Table 3.3 Time effect

Sample no.	Depth	LL%	PL%	W%	N (Blows/30 cm)	c_u (t/m ²)
					Vane test	Lab. test
1	6	76	28	38		4.2
2	8.5	58	26	36	4	2.6
3	10.5	62	30	42		4.5
4	14.0	48	30	37		4.9

Date of sampling: 05 04 76

Date of testing: 25 06 76

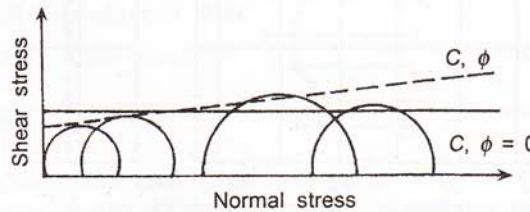


Fig. 3.8 UU triaxial test: Mohr's circles.

Effective stress parameters: The effective stress parameters are required for analysis of long term stability when all the excess pore pressures developed during construction have dissipated. However, in case of granular soils, effective stress parameters are to be used even for short-term stability because the high permeability of the soil generally ensures that all the excess pore-pressure get dissipated during construction itself. The effective shear parameters of a soil are determined from consolidated drained triaxial test or the consolidated undrained triaxial test with pore-pressure measurement. The latter is particularly useful in problems of stage construction of embankment where stability of the embankment is to be investigated for undrained loading after each stage of construction (Gangopadhyay and Som, 1974). The pore-pressure parameter A is also required for such an analysis.

For partially saturated soils and for soils with high silt content where partial drainage may occur even during load application, the total stress parameters of soil (c_u and ϕ_u) may have to be evaluated for stability analysis.

Consolidation: Consolidation tests are often done for pre-determined pressure ranges without any reference to the depth of the samples. In particular, if the sample is derived from deeper strata or it appears overconsolidated, the virgin compression curve has to be determined by loading the sample to sufficiently high pressures for establishing the field compression curve. Only then is it possible to determine if a soil is normally consolidated or preconsolidated. In the latter case, the C_c value in the overconsolidation range and the preconsolidation pressure are important in selecting the design parameters. Moreover, calculating the m_v value for different stress ranges from the laboratory curve may not represent the field behaviour correctly because of sampling disturbances. It would be more appropriate to obtain the virgin curves from the test data—using Schmertmann's procedure, as shown in Fig. 3.9.

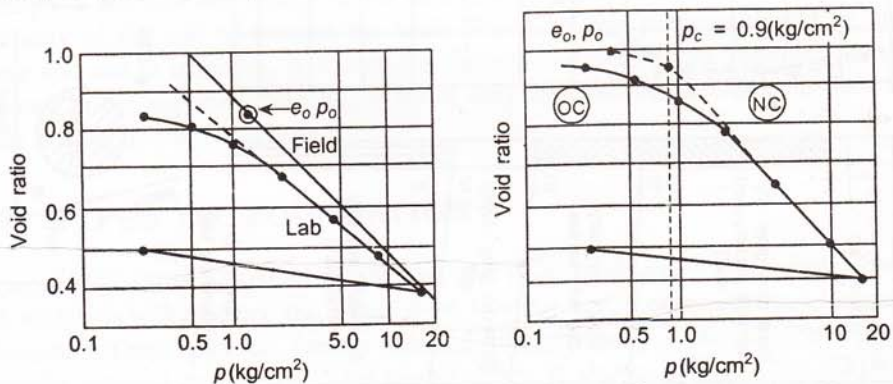


Fig. 3.9 Virgin consolidation curve (after Schmertmann 1953).

Design parameters

On the basis of field and laboratory test data, it should be possible to assign appropriate values of design parameters for each stratum. Considerable judgement is required to evaluate the data. Individual values may be erratic for various reasons described earlier. But an overall assessment for a particular stratum is necessary. Figure 3.10 gives the results of a controlled exploration programme for a failure investigation. The consistency of data becomes evident from such presentation and the results inspire confidence. The average engineering properties of each stratum can thus, be obtained without much difficulty.

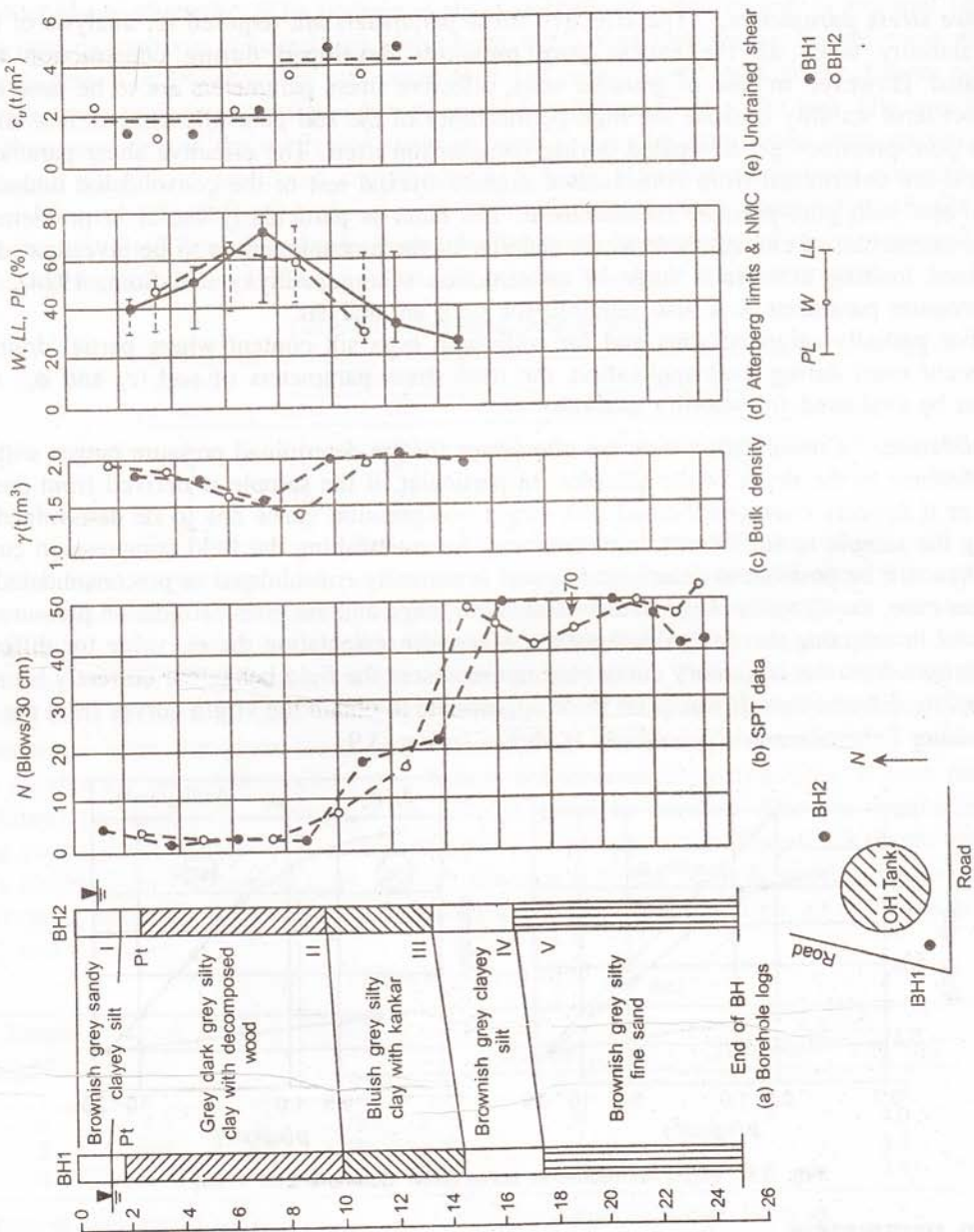


Fig. 3.10 Soil profile and test data for a failure investigation.

REFERENCE

Gangopadhyay, C.R. and N.N. Som (1974), *An Approach to $\phi_u = 0$ Analysis for Stage Construction*, Proceedings ASCE, Vol. 100, GT6, pp. 699–703.

4

Foundations: Types and Design Criteria

4.1 INTRODUCTION

Foundation is that part of a structure which provides support to the structure and the loads coming from it. Thus, foundation means the soil or rock that ultimately supports the load and any part of the structure which serves to transmit the load into the soil. The design of foundation for a structure, therefore involves the following:

1. Evaluation of the capacity of the soil to support the loads and
2. Designing proper structural elements to transmit the super structure load into the soil.

Often the term *foundation* describes only the structural elements but this definition is incomplete, because the ability of the structural element to transmit the load is limited by the capability of the soil to support the load. Therefore, the problem should be considered as a whole and not in isolation. A foundation failure may destroy the superstructure as well while a failure in the superstructure might result only in localized damage and does not essentially mean failure of the foundation.

4.2 TYPES OF FOUNDATION

Foundations can be classified as shallow and deep foundations depending upon the depth of soil which is affected by the foundation loading and, consequently, affect the foundation behaviour. These can be further divided into different types of foundations which are normally adopted in practice. This classification is shown in Fig. 4.1.

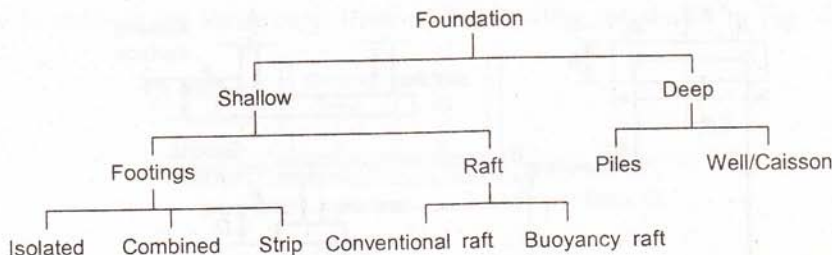


Fig. 4.1 Types of foundation.

4.2.1 Shallow Foundations

In shallow foundations, the load is transmitted to the soil lying immediately below the substructure, as shown in Fig. 4.2. Such foundations are used when the subsoil near the ground surface has adequate strength to support the load.

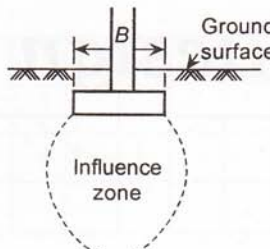


Fig. 4.2 Shallow foundation.

Footings

Isolated footing: Isolated footings are provided to support the columns of a building frame individually. Figure 4.3 depicts an isolated footing. Such footings behave independently of each other without being influenced by adjacent footings in any way.

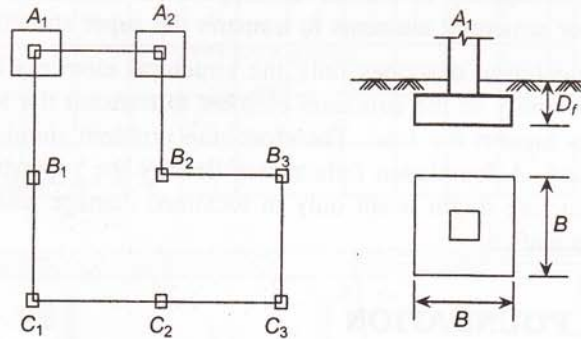


Fig. 4.3 Isolated footing.

Combined footing: Combined footings are designed to support two or more adjacent columns in a building frame where isolated footings either overlap or come very close to one another (refer Fig. 4.4).

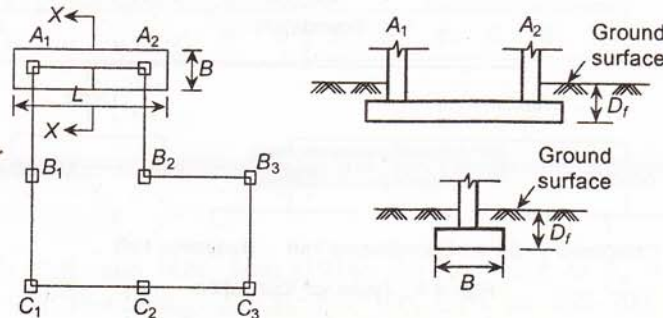


Fig. 4.4 Combined footing.

Strip footing: Strip footings support a load bearing wall or a number of closely spaced columns in a row. They form a long, narrow continuous foundation, with the width small compared to the length, as illustrated in Fig. 4.5.

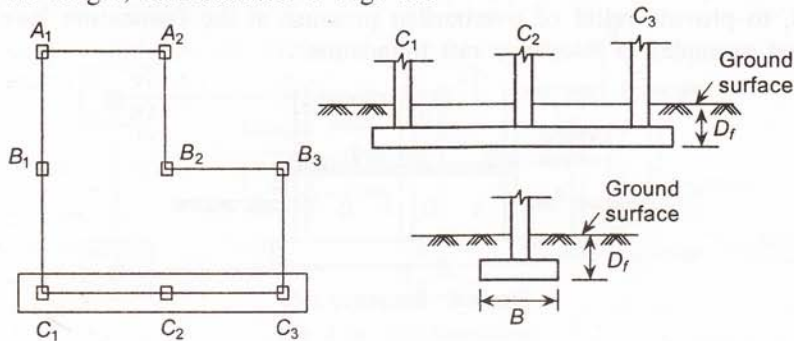


Fig. 4.5 Strip footing.

Raft or mat foundation

A large number of columns or often, the entire structure is founded on one single slab or raft. When individual column footings are, together, found to occupy more than 70% of the plan area of the building, raft foundations are provided. This is shown in Fig. 4.6. The basic difference between footings and rafts lies in their size—the latter being much larger and affecting a greater area of the soil in determining its behaviour.

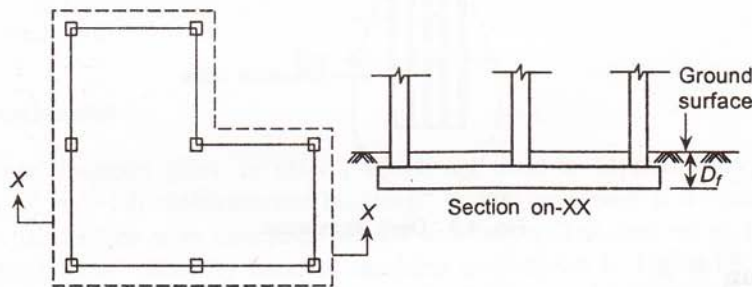


Fig. 4.6 Raft foundation.

Conventional raft: Conventional rafts are provided at shallow depth beneath the ground surface and backfilling is done on the raft to reach the original ground surface. Thereafter plinth filling is done to lay the ground floor of the building, as shown in Fig. 4.7.

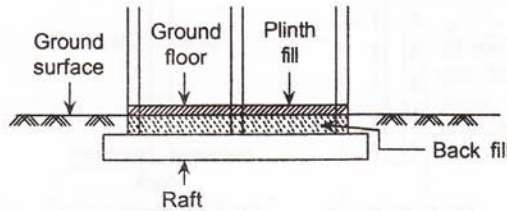


Fig. 4.7 Conventional raft.

Buoyancy raft: Buoyancy rafts are placed at some depth beneath the ground surface but no backfilling is done on the raft. A ground floor slab is provided at the desired height above the ground and the space between the ground floor slab and the foundation raft is kept void, refer Fig. 4.8, to provide relief of overburden pressure at the foundation level. Basement rafts are typical examples of buoyancy raft foundation.

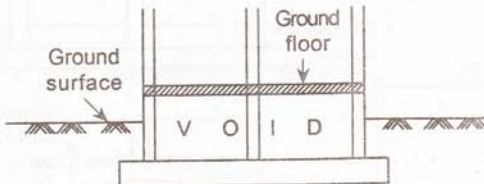


Fig. 4.8 Buoyancy raft.

4.2.2 Deep Foundations

In deep foundations, the load is transmitted well below the bottom of the substructure, as shown in Fig. 4.9. Deep foundations are provided when soil immediately below the structure does not have adequate bearing capacity but the soil at deeper strata have.

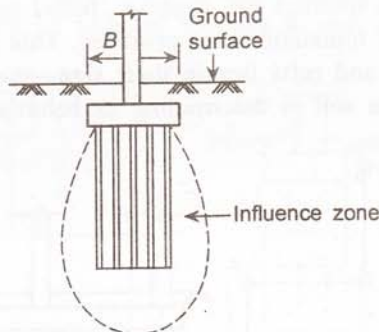


Fig. 4.9 Deep foundation.

Pile foundation

Piles transfer the load through soft upper strata either by end bearing on hard stratum or by friction between the soil and the pile shaft and are accordingly called end bearing piles or friction piles, Fig. 4.10.

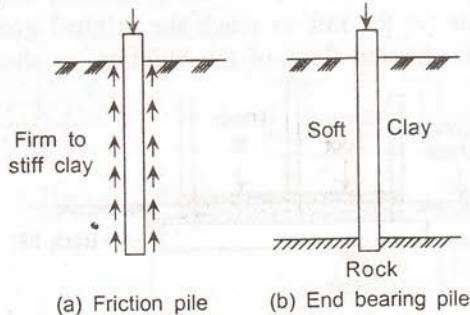


Fig. 4.10 Pile foundations.

Usually a column load is supported on a group of piles through a pile cap, as shown in Fig. 4.11. Rafts and piles are sometimes combined to form a piled raft illustrated in Fig. 4.12.

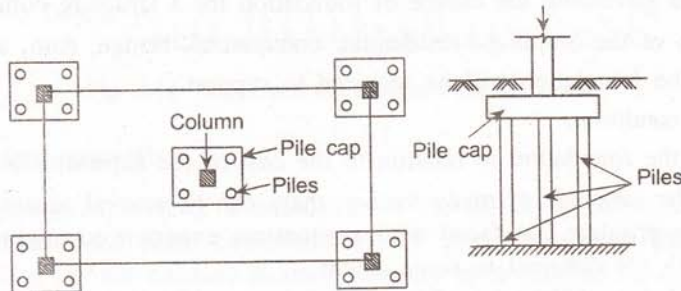


Fig. 4.11 Pile foundation.

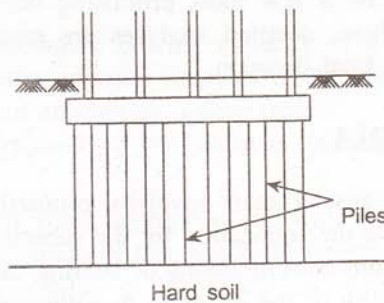


Fig. 4.12 Piled raft.

Piers and caissons

These are large diameter piles, in effect, which are used to support heavy structural load from bridges or very tall multistoreyed buildings. A pier or a well is a shaft drilled into the soil which is then filled with concrete, gravel, and so on. The bottom of the shaft may be undercut or belled out, either by hand or machine as depicted in Fig. 4.13 to afford a large bearing area. Wells are rigid structural elements and can take large lateral forces while piles are slender and liable to bend under flexural stress. Caissons are large diameter wells which are installed by special construction technique.

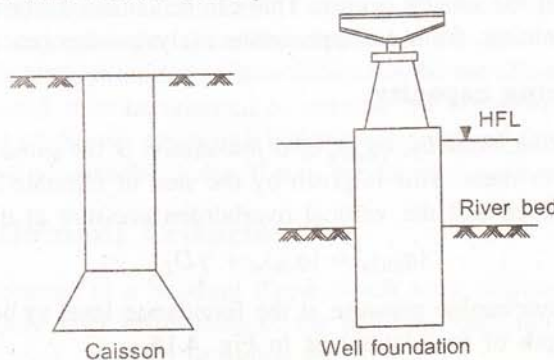


Fig. 4.13 Caisson and well foundation.

4.2.3 Choice of Foundation Type

The main criteria governing the choice of foundation for a structure comprise

- Function of the building—residential, commercial, bridge, dam, and so on.
- Loads, the foundation will be required to support.
- Subsoil condition.
- Cost of the foundation in relation to the cost of the superstructure.

On account of the interplay of many factors, there can be several acceptable solutions to a given foundation problem but faced with a situation, experienced engineers may arrive at conclusions which are different to some extent.

Often the choice of the type of foundation is arrived at by the process of elimination. An experienced engineer first discards, almost instinctively, the most unsuitable types of foundation and concentrates on a few most promising ones. When the choice has been narrowed down to two or three, detailed analyses are made and their relative economy studied before arriving at the final decision.

4.3 DESIGN CRITERIA

The design of foundation for any structure involves, primarily the determination of the net permissible bearing pressure on the foundation for the subsoil prevailing at the building site. This should be determined from considerations of bearing capacity, the magnitude and the rate of settlement, and the ability of the structure to withstand settlement. Foundations for a building should, therefore satisfy the following design criteria:

- There must be adequate factor of safety against bearing capacity failure, and
- The settlement of the foundation must be within permissible limits.

4.3.1 Bearing Capacity

Net ultimate bearing capacity

The *net ultimate bearing capacity*, $(q_{ult})_n$ of a foundation is the applied pressure at which complete shear failure of the subsoil occurs. This can be obtained, for a given foundation and for a given subsoil condition, from an appropriate analysis—theoretical or empirical.

Gross ultimate bearing capacity

The *gross ultimate bearing capacity*, $(q_{ult})_g$ of a foundation is the gross foundation pressure at which the subsoil fails in shear. This is given by the sum of ultimate bearing capacity of the soil at the depth considered and the vertical overburden pressure at that depth. Therefore,

$$(q_{ult})_g = (q_{ult})_n + \gamma D_f \quad (4.1)$$

where γD_f is the total overburden pressure at the foundation level (γ being the unit weight of the soil and D_f , the depth of foundation) as in Fig. 4.14.

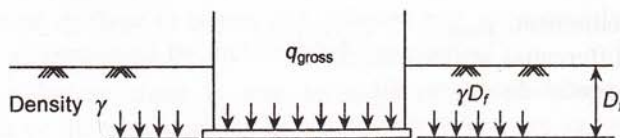


Fig. 4.14 Gross and net ultimate bearing capacity.

Allowable bearing capacity

The *allowable bearing capacity* of a foundation is the maximum allowable net pressure on the foundation determined from considerations of shear failure of the ground. This is obtained by dividing the net ultimate bearing capacity by a suitable factor of safety, that is,

$$q_{\text{all}} = \frac{(q_{\text{ult}})_n}{F}$$

where, F = factor of safety.

The determination of allowable bearing capacity of a foundation from shear failure consideration involves a bearing capacity analysis of the foundation with the relevant soil properties and the choice of an appropriate safety factor.

A factor of safety is applied on the ultimate bearing capacity of a foundation to safeguard against:

- (i) natural variation in the shear strength of the soil.
- (ii) uncertainties in the accuracy of test results to determine shear strength.
- (iii) uncertainties in the reliability of theoretical and empirical methods of determining bearing capacity.
- (iv) excessive yielding of the foundation when the soil approaches shear failure.

Of the above, natural variation in subsoil properties and uncertainty about the accuracy of test results are the primary reasons for requiring an adequate factor of safety in determining the allowable bearing capacity of a foundation. Subsoil properties at a site by their very nature, are heterogeneous and there is usually wide variation of test results. Therefore, a high degree of judgement is required in selecting the shear strength parameters for design. Any general guidance in this regard is neither possible nor always desirable, but a safety factor of 2.5–3.0 may be adopted to guard against the variations and uncertainties listed above. Lower factor of safety, say, 2.0 may be adopted for a temporary construction or on sites where subsoil condition is well known and uniform. Lowering the factor of safety even further may lead to local yielding and excessive shear deformation of the soil.

The first step in a foundation design is to determine the net allowable bearing capacity, as described above. It would, then be required to estimate the settlement of the foundation for a bearing pressure equal to the net allowable bearing capacity and then to see if the estimated settlement is within the permissible limits. If not, the foundation is to be redesigned.

4.3.2 The Settlement Criteria

Let us consider the columns in a building frame which were originally at the same level but have settled differentially after application of the building load, illustrated in Fig. 4.15. The different settlement criteria can then be stated as:

- (a) Maximum settlement, ρ_{\max}
- (b) Maximum differential settlement, Δ
- (c) Maximum angular distortion, δ/l

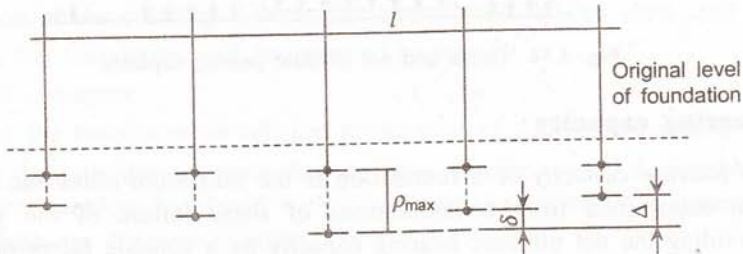


Fig. 4.15 Settlement of foundation and settlement criteria.

All these criteria can be evaluated from an adequate settlement analysis of the foundation. However, it is obvious that mere prediction of settlement is only of limited practical value unless some idea about how much settlement the building is going to tolerate without suffering damage, is obtained. If a building frame settles uniformly over its area, no matter by whatever amount, it has no adverse effect on the behaviour of its structural components. Maximum settlement is important in relation to access and services of the building and is generally of not much significance when it is within reasonable limits. Damage to structural components may, however, occur if there is excessive differential settlement.

Damages due to differential settlement may be classified under the following categories (Skempton and McDonald 1955),

- (i) Structural damage involving frame members, namely, beams, columns, and their joints.
- (ii) Architectural damage involving the walls, floors, and finishes.
- (iii) Combined structural and architectural damage, and
- (iv) Visual effects.

Structural damage: Building frames are generally designed to achieve uniform settlement. Since differential settlement occurs in most cases, secondary stresses are induced in the members of the framed structure, the evaluation of which is yet to become a standard practice, although with the advent of numerical analysis using computers, it is now possible to undertake theoretical analysis of complicated building frames for different conditions of total and differential settlement.

In steel frames, local failure may be prevented by yielding of the joints, provided mild steel is used because the relative rotation required to cause fracture is in most cases greater than that which can occur. However, with increasing use of welding in recent years, secondary stresses are of greater importance since yielding of welded connections would result in rupture and failure.

Architectural damage: This refers to cracks in the walls, floors, and finishes which is apparently a more immediate effect of differential settlement than the overstressing of structural members. Excessive cracking may cause damage to the functional aspects of the building. For example, major cracks are considered detrimental to hospital buildings, cold storage, and the like. Hence, in most cases, the cracks or the architectural damages are the guiding factor in determining the allowable settlement of buildings.

Combined architectural and structural damage: Usually, architectural damage occurs long before there is structural damage in beams and columns and consequently a structural damage is almost invariably accompanied by architectural damage.

Visual effect: Even before there is any architectural or structural damage, excessive differential settlement or tilt which can be recognised by naked eye cannot be accepted either psychologically or aesthetically.

Allowable settlement

The allowable settlement of a building can be determined from an integrated analysis of the building frame for given magnitudes of settlement. This is, however, laborious and time consuming and has to be done separately for each building. Therefore, attempts have been made to estimate the allowable settlement from statistical correlation between damage and settlement criteria.

The allowable settlement of buildings depends upon the type of construction, the type of foundation, and the nature of soil (sand or clay). The angular distortion appears to be the more useful criterion for establishing the allowable limits. Terzaghi (1938) studied the settlement pattern of a number of brick walls in Vienna. He found that the walls reached their ultimate strength when the angular distortion was 1/285 and concluded that an average settlement of 5–7.5 cm would be considered normal.

Skempton and McDonald (1955) derived a statistical correlation between damage and settlement of 98 buildings from different parts of the world and concluded that an angular distortion of 1/300 should be considered the allowable limit for conventional buildings. Jappeli (1965) observed the damages to a three-storeyed building on clay due to differential settlement and confirmed that an angular distortion of greater than 1/300 would lead to severe damages in walls of ordinary buildings. Whitman and Lambe (1964), on the other hand, studied the settlement pattern of buildings in MIT Campus and observed that an angular distortion of as little as 1/800 was sufficient to cause cracks in bricks and masonry elements. Mackinley (1964) made a study of more than fifteen structures damaged by settlement. He observed that there was no simple rule to define the tolerance of structures to settlement. A cement silo had collapsed in New York after only 5 cm of differential settlement whereas some public buildings in Mexico City had been in use even after differential settlement of more than 10 cm.

Rethati (1961) carried out an investigation of twelve buildings on fill. This time, the rigidity of the structure as represented by the number of storeys was also considered. While the critical angular distortion of 1/300 agreed well with those proposed by Skempton and McDonald, it was found that 91% of the buildings that suffered structural damage were two storeys or lower. Hence, the author concluded, the critical angular distortion should be related to the rigidity of the building. Some further studies on allowable settlement have been made by Feld (1964) and Grant et al. (1974).

While much work still remains to be done on the subject to recommend some readily acceptable values of allowable settlement, it seems there is a common agreement that an angular distortion of more than 1/300 may lead to damages in conventional load bearing wall and framed construction. There is, as yet, no agreed guideline as regards the allowable maximum settlement of a building. Skempton and McDonald (1955) have proposed some tentative damage limits which are shown in Table 4.1.

Table 4.1 Damage limits for load bearing walls in traditional type framed buildings

	<i>Isolated foundation</i>	<i>Raft foundation</i>
Sand	5 cm	5–7.5 cm
Clay	7.5 cm	10–12.5 cm

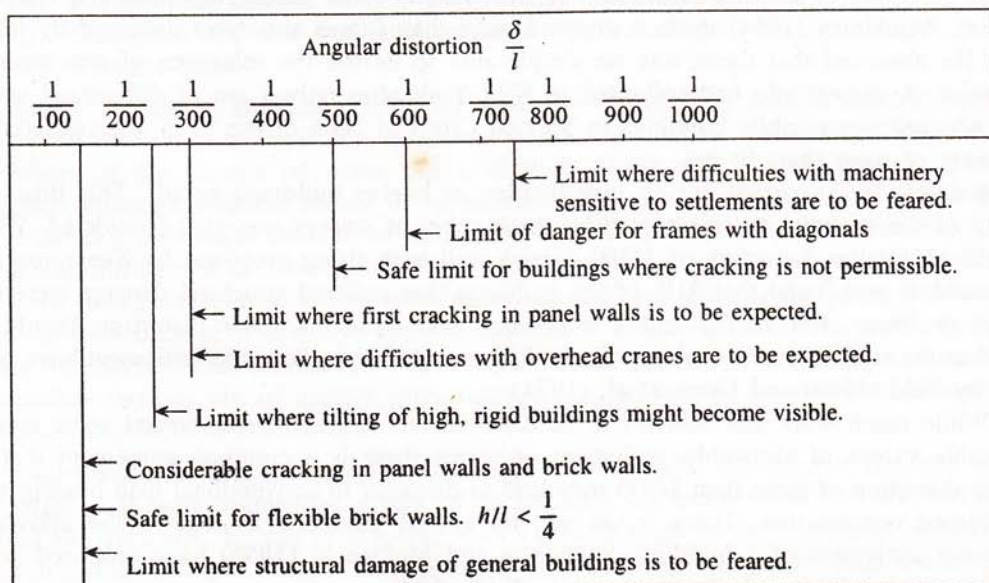
Indian Standard Code of Practice (IS 1904-1986) recommends the following (Table 4.2) permissible total settlement for RCC framed buildings on different types of foundation.

Table 4.2 Permissible settlement (IS 1904–1986)

	ρ_{\max}	Isolated footings		Raft foundation	
		Sand/hard clay	Plastic clay	Sand/hard clay	Plastic clay
Steel structure	$\delta/1$	50 1/300	50 1/300	75 1/300	1/300
RCC structure	ρ_{\max} $\delta/1$	50 1/666	75 1/666	75 1/500	100 1/500
Multistorey buildings	ρ_{\max}	60	75	75	125
RCC/steel framed Bldg.	$\delta/1$	1/500	1/500	1/400	1/300

An allowable limit of angular distortion of 1/300 has been proposed for framed buildings of both traditional and modern construction. This may not eliminate the chances of cracks in walls and floors altogether, but structural damage would, by and large, be eliminated. Bjerrum (1963) has given the damages limits for different performance criteria, which are shown in Table 4.3. To eliminate cracks in a building, the angular distortion should be less than 1/500.

Table 4.3 Damage limits of angular distortion for different settlement criteria



Net permissible bearing pressure

The net permissible bearing pressure on a foundation is to be determined from considerations of safe bearing capacity and permissible settlement, so as to satisfy both design criteria. Starting with the net allowable bearing capacity, if the estimated settlement appears to go beyond the permissible limits, the bearing pressure should be correspondingly reduced until the criterion of allowable settlement is also satisfied although this may mean a higher factor of safety against bearing capacity failure. For soft clays, in general, the settlement criterion governs the choice of net permissible bearing pressure. This is particularly so for raft foundations.

REFERENCES

- Bjerrum, L. (1963), *Relation between Observed and Calculated Settlement of Structures in Clay, and Sand*, Norwegian Geotechnical Institute Bulletin, Oct 1969.
- Grant, R., J.T. Christian, and E. Van Marcke (1974), *Differential Settlement of Buildings*, Proceedings ASCE, Vol. 100, GT9, pp. 973–991.
- I.S. 1904 (1986), *Code of Practice for Design of Shallow Foundations*, Bureau of Indian Standards, New Delhi.
- Jappeli (1965), *Settlement Studies of Some Structures in Europe*, Proceedings 6th International Conference on Soil Mechanics and Foundation Engineering, Vol. 2, pp. 88–92.
- Rethati (1961), *Behaviour of Building Foundations on Embankments*, Proceedings 5th ICSMFT, Vol. 1, p. 781.
- Skempton, A.W. and D.H. McDonald (1955), *A Survey of Comparison Between Calculated and Observed Settlement of Structures in Clay*, Proceedings Conference on Correlation of Calculated and Observed Stresses and Displacement of Structures, Institute of Civil Engineers, London, Vol. 1, p. 38.
- Terzaghi, K. (1938), *Settlement of Structures in Europe and Methods of Observation*, Proceedings ASCE, Vol. 103, p. 1432.
- Whitman, R.V. and T.W. Lambe (1964), *Soil Mechanics*, McGraw-Hill Publication, New York.

5

Stress Distribution in Soils

5.1 INTRODUCTION

An essential step in foundation design is to determine the magnitude and distribution of stresses that are developed in the soil due to the application of structural load. It is these stresses which not only cause settlement of the foundation but determine its stability against shear failure.

The stresses and strains in soil mass depend on the stress-deformation characteristics, anisotropy and non-homogeneity of the soil, and also on the boundary conditions. But the task of analyzing stresses taking all these factors into consideration is extremely complex and, therefore, the attempts that have been made to date are based on simplifying assumptions. The most widely used method of analysis is based on the consideration of soil as homogeneous, isotropic, elastic medium.

It is well understood that the assumption of linearity of the stress-strain relationship which forms the basis of elastic behaviour is a questionable simplification because soils in their behaviour are essentially non-linear. No other widely acceptable theory has yet been developed for practical use to describe the response of soils to stress changes. Also within the comparatively small range of stresses that are normally imposed by structural loads, the assumption of linearity, for most soils, may be considered to be reasonably valid. Also, limited field evidence reported by Plantema (1953) and Turnbull et al. (1961) show that measured stresses correspond fairly well to those predicted by elastic theory. Therefore, refinement of the methods of stress analysis based on the theory of elasticity—still assuming the validity of the linear stress-strain relationship, but taking into consideration the variations of properties within the soil mass—has often been attempted.

5.2 IN-SITU STRESS

The stresses in the subsoil due to the over burden are called in-situ or geostatic stresses. Figure 5.1 shows the in-situ stresses in a soil element at a depth z , below the ground surface.

$$\text{Total vertical stress, } \sigma_v = \gamma z \quad (5.1)$$

where, γ = unit weight of soil, and

z = depth below ground surface.

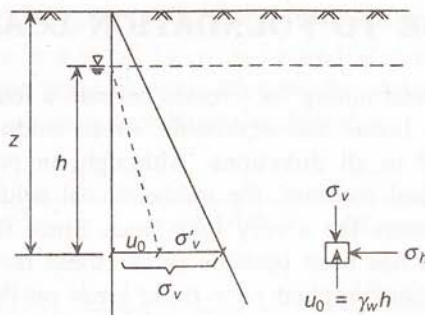


Fig. 5.1 In-situ stresses in soil.

$$\text{Total horizontal stress, } \sigma_h = K\sigma_v = K\gamma z \quad (5.2)$$

where, K is the coefficient of lateral pressure at rest with respect to total stress.

$$\text{Pore water pressure, } u_0 = \gamma_w h \quad (5.3)$$

where, γ_w = unit weight of water, and

h = depth of the point below water table.

$$\begin{aligned} \text{Effective vertical stress, } \sigma'_v &= \sigma_v - u_0 \\ &= \gamma z - \gamma_w h \end{aligned} \quad (5.4)$$

$$\begin{aligned} \text{Effective horizontal stress, } \sigma'_h &= \sigma_h - u_0 \\ &= K\gamma z - \gamma_w h \\ &= K_o \sigma'_v \end{aligned} \quad (5.5)$$

where K_o = coefficient of earth pressure at rest with respect to effective stress.

The value of K_o depends on the type of soil and its stress history. For normally consolidated soils, it varies from 0.4–0.7. For over consolidated soils, K_o depends on the overconsolidation ratio and generally becomes greater than 1 for overconsolidation ratio exceeding 4 (Som 1974).

Some empirical formulae for computing K_o values for soils are as follows:

For sand and normally consolidated clays, Jaky (1944) gave a relationship between K_o and the angle of shear resistance, ϕ' ,

$$K_o = 1 - \sin \phi' \quad (5.6)$$

This was subsequently modified by Brooker and Ireland (1965) as

$$K_o = 0.95 - \sin \phi' \quad (5.7)$$

For overconsolidated soils, Alpan (1967) gave the relationship,

$$(K_o)_{OC} = (K_o)_{NC} (OCR)^\lambda \quad (5.8)$$

where λ is a factor depending on the plasticity index of the soil and is given by

$$I_p = -281 \log(1.85\lambda) \quad (5.9)$$

Ladd (1977) suggested the value of 0.41 for λ .

5.3 STRESSES DUE TO FOUNDATION LOADING

It is generally assumed, in determining the stresses beneath a foundation, that the soil behaves as an elastic medium (i.e. linear and reversible stress-strain relationship) with identical properties at all points and in all directions. Although, in practice, a soil can hardly be approximated to such an ideal medium, the mathematical solution to this problem was the only one available to engineers for a very long time. Since the principle of superposition holds for such a medium, it has been possible to use these results to determine the stresses and deflections caused by loads applied over finite areas on the surface. Love (1923) gave equations for stresses and deflections caused by a loaded circular rigid plate and Newmark (1942) derived the expression for the stresses under the corner of a uniformly loaded rectangular area. The tables and charts prepared by Newmark and later by Fadum (1948) are extensively used to calculate the vertical stresses beneath a foundation. The case of a uniformly loaded strip was solved by Carothers (1920) and Jurgenson (1934). Bishop (1952) used stress functions and relaxation technique to calculate the stresses in and underneath a triangular dam. The most complete pattern of stresses, strains and deflections beneath a uniform circular load on a homogeneous half space can be obtained from tables prepared by Ahlvin and Ulery (1962). From all these results, it can be seen that the vertical stresses in a homogeneous, isotropic elastic body is a function only of the dimensions of the loaded area and independent of the elastic properties of the soil. However, this is not true in case of the lateral stresses and displacements.

5.3.1 Boussinesq Analysis: Point Load

Boussinesq (1885) (see Terzaghi 1943) was the first to obtain solution for the stresses and deformations in the interior of a soil mass due to a vertical point load applied at the ground surface, refer Fig. 5.2. He considered the soil mass as a half space bounded on the top by a horizontal plane (ground surface) and extending to infinity along depth and width.

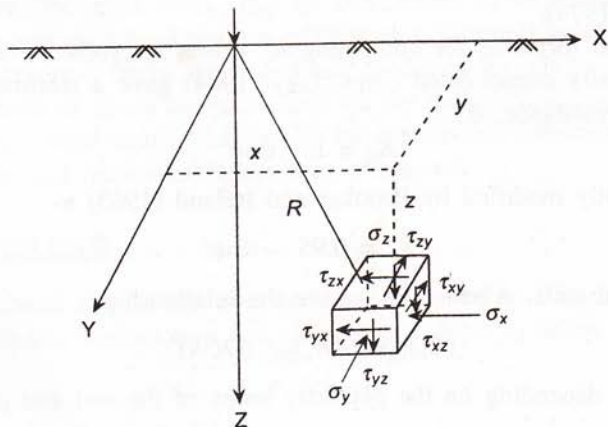


Fig. 5.2 Stress in the soil due to point load at surface (rectangular coordinates).

Considering soil as a homogeneous, isotropic, and elastic medium, Boussinesq obtained the expressions for stresses at a point (x, y, z) located at a distance, R from the origin of coordinates which is also the point of application of the vertical load, Q . The stress components in Cartesian coordinates are given as:

$$\begin{aligned}\sigma_x &= \frac{3Q}{2\pi} \left[\frac{x^2 z}{R^5} - \frac{1-2v}{3} \left\{ -\frac{1}{R(R+z)} + \frac{(2R+z)x^2}{(R+z)^2 R^3} + \frac{z}{R^3} \right\} \right] \\ \sigma_y &= \frac{3Q}{2\pi} \left[\frac{y^2 z}{R^5} - \frac{1-2v}{3} \left\{ -\frac{1}{R(R+z)} + \frac{(2R+z)y^2}{(R+z)^2 R^3} + \frac{z}{R^3} \right\} \right] \\ \sigma_z &= \frac{3Q}{2\pi} \frac{z^3}{R^5} \\ \tau_{yz} &= \frac{3Q}{2\pi} \frac{yz^2}{R^5} \\ \tau_{xz} &= \frac{3Q}{2\pi} \frac{xz^2}{R^5} \\ \tau_{xy} &= \frac{3Q}{2\pi} \left[\frac{xyz}{R^5} - \frac{1-2v}{3} \left\{ \frac{(2R+z)xy}{(R+z)^2 R^3} \right\} \right]\end{aligned}\quad (5.10)$$

Here, $R = \sqrt{(x^2 + y^2 + z^2)}$ and

v = Poisson's ratio of the soil

It may be observed that the vertical stress is independent of both the stress-strain modulus and Poisson's ratio. The lateral stresses and shear stresses, however, depend on Poisson's ratio but even these are independent of stress-strain modulus. Values of $v = 0.5$ for saturated cohesive soils under undrained condition (no volume change) and 0.2–0.3 for cohesionless soils, are generally valid.

In cylindrical coordinates, the stress components (refer Fig. 5.3), are:

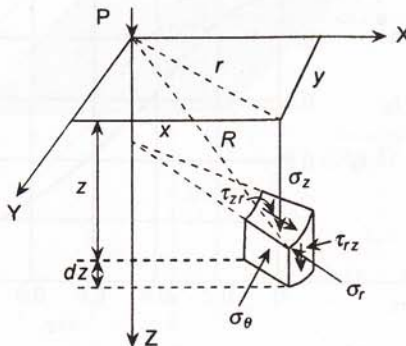


Fig. 5.3 Stresses in the soil due to point load at surface (cylindrical coordinates).

The stress components in cylindrical coordinates are written as:

$$\begin{aligned}\sigma_z &= \frac{3Q}{2\pi} \frac{z^3}{R^5} \\ \sigma &= \frac{Q}{2\pi} \left[\frac{3zr^2}{R^5} - \frac{1-2\nu}{R(R+z)} \right] \\ \sigma_\theta &= \frac{Q}{2\pi} (1-2\nu) \left[\frac{1}{R(R+z)} - \frac{2}{r^3} \right] \\ \tau_{rz} &= \frac{3Q}{2\pi} \frac{z^2 r}{R^5}\end{aligned}\tag{5.11}$$

The above expressions for stresses are valid only at distances, away from the point of load application. At the point of load application, the stresses are theoretically infinite.

For foundation analysis, the vertical stresses on horizontal plane (σ_z) are mostly required.

$$\text{Putting } R = \sqrt{(x^2 + y^2 + z^2)} = \sqrt{(r^2 + z^2)}$$

$$\sigma_z = \frac{3Q}{2\pi} I_B\tag{5.12}$$

$$\text{where } I_B = \frac{3}{2\pi [1 + (r/z)^2]^{5/2}}$$

I_B is the influence coefficient for vertical stress at any point within the soil mass, for the Boussinesq problem. The values of I_B for different values of r/z are given in Fig. 5.4.

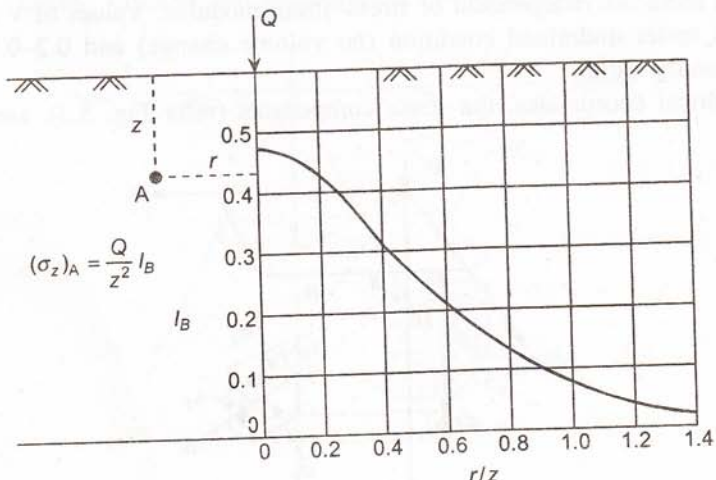


Fig. 5.4 Stress influence factor for point load (Boussinesq).

If a number of point loads Q_1 , Q_2 , and Q_3 are applied to the surface of soil, then the vertical stress on horizontal plane at any point M, is obtained by adding the stresses caused by the individual point loads, Fig. 5.5.

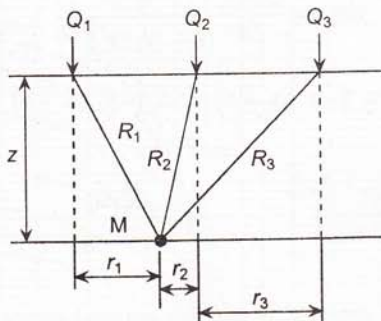


Fig. 5.5 Vertical stress in the soil due to a number of point loads.

In this case,

$$\sigma_z = \frac{Q_1}{z^2} I_{B1} + \frac{Q_2}{z^2} I_{B2} + \frac{Q_3}{z^2} I_{B3} \quad (5.13)$$

where the coefficients I_{B1} , I_{B2} , and I_{B3} are obtained from Fig. 5.4 for the corresponding ratios, r/z .

5.4 VERTICAL STRESSES BELOW UNIFORM RECTANGULAR LOAD

The vertical stress at the point M at depth z below the corner of a rectangular area of length $2a$ and width $2b$, due to a uniform vertical pressure q per unit area, can be obtained by integration of Boussinesq equation, which is given as Eq. (5.10). Figure 5.6 depicts this arrangement effectively.

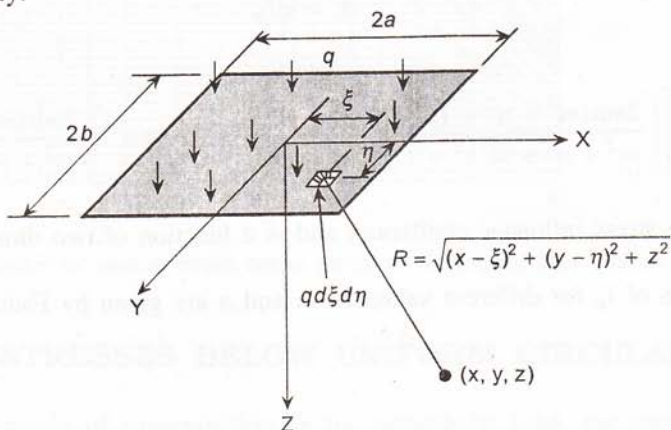


Fig. 5.6 Stresses below the corner of rectangular loaded area.

The equivalent point load on the infinitesimal area $dx dy$ is given by $dQ = q dx dy$
The vertical stress at M due to point load dQ (Eq. 5.12)

$$d\sigma_z = \frac{3dQ}{2\pi} \frac{z^3}{[1 + (r/z)^2]^{5/2}} \quad (5.14)$$

Integrating Eq. (5.14) between $[-a$ to $+a]$ and $[-b$ to $+b]$ along the x and y directions respectively we get,

$$\sigma_z = \frac{3qz^3}{2\pi} \int_{-a-b}^a \int_{-b}^b \frac{d\xi d\eta}{[(x-\xi)^2 + (y-\eta)^2 + z^2]^{5/2}} \quad (5.15)$$

Evaluation of this double integral gives the general expression for vertical stress at any point within the soil mass. Let us now consider the vertical stress at the origin ($x = y = 0$). Then,

$$\sigma_z(0,0, z) = \frac{2q}{\pi} \left(\frac{abz(a^2 + b^2 + 2z^2)}{(a^2 + z^2)(b^2 + z^2)\sqrt{a^2 + b^2 + z^2}} + \sin^{-1} \frac{ab}{\sqrt{a^2 + z^2} \sqrt{b^2 + z^2}} \right) \quad (5.16)$$

Now taking one quarter of this expression, the vertical stress below the corner of a flexible rectangular area ($a \times b$) (i.e. one quarter of the original rectangle $2a \times 2b$) is obtained as

$$\sigma_z = \frac{q}{4\pi} \left[\left(\frac{2mn(m^2 + n^2 + 1)^{1/2}}{m^2 + n^2 + m^2n^2 + 1} \right) \left(\frac{m^2 + n^2 + 2}{m^2 + n^2 + 1} \right) + \tan^{-1} \left(\frac{2mn(m^2 + n^2 + 1)^{1/2}}{m^2 + n^2 - m^2n^2 + 1} \right) \right] \quad (5.17)$$

where $m = \frac{a}{z}$ and $n = \frac{b}{z}$

or

$$\sigma_z = qI_\sigma \quad (5.18)$$

where

$$I_\sigma = \frac{1}{4\pi} \left[\left(\frac{2mn(m^2 + n^2 + 1)^{1/2}}{m^2 + n^2 + m^2n^2 + 1} \right) \left(\frac{m^2 + n^2 + 2}{m^2 + n^2 + 1} \right) + \tan^{-1} \left(\frac{2mn(m^2 + n^2 + 1)^{1/2}}{m^2 + n^2 - m^2n^2 + 1} \right) \right]$$

I_σ is called the stress influence coefficient and is a function of two dimensionless parameters m and n .

The value of I_σ for different values of m and n are given by Fadum (1948), are shown in Fig. 5.7.

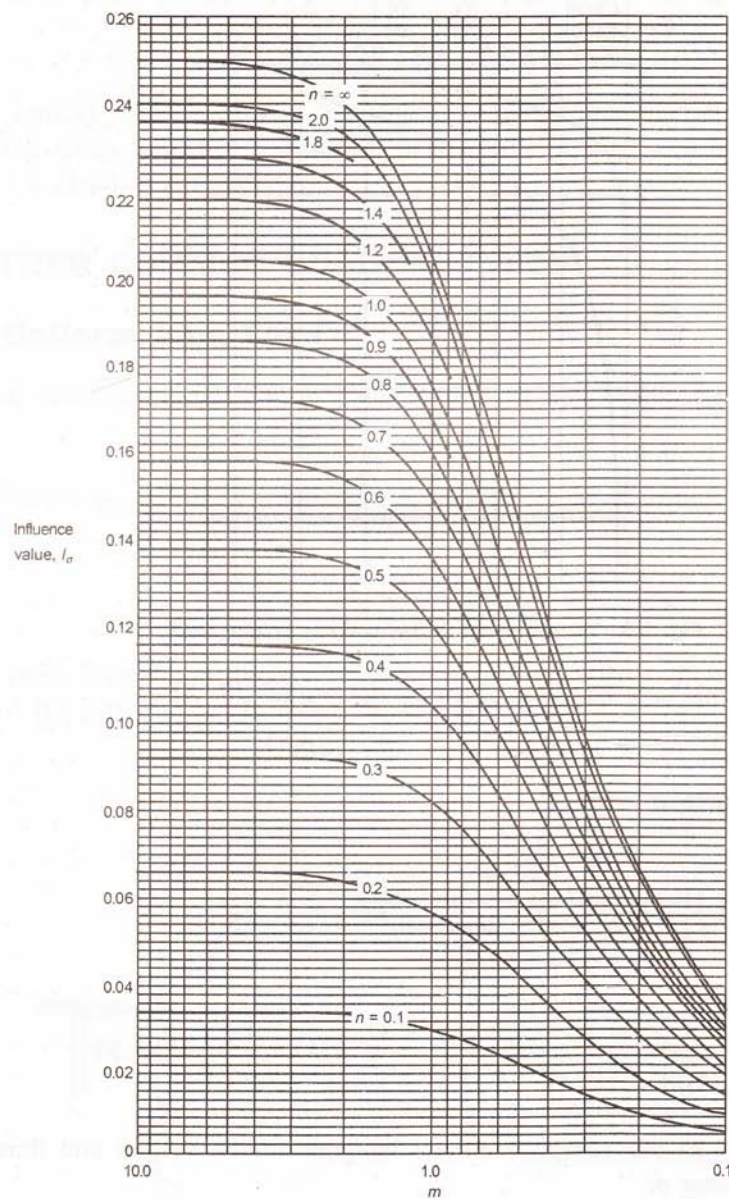


Fig. 5.7 Influence factor for vertical stress below corner of rectangular load, Fadum (1948).

5.5 VERTICAL STRESSES BELOW UNIFORM CIRCULAR LOAD

Following the same principle of superposition as for rectangular load, the vertical stresses below a uniformly distributed circular load may be obtained as in Fig. 5.8.

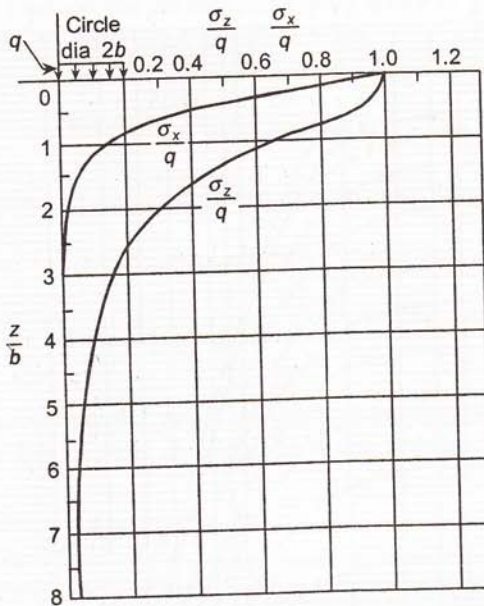


Fig. 5.8 Vertical stress below uniform circular load.

The load on infinitesimal area $rdrd\theta$ is given by $dQ = qrdrd\theta$. Also,

$$R = (r^2 + b^2 + z^2 - 2br \cos\theta)^{1/2}$$

Integrating over the circular area,

$$\sigma_z = \frac{3qz^3}{2z} \int_0^{2\pi} \int_0^a \frac{rdrd\theta}{[r^2 + b^2 + z^2 - 2br \cos\theta]^{5/2}} \quad (5.19)$$

$$= q \left\{ A - \frac{n}{\pi \sqrt{n^2 + (1+t)^2}} \left[\frac{n^2 - 1 + t^2}{n^2 + (1-t^2)} E(k) + \frac{1-t}{1+t} \Pi_0(k, p) \right] \right\} \quad (5.20)$$

where $E(k)$ and $\Pi_0(k, p)$ are complete elliptic integrals of the second and third kind of modulus k and parameter p .

$$\begin{aligned} t &= r/a & A &= \begin{cases} 1 & \text{if } r < a \\ \frac{1}{2} & \text{if } r = a \\ 0 & \text{if } r > a \end{cases} \\ n &= z/a \\ k^2 &= \frac{4t}{n^2 + (t+1)^2} \end{aligned}$$

For the special case of the points beneath the centre of the load, $r = 0$

$$(\sigma_z)_{r=0} = q \left\{ 1 - \frac{1}{[1 + (a/z)^2]^{3/2}} \right\} \quad (5.21)$$

The vertical stresses beneath the centre of a uniform circular load are shown in Fig. 5.8. The stress influence coefficient for a circular loaded area for different values of r/a and z/a is given in Appendix A.

5.6 OTHER COMMON LOADING TYPES

5.6.1 Uniform Line Load

The vertical stress in the soil due to a line load p per unit length, applied at the surface is given by

$$\begin{aligned} \sigma_z &= \frac{2p}{\pi} \frac{z^3}{(x^2 + z^2)^2} \\ &= \frac{p}{z} \left(\frac{2}{\pi(1 + x^2/z^2)^2} \right) \end{aligned} \quad (5.22)$$

The stress distribution directly beneath the load ($x = 0$) is shown in Fig. 5.9(a). The variation of $\sigma_z/(p/z)$ with x/z is shown in Appendix A.

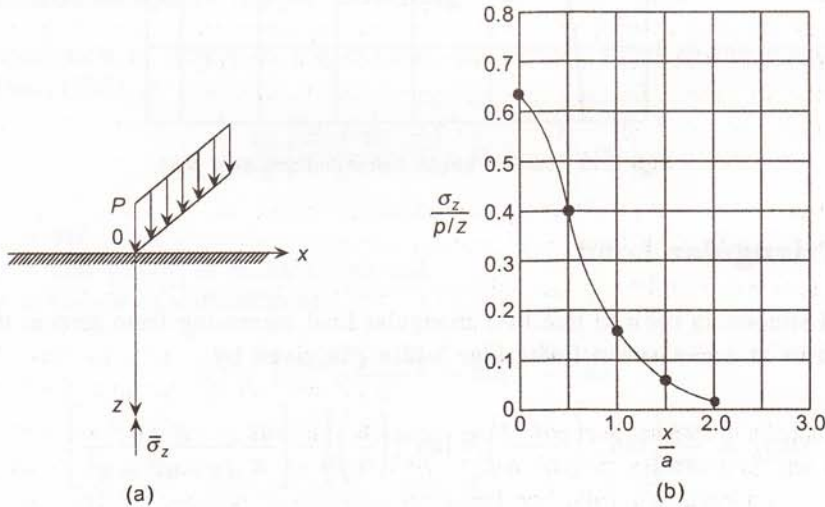


Fig. 5.9 Vertical stresses in the soil due to a line load.

5.6.2 Uniform Strip Load

The vertical stresses in the soil due to a uniformly distributed strip load is given by the expression,

$$\sigma_z = \frac{q}{\pi} \left[\tan^{-1} \left(\frac{z}{x-a} \right) - \tan^{-1} \left(\frac{z}{x+a} \right) - \frac{2az(x^2 - z^2 - a^2)}{(x^2 + z^2 - a^2)^2 + 4a^2 x^2} \right] \quad (5.23)$$

The corresponding stress distribution below the centre line and the edge are shown in Fig. 5.10. The variation of σ_z/q with x/a and z/b is tabulated in Appendix A.

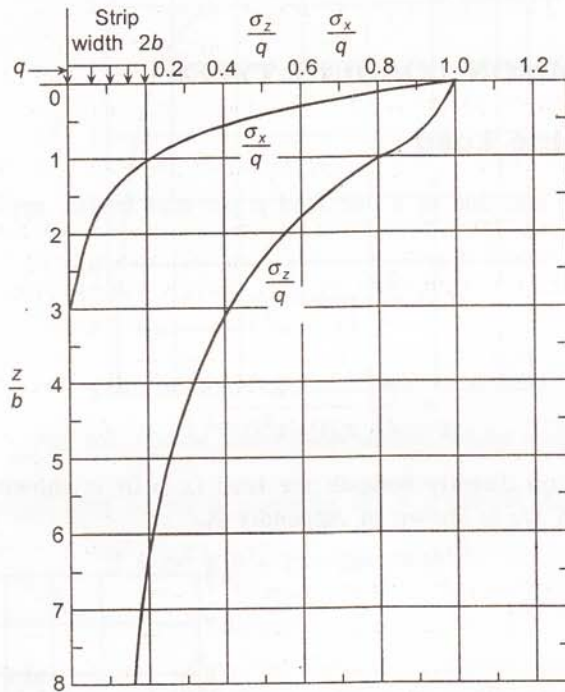


Fig. 5.10 Vertical stress below uniform strip load.

5.6.3 Triangular Load

The vertical stresses in the soil due to a triangular load increasing from zero at the origin to q per unit area at a distance a [refer Fig. 5.11(a)] is given by,

$$(\sigma_z)_A = \frac{qx}{\pi a} \left[\tan^{-1} \left(\frac{z}{x-a} \right) - \tan^{-1} \left(\frac{z}{x} \right) \right] - \left[\frac{qz}{\pi} \frac{x-a}{(x-a)^2 + z^2} \right] \quad (5.24)$$

or

$$\frac{\sigma_z}{q} = \frac{1}{\pi} \left[\frac{x}{a} \left\{ \tan^{-1} \left(\frac{z}{x-a} \right) - \tan^{-1} \frac{z}{x} \right\} - \frac{z}{a} \frac{\frac{x}{a} - 1}{\left(\frac{x}{a} - 1 \right)^2 + \left(\frac{z}{a} \right)^2} \right]$$

For $x = a$, that is, for points below B,

$$\sigma_z = qI'$$

where $I' = \frac{1}{\pi} \left(\frac{\pi}{2} - \tan^{-1} \frac{z}{a} \right)$.

The variation of I' with z/a is shown in Fig. 5.11(b). The tabulated values of σ_z/q for different values of x/a and z/a are given in Appendix A.

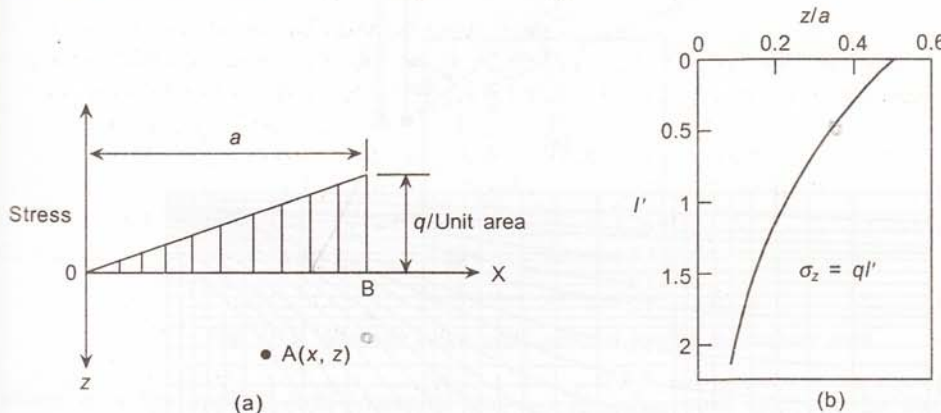


Fig. 5.11 (a) Vertical stress due to a triangular load. (b) Variation of I' with z/a (stress below point B).

5.6.4 Embankment Type Loading

For an embankment of height H , Fig. 5.12(a), the vertical stress at any point below B is given as, Das (1997)

$$\Delta p = \frac{q_o}{\pi} \left[\frac{B_1 + B_2}{B_2} (\alpha_1 + \alpha_2) - \frac{B_1}{B_2} \alpha_2 \right] \quad (5.25)$$

where $q_o = \gamma H$

γ = unit weight of embankment soil

H = Height of embankment

$$\alpha_1 = \tan^{-1} \frac{B_1 + B_2}{z} - \tan^{-1} \frac{B_1}{z} \text{ rad}$$

$$\alpha_2 = \tan^{-1} \frac{B_1}{z}$$

$$\Delta p = q_o I' \quad (5.26)$$

where $I' = f \left(\frac{B_1}{z}, \frac{B_2}{z} \right)$.

The variation of I' with $\frac{B_1}{z}$ and $\frac{B_2}{z}$ is shown in Fig. 5.12.

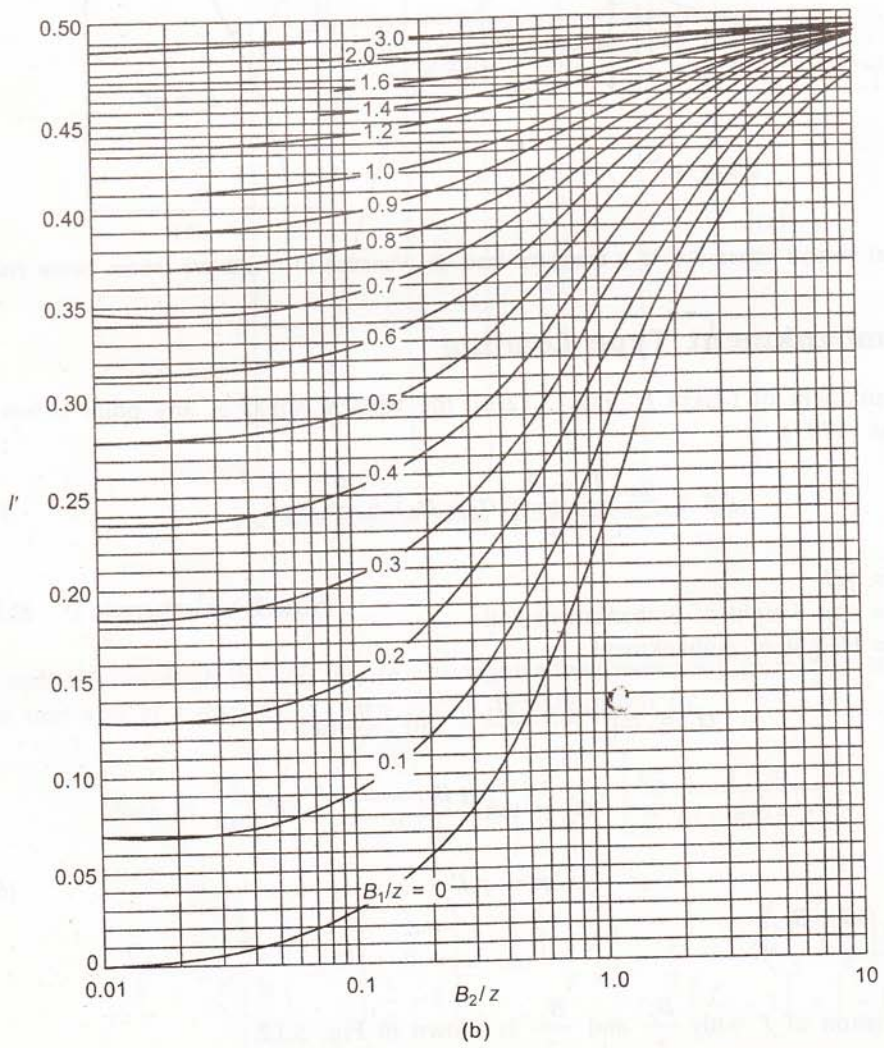
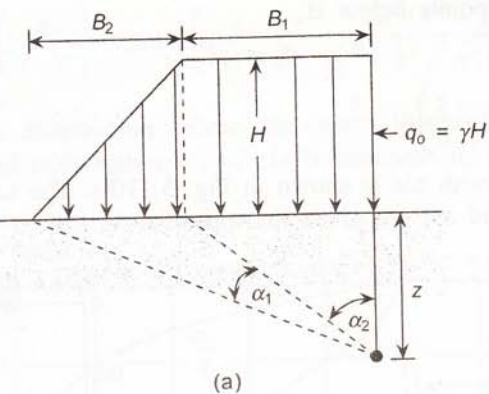


Fig. 5.12 Stresses due to embankment type loading, Das (1997).

5.7 STRESS AT ANY POINT BELOW RECTANGULAR LOAD

The principle of superposition allows determination of vertical stress at any point below a rectangular loaded area. For point A, for example, Fig. 5.13, the loaded area may be divided into four smaller rectangles keeping the point A at the corner of each rectangle. Then,

$$(\sigma_z)_A = q[I_{\sigma_I} + I_{\sigma_{II}} + I_{\sigma_{III}} + I_{\sigma_{IV}}] \quad (5.27)$$

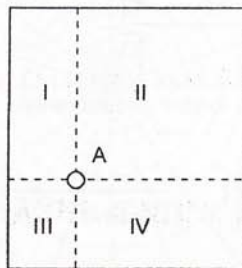


Fig. 5.13 Stresses below point within a loaded rectangular area.

where q is the applied load intensity and I_{σ_I} , $I_{\sigma_{II}}$, $I_{\sigma_{III}}$ and $I_{\sigma_{IV}}$ are the stress influence factors for points below the corner of respective rectangular areas.

Similarly, for points outside the loaded rectangle, Fig. 5.14, the vertical stress below point B may be obtained as,

$$(\sigma_z)_B = q[I_{\sigma_{I+II}} + I_{\sigma_{I+IV}} - I_{\sigma_{III}} - I_{\sigma_{IV}}] \quad (5.28)$$

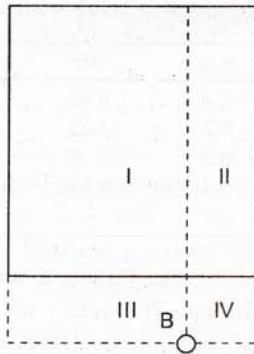


Fig. 5.14 Stresses below point outside a loaded rectangular area.

5.8 NEWMARK'S CHART

Newmark (1942) derived a simple graphical calculation for determining the vertical stress at any point within a soil mass for any shape of loaded area.

Let us consider the stress beneath the centre of a loaded circular area, Fig. 5.15.

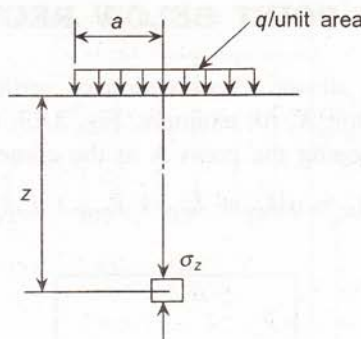


Fig. 5.15 Stress beneath centre of a loaded circular area: construction of Newmark's chart.

$$\sigma_z = q \left\{ 1 - \frac{1}{[1 + (a/z)^2]^{3/2}} \right\} \quad (5.29)$$

On rearranging the above equation,

$$\frac{a}{z} = \left(1 - \frac{\sigma_z}{q} \right)^{-2/3} - 1 \quad (5.30)$$

The interpretation of this equation is that a/z ratio is the relative size of a circular loaded area in terms of the depth z such that when loaded it gives a unique pressure ratio, σ_z/q on the soil at that depth. By substituting different values of σ_z/q in Eq. (5.30), corresponding values of a/z can be obtained, as in Table 5.1.

Table 5.1 Relationship between a/z and σ_z/q

a/z	σ_z/q	a/z	σ_z/q
0.27	0.1	0.92	0.6
0.40	0.2	1.11	0.7
0.52	0.3	1.39	0.8
0.64	0.4	1.91	0.9
0.77	0.5	∞	1.0

Then, taking an arbitrary value of z (say, 1 cm), a series of concentric circles of radius 0.27 cm, 0.4 cm, and so on can be drawn. The series of rings is further subdivided into a number of units (say 200) by drawing radial lines from the centre, as shown in Fig. 5.16. The value of each unit then becomes $(1/200)q = 0.005q$.

To obtain the stress at a point A located at depth z below a footing, the loaded area is drawn on a tracing paper to a scale z equal to the scale for which the Newmark's chart to be used has been drawn. The plan on the tracing paper is placed on the Newmark's chart such that the point A is placed at the centre of the chart. Then, the number of units of the Newmark's Chart (N) enclosed within, are counted. The stress at A is given by,

$$(\sigma_z)_A = q \times N \times \text{value of each unit.}$$

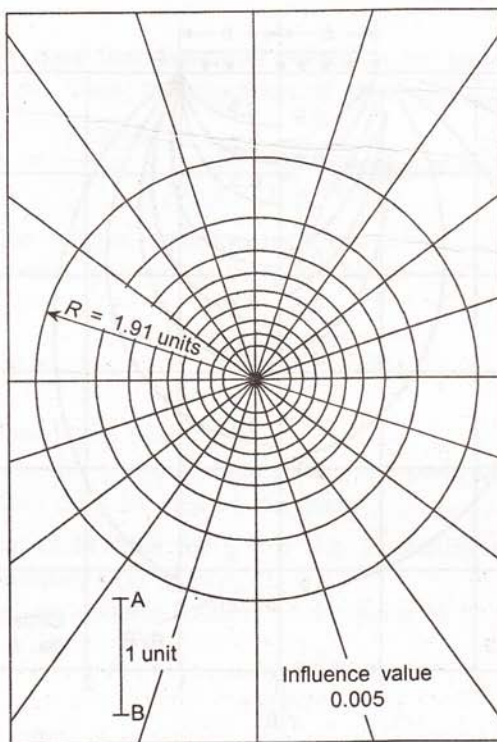


Fig. 5.16 Newmark's chart.

By moving the plan of the building and bringing different points at the centre of the Newmark's chart, the stresses at different points may be obtained. For different depths, the plan of the building is to be drawn fresh to the appropriate scale.

5.9 PRESSURE BULB

When a soil is subjected to a foundation load, it is important to know the zone of soil beneath the foundation which is significantly stressed by the applied load. This is generally expressed graphically by isobars or pressure bulb.

An *isobar* for a given surface load is a curve which connects all points below the ground surface having equal stress. The procedure for obtaining isobars is as follows:

1. Divide the half space in the vicinity of the load area into sufficient number of grid points.
2. Compute vertical stress at each grid point using an appropriate formula/table/chart.
3. Draw contours of equal vertical stresses, say $0.8q$, $0.5q$, $0.2q$, $0.1q$ and so on.

The bulb formed by the set of isobars is called a pressure bulb. Figure 5.17 shows pressure bulbs for vertical stress due to uniform circular and strip loads. It can be seen that for strip loading, the depth of pressure bulb upto which significant vertical stress exists ($\sigma_z/q > 0.1$) is about three times the width of the load area. For circular loading, this depth is about twice the width of load area.

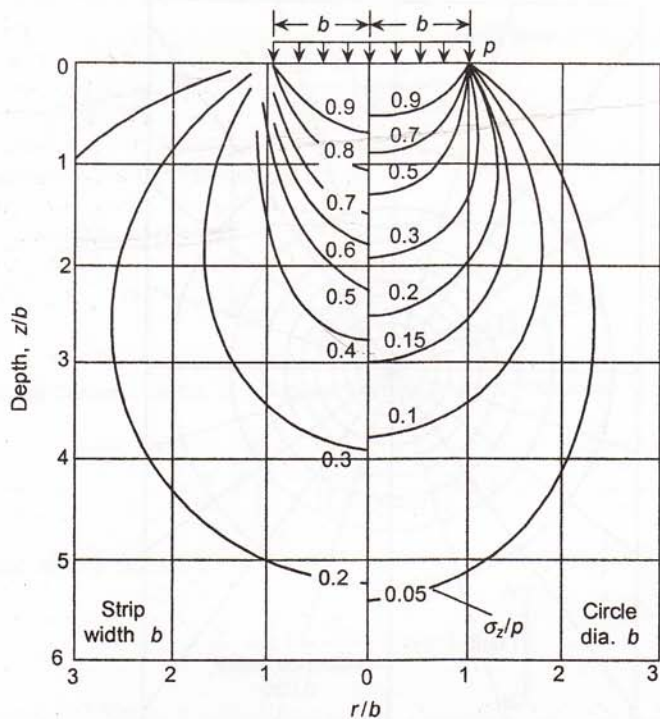


Fig. 5.17 Pressure bulb for circular and strip footings.

The pressure bulb gives the zone of soil which influenced by the foundation loading and is useful in planning soil exploration programmes, and in the study of settlement and interference of footing.

5.10 RIGIDITY OF FOOTINGS: CONTACT PRESSURE

Most footings possess a definite rigidity. It is important to estimate the effect of rigidity on the distribution of pressure on the footing base (contact pressure), and on the stress distribution within the soil mass.

According to Boussinesq analysis, the vertical deformation of a point on the surface of an elastic half space under the action of a concentrated load P is given by

$$W = \frac{P}{\pi R} (1 - \nu^2) E \quad (5.31)$$

For an arbitrary loading area (Fig. 5.13), the vertical displacement of the point A is given by

$$w_z = \frac{1 - \nu^2}{\pi E} \iint_F \frac{p(\xi - \eta) d\xi d\eta}{\sqrt{(x - \xi)^2 + (y - \eta)^2}} \quad (5.32)$$

where F is the loading area over which integration has to be done.

With an absolutely rigid foundation, all points on the surface of contact will have the same vertical displacement. Thus, the condition of absolute rigidity of a foundation is,

$$w_z = \frac{1-v^2}{\pi E} \iint_F \frac{p(\xi-\eta)d\xi d\eta}{\sqrt{(x-\xi)^2 + (y-\eta)^2}} = \text{constt} \quad (5.33)$$

The solution of the integral equation for an absolutely rigid circular footing with a central load gives the contact pressure at the point M as:

$$p(x, y) = \frac{p_m}{2\sqrt{[1 - (\zeta/a)^2]}} \quad (5.34)$$

where,

a = radius of foundation base

ζ = distance from the centre of base to a given point ($\zeta \leq a$)

p_m = mean pressure per unit area of the base

It can be seen from Eq. (5.34) that for $\zeta = a$ (i.e. at footing edge), $p(x, y) = \infty$ and for $\zeta = O$ (i.e. at footing centre), $p(x, y) = p_m/2$.

For a strip footing, the contact pressure at the point M is given by,

$$P(x, y) = \frac{2 p_m}{\pi \sqrt{[1 - (y/b)^2]}} \quad (5.35)$$

where,

y = horizontal distance of the point M from the centre of footing

b = half width of footing

The distribution of contact pressure for an absolutely rigid footing on an elastic half space will have a saddle like shape with infinite pressure at the ends, as shown in Fig. 5.18. However, in actual practice, there is redistribution of stresses over the base (the stresses at the edge of footing cannot exceed the bearing capacity of the soil) and the contact pressure at the base of a rigid footing becomes much more uniform as shown by curves in Fig. 5.18.

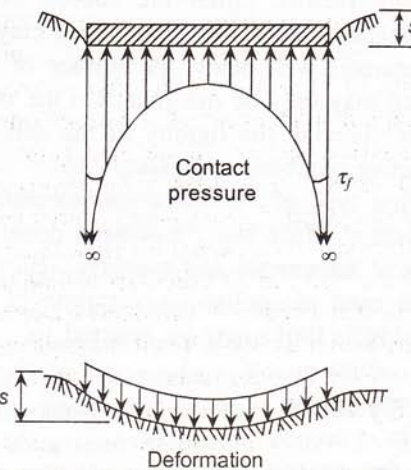


Fig. 5.18 Rigid footing: contact pressure.

For foundation of finite rigidity, the contact pressure can be obtained by solving the integral equation, Eq. (5.32) together with the differential equation for bending of plates. Using such an approach, Borowicka (1936, 1938) obtained the contact pressure distribution for a uniformly loaded circular/strip footing on a semi-infinite elastic mass. The shearing stress along the base of the foundation was assumed to be zero. It was found that the distribution of contact pressure is strongly dependent on a dimensionless factor, termed flexibility factor, of the form,

$$K = \frac{1}{6} \left(\frac{1 - v_S^2}{1 - v_F^2} \right) \left(\frac{E_F}{E_S} \right) \left(\frac{T}{b} \right)^3 \quad (5.36)$$

where,

v_S = Poisson's ratio of soil

v_F = Poisson's ratio of footing material

E_F, E_S = Young's Modulus of footing material and soil, respectively

b = radius for circular footing

T = Thickness of footing

It should be noted that for an elastic footing, the distribution of contact pressure depends on the elastic properties of the supporting medium, on the flexural rigidity of the footing, and on distribution of loads on the footing.

The nonuniform distribution of contact pressure influences stress distribution in the soil only upto a small depth from the base, and the pressure bulb is slightly affected. As a result, the influence of rigidity of footing on settlement is relatively small.

5.11 NON-HOMOGENEOUS SOILS

The engineering properties of a soil are not generally uniform throughout its mass. This non-uniformity may manifest itself in both spatial (non-homogeneous) and directional (anisotropic) variation of the modulus of deformation. The variation of soil properties with depth may be due to many factors. Often the subsoil consists of different geological formations with different characteristics, for example, a clay deposit underlain by sand or rock. If the underlying stratum is well below the surface of the clay relative to the size of the loaded area, its influence may only be marginal. On the other hand, even in a deep layer of apparently homogeneous material, the rigidity of the soil generally increases with depth due to the increase in effective overburden pressure.

In dealing with the first type of non-homogeneity mentioned above, a subsoil is often considered as a layered system. Much work has been done on this subject, particularly in connection with the design of pavements and runways. (Biot 1938, Pickett 1938, Burmister 1943, Poulos 1967). In the case of continuous variation of elastic parameters with depth, Gibson's analysis (Gibson 1967, 1968) may be referred to.

5.11.1 Two-layer System

A simple two-layer system, Fig. 5.19, may consist of either two elastic layers with different engineering properties or single elastic layer on a rigid base.

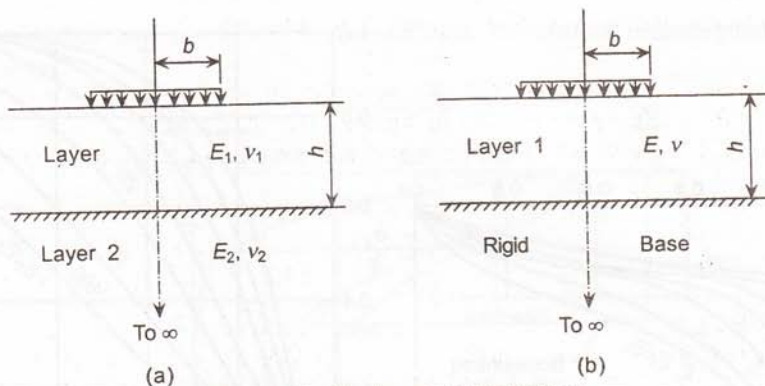


Fig. 5.19 Two-layer elastic system.

Two layers with different elastic parameters

This situation is often encountered in the case of pavements where stiffer layers are placed on a soft subgrade. However, in the case of foundations, the situation is often reversed and one may encounter a layer of soft soil overlying a stronger deposit.

Biot (1935) and Pickett (1938) were among the first to solve the problem of stress distribution in the two-layer rigid base system. However, their results could only be used to determine the stresses at the surface of the base layer. In a series of papers in 1943 and 1945, Burmister (1943, 1945a, b, c) presented the general theory of stresses and displacements in layered soils from which exact solutions could be obtained for axi-symmetric loading. Using Burmister's analysis, Fox (1948) published tabulated values of stresses due to a uniform circular loading with or without friction at the interface for the case of Poisson's ratio, $\nu = 1/2$. The case of the line or strip loading was analyzed by Lemcof (1961) who developed equations of stresses for a general two-layer system and tabulated numerical values for the particular case of $E_1/E_2 = 50$ and $\nu_1 = \nu_2 = 1/4$.

In the general two-layer system for a circular load, the stresses depend on the values of ν_1 and on the two parameters (refer Fig. 5.19).

$$a = \frac{b}{h} \quad \text{and} \quad K = \frac{E_1}{E_2} \quad (5.37)$$

where,

b = radius of the loaded area

h = thickness of the top layer and

E_1, E_2 are the elastic modulii of, respectively the top and bottom layers.

In Fig. 5.20 are plotted the distribution of vertical stresses beneath the centre of a circle for the special case of $a = 1$ and where the upper layer is stiffer than the lower. It can be seen that the presence of the stiff upper layer has a considerable influence on the stresses, particularly in the vicinity of the interface. For example, a rigid upper layer which is five times stiffer than the subgrade (i.e. $E_1/E_2 = 5$) reduces the stress at the interface to 60% of the Boussinesq value. This load spreading capacity of the stiff upper layer has been successfully employed in the design of pavements on soft subgrades.

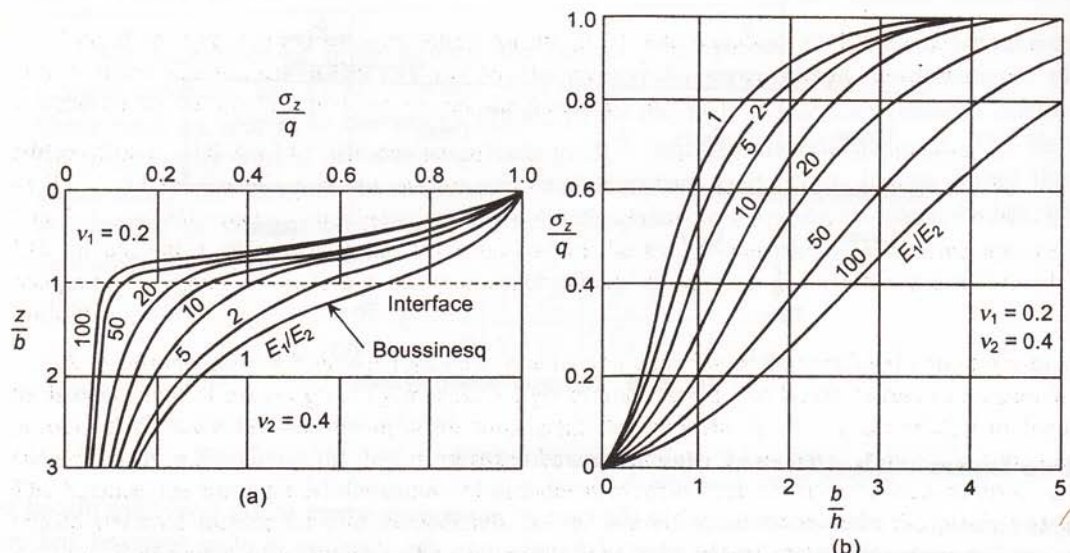


Fig. 5.20 Two-layer elastic system: Effect of rigidity of upper layer on the vertical stress beneath centre of a uniform circular load (after Burmister 1963).

The effect of relative size of loaded areas and thickness of the upper layer on the vertical stresses at the interface is shown in Fig. 5.19b. The upper layer is most effective in spreading the load when its thickness lies between b and $3b$ while for very thin and very thick layers, they approach the Boussinesq values.

The case of a foundation where a soft layer is underlain by a stiffer deposit ($E_1/E_2 < 1$) has not been evaluated but from extrapolation, it can be concluded that the stresses in the upper layer will, if anything, be greater than those for a homogeneous medium.

Single elastic layer on a rigid base

This is a special case of the above problem with the elastic modulus of the bottom layer $E_2 = \infty$. The problem was first solved by Burmister (1956) who extended his earlier work to analyze the stresses and strains in the upper layer of a two-layer rigid base system. From his influence charts, it is possible to obtain the complete pattern of stresses and displacements under the corner of a uniformly loaded rectangle for Poisson's ratio, $v = 0.2$ and 0.4 .

The same problem was considered in detail by Poulos (1967), who used Burmister's theory to compute a set of influence factors for stresses and surface displacements due to a point load, for values of Poisson's ratio, $v = 0, 0.2, 0.4$, and 0.5 . By integration of these point load factors, he then calculated the corresponding influence factors for different loading types.

The vertical and radial stresses beneath the centre of a loaded circle for values of $h/b = 1, 2, 4$, and 8 and $v = 1/2$ are shown in Fig. 5.21. The stresses for the homogeneous half-space (Boussinesq) are also plotted for comparison. It can be seen that the presence of a rigid layer at a shallow depth relative to the size of the loaded area significantly alters the stress pattern. For small values of h/b just underneath the load, vertical stresses may even be greater than the applied pressure. However, with increasing depth, the effect of the rigid base

gradually diminishes and for $h/b > 8$, the stresses are almost indistinguishable from the Boussinesq values.

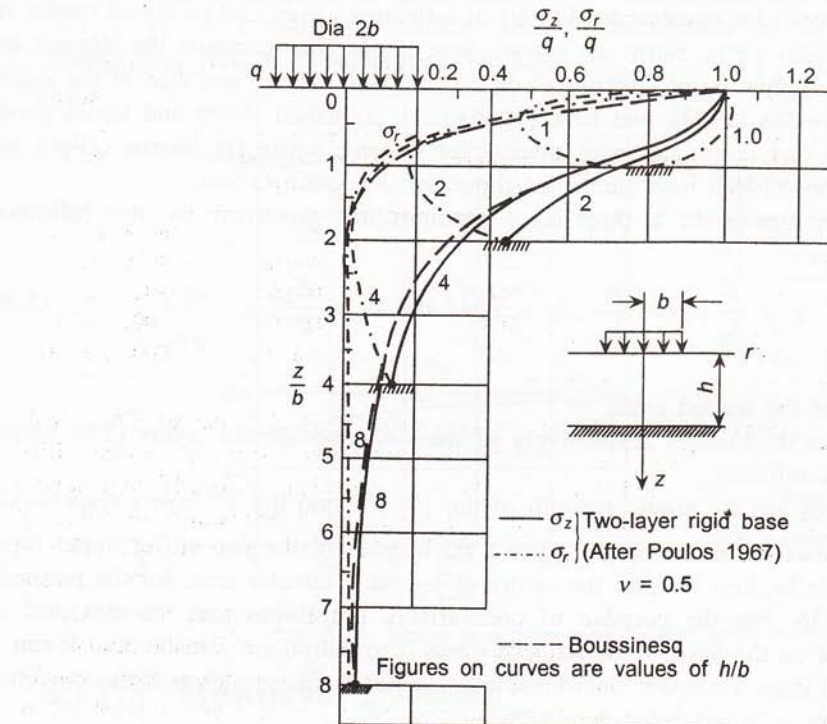


Fig. 5.21 Distribution of stresses in two-layer rigid base system (after Poulos, 1967).

5.11.2 Three-layer Systems

The analyses of three-layer soil systems (Fig. 5.22) are much more complex than for two-layers and solutions have only been obtained for stresses and deflections beneath a uniform circular load. Burmister (1945) was the first to develop the general theory for such a system with both rough and smooth interfaces.

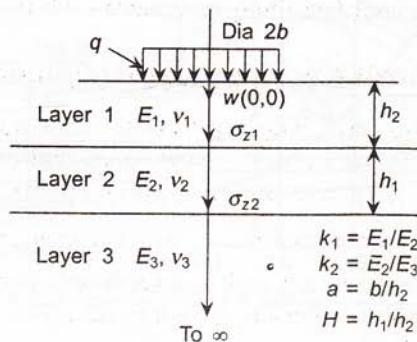


Fig. 5.22 Three-layer elastic system.

Burmister's equations were used by Acum and Fox (1951) to calculate the stresses at the interfaces (for $v_1 = v_2 = 0.5$ and for full continuity between the layers). Schiffman (1957) presented methods for numerical solutions of influence values and tabulated results for a particular case. In later years, Burmister's work was extended to compute the stresses and deflections for any combination of thicknesses of the individual layers and size of the loaded area. Jones (1962), Peattie (1962), and Kirk (1966) have published charts and tables giving the stress factors for any combination of three-layer systems while De Barros (1966) and Uyeshita and Meyerhof (1967) have published those for deflection factors.

The stress and strains in a three-layer medium are governed by the following dimensionless parameters:

$$a = \frac{b}{h_2}; H = \frac{h_1}{h_2}; k_1 = \frac{E_1}{E_2}; \text{ and } k_2 = \frac{E_2}{E_3} \quad (5.38)$$

where,

b is radius of the loaded circle

h_1 and h_2 are thicknesses respectively of the first and second layers (The bottom layer is semi-infinite).

E_1 , E_2 , and E_3 are the elastic modulii of the 1st, 2nd, and the 3rd layers respectively.

Figure 5.23 shows the effect of the relative thicknesses of the two stiffer upper layers on the stresses and deflections beneath the centre of a loaded circular area, for the particular case of $h_1 + h_2 = 2b$. For the purpose of comparison, the Boussinesq stresses and the deflections calculated on the basis of Boussinesq stress distribution are also plotted. It can be seen that the actual values are lower than those given by Boussinesq although the maximum discrepancy in deflection is not more than 25%.

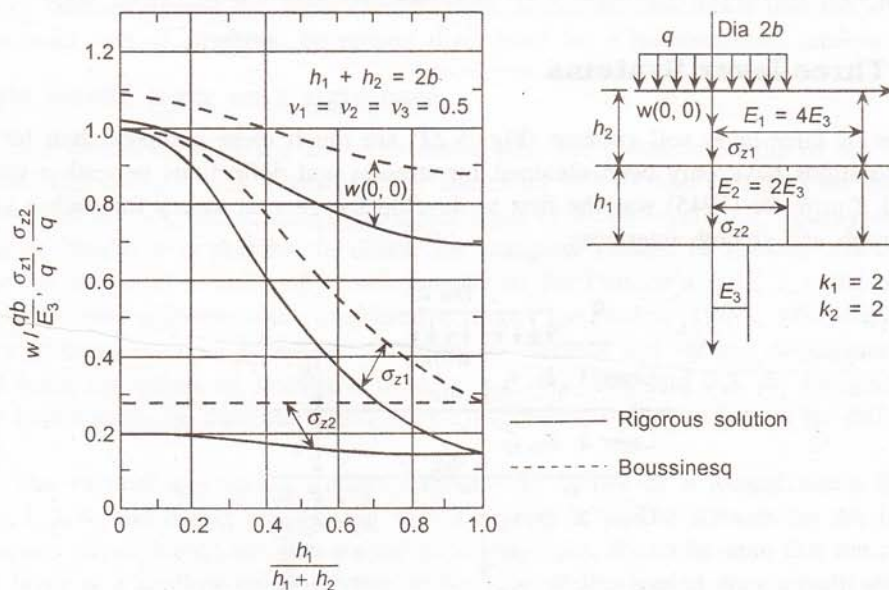


Fig. 5.23 Stress and displacement in three-layer system (after Jones 1962, Uyeshita and Meyerhof 1967).

For the situation where the layers become successivley stiffer with depth ($k_1 = 0.2$, $k_2 = 0.2$), the assumption of homogeneity will underestimate the stresses by up to 30% for $h_1/h_1 + h_2 \rightarrow 1$ while for smaller relative thicknesses of the top layer, the error is considerably less, as illustrated in Fig. 5.24.

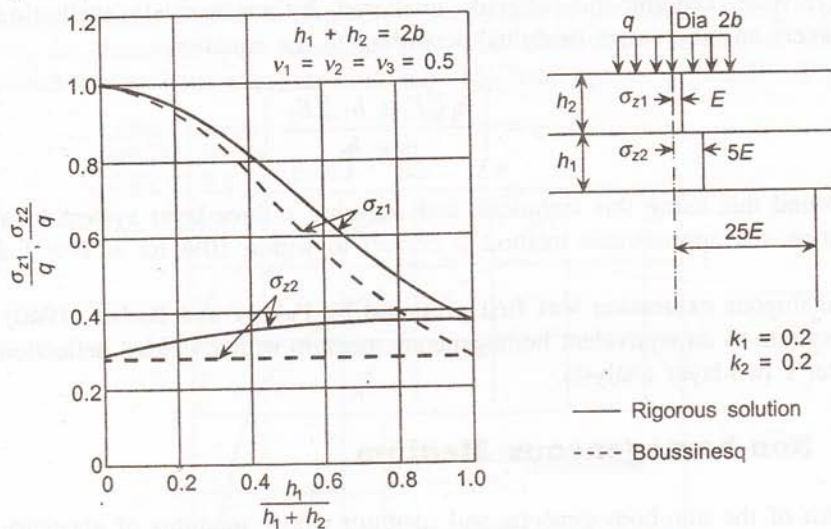


Fig. 5.24 Stress in a three-layer system (after Jones 1962).

5.11.3 Multilayer Systems

The problem of multilayer system involves immense complexity and to date no analytical solution is available for anything consisting of more than three layers. Vesic (1963) has suggested an approximate method of calculating the elastic settlement of a foundation on a multilayered medium assuming Boussinesq stress distribution but using the proper elastic modulus for the respective layers. His charts and method of calculation are shown in Fig. 5.25.

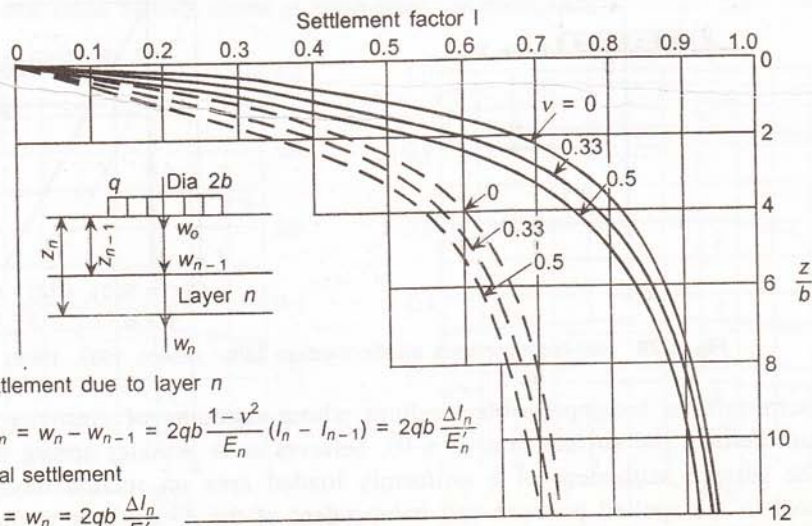


Fig. 5.25 Approximate method of calculating settlement in multilayer elastic systems (after Vesic 1963).

Vesic observed that in three-layered systems, the shape of the deflected surface computed by this approximate technique agrees better with measured deflections of pavements than the more rigorous analyses.

De Barros (1966) proposed an approximate method of reducing a multilayer system to a three-layer one, keeping the subgrade unaltered, by successively attributing to the two adjacent layers an 'equivalent modulus' according to the equation

$$E_{1,2} = \left(\frac{h_1 \sqrt[3]{E_1 + h_2} \sqrt[3]{E_2}}{h_1 + h_2} \right)^3 \quad (5.39)$$

He found that using this technique and reducing a three-layer system to an equivalent two-layer one, the approximate method is correct to within 10% for $h_2/b^3 > 1$ and 14% for $h_2/b > 2$.

An analogous expression was first proposed by Palmer and Barber (1940) to reduce a two-layer system to an equivalent homogeneous medium which yielded deflections very close to Burmister's two-layer analysis.

5.11.4 Non-homogeneous Medium

The problem of the non-homogeneous soil medium whose modulus of elasticity varies as a continuous function of depth has received only limited attention so far. Korenev (1957), Sherman (1959), Golecki (1959), Hruban (1959), and Lekhnitskii (1962) have studied particular problems of non-homogeneity, but no comprehensive theory had been presented until Gibson developed the theory (Gibson 1967, 1968) of stresses and displacements in a non-homogeneous, isotropic elastic half-space subjected to strip or axially symmetric loading normal to its place boundary, Fig. 5.26.

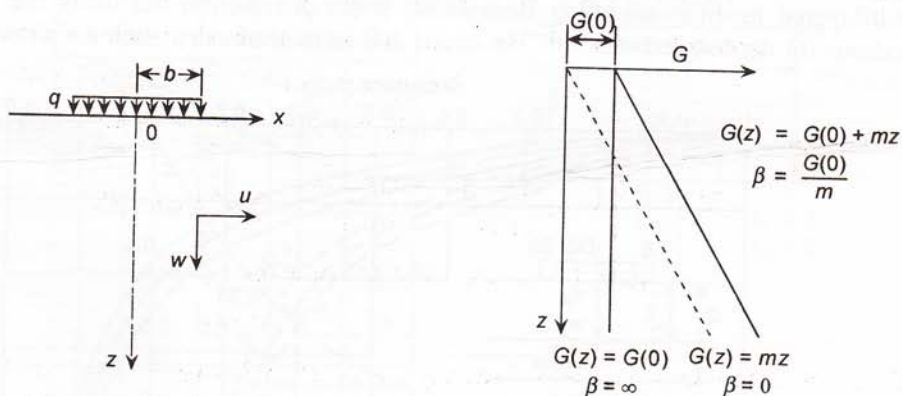


Fig. 5.26 Non-homogeneous elastic medium (after Gibson 1967, 1968).

A semi-infinite incompressible medium whose modulus of elasticity increases with depth from zero at the surface (i.e. $\beta = 0$), behaves as a Winkler spring model. In other words, the surface settlement of a uniformly loaded area on such a medium is directly proportional to the applied pressure and independent of the dimensions of the load.

The distribution of stresses in a semi-infinite medium is not significantly affected by this type of non-homogeneity. Figure 5.27 shows the stress distribution for $\beta/b = 0.1$ and 10. Indeed, the two limiting cases $\beta/b = 0$ and $\beta/b = \infty$ give exactly the same stresses while in the intermediate range $0 < \beta/b < \infty$, both the vertical and horizontal stresses tend to be a little higher than the corresponding stresses for the homogeneous medium, though the difference is never greater than 10%. However, over most of the range ($0 < \beta/b < 0.5$ and $5 < \beta/b < \infty$), the discrepancy is less than 5%. This observation is true of vertical and horizontal stresses due to both axi-symmetric and strip loadings, as depicted in Fig. 5.28.

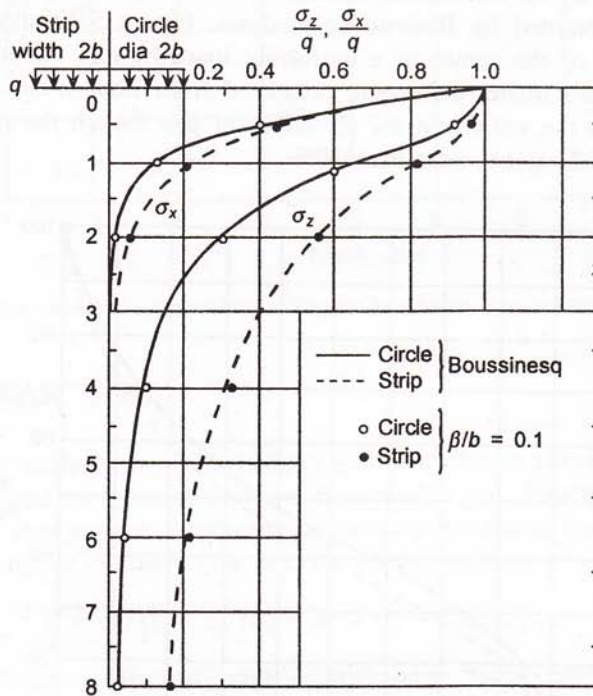


Fig. 5.27 Vertical stress beneath centre of foundations: non-homogeneous medium (Som 1968).

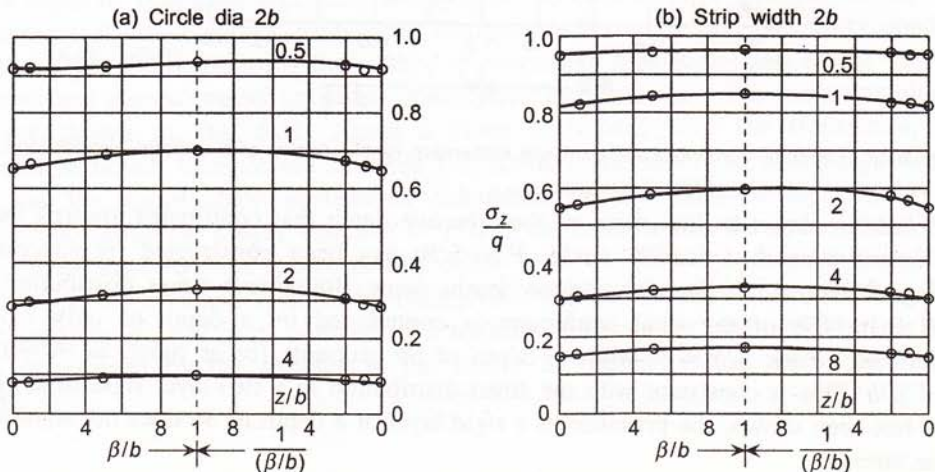


Fig. 5.28 Effect of non-homogeneity on the vertical stresses beneath centre of foundations (Som 1968).

Extensive field measurements of stresses reported by Plantema (1953), Turnbull et al. (1961), and the Waterways Experimental Station (1953, 1954) have shown very close agreement with the predictions based on Boussinesq analysis even though the soil media varied from non-homogeneous deposits (Plantema) to fairly homogeneous test sections of clayey silt and sand (Turnbull et al.). This is certainly in agreement with the theoretical results presented here.

If the foregoing conclusions are correct, the settlement of a foundation on a non-homogeneous medium may be calculated reasonably accurately by assuming that the stress distribution could be obtained by Boussinesq analysis. Figure 5.29 shows a comparison between the settlements of the centre of a uniformly loaded circle obtained from rigorous computation and the approximate settlements calculated from Boussinesq stress distribution. The latter underestimates the settlement for all values of β/b though the maximum error (in the range $0.5 < \beta/b < 1.5$) is no more than 10%.

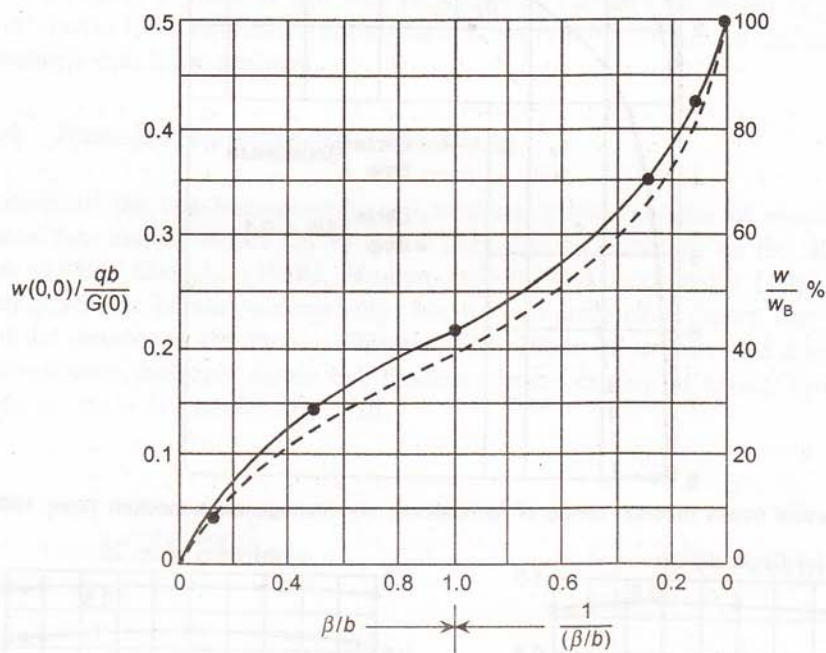


Fig. 5.29 Effect of non-homogeneity on the settlement of the centre of a uniform circular load.

In order to obtain an indication of the effective depth that contributes towards most of the settlement beneath a loaded circle, Fig. 5.30 has been constructed by successively integrating the vertical strains for various depths using Boussinesq stress distribution. It is observed that 80% of the total settlement is contributed by a depth of only $1.5b$ for $\beta/b = 0.1$ and $5b$ for $\beta/b = \infty$ while a depth of $8b$ accounts for as much as 90% for all values of β/b . This is consistent with the stress-distribution in a two-layer rigid base system, where, it has been shown, the presence of a rigid layer at a depth of $8b$ does not significantly affect the stresses.

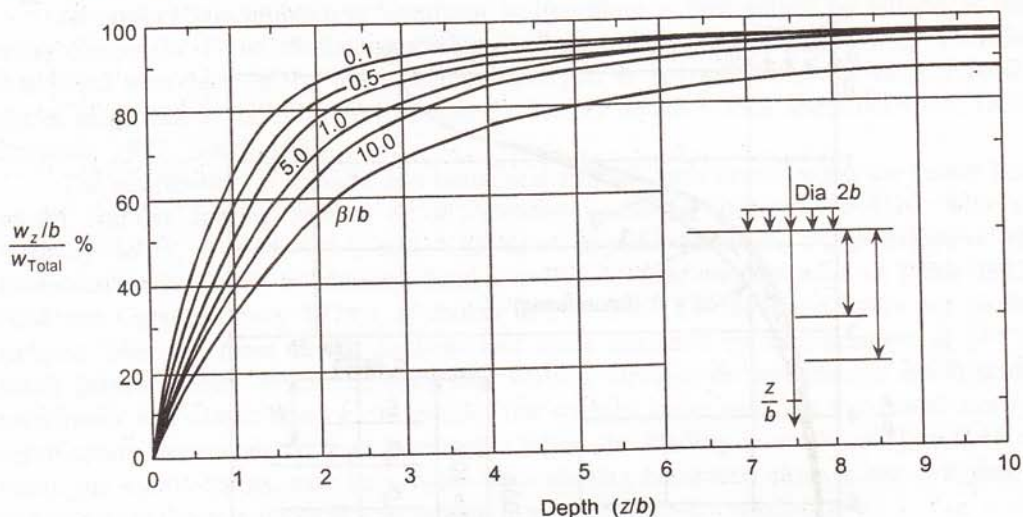


Fig. 5.30 Effective depth of soil beneath a circular foundation: non-homogeneous medium.

5.12 NONLINEAR SOIL

The problem of stress analysis in a soil medium with a nonlinear stress-strain relationship is immensely complex and no general solution is available yet. Huang (1968) presented a method of analyzing stresses and displacements beneath a circular load in a nonlinear soil medium whose modulus of elasticity is a function of the stresses.

$$E = E_0 [1 + c_\beta (\sigma_z + \sigma_r + \sigma_\theta + c_\gamma \gamma_z b)] \quad (5.40)$$

where c_β (the nonlinear coefficient) and c_γ (the body force coefficient) are material parameters. He divided the semi-infinite medium into a multilayer system assuming a rigid base at a depth of $100b$ (see Fig. 5.28) and assigned to each layer, a modulus corresponding to the stresses at the midpoint. Employing Burmister's boundary and continuity conditions (Burmister 1943, 1945) and using the method of successive approximations, Huang calculated the stresses and displacements until two consecutive iterations gave the same modulus. His results are shown in Fig. 5.31. Again a close agreement with the Boussinesq stress distribution is noted. Comparison between the actual settlements calculated rigorously by Huang and the approximate settlements calculated on the basis of Boussinesq stress distribution but using the proper variation of E with depth show that the two methods do not differ by more than 10%, as shown in Fig. 5.32.

However, the assumption made by Huang, that each layer has uniform modulus means that the problem is, in effect, reduced to a multilayer Burmister problem with the elastic moduli determined by the stresses in the centre of the individual layers as shown in Fig. 5.32.

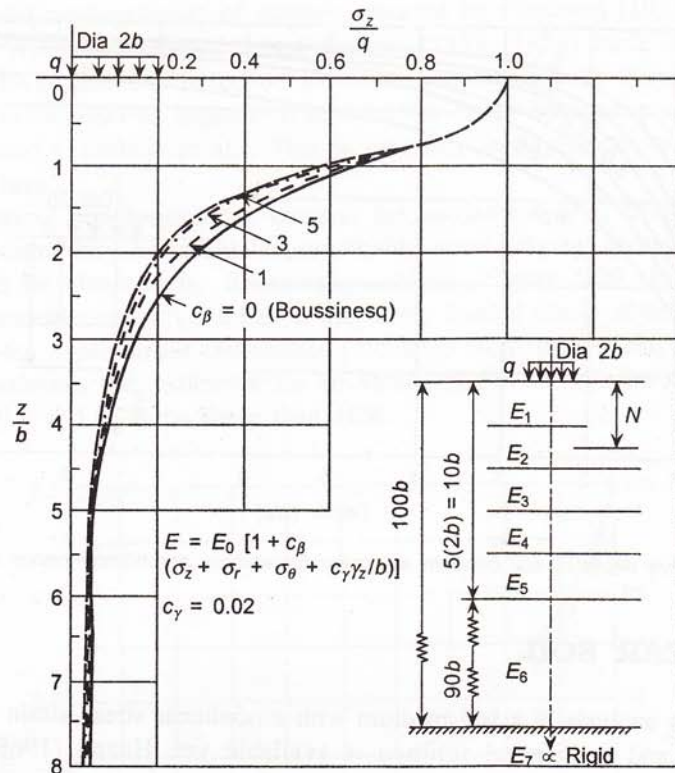


Fig. 5.31 Stresses in nonlinear soil medium (after Huang 1968).

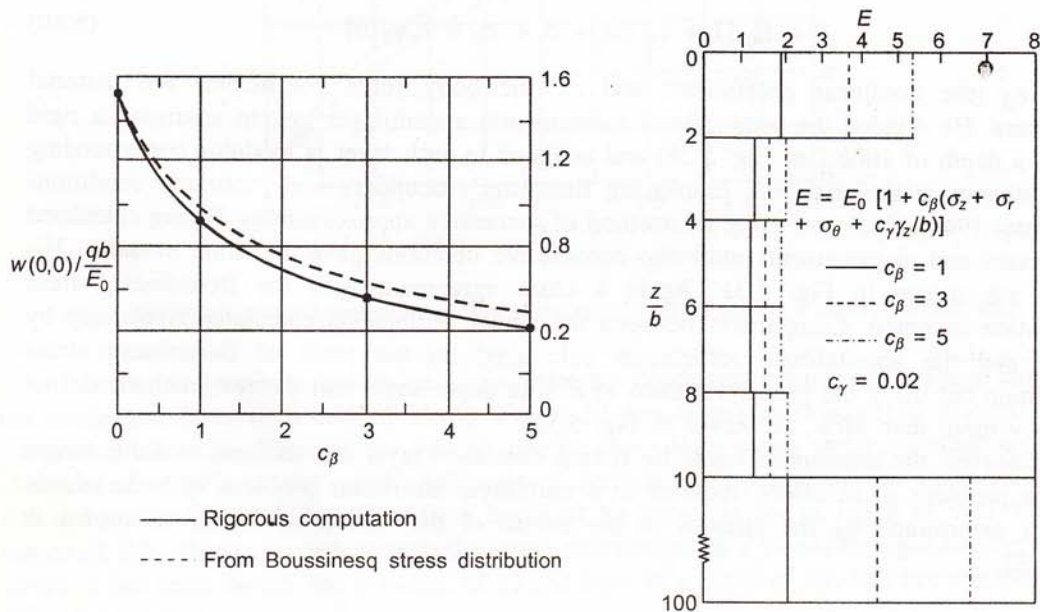


Fig. 5.32 Settlement at centre of circular load: nonlinear medium.

At present, the problem of nonlinear soil medium is best solved by numerical methods using computers. Finite element modelling is most widely used (Zienkiewicz 1971). However, a detailed treatment of the finite element analysis is beyond the scope of this book. The reader may refer to the relevant literature for further details (Desai and Abel 1972, Desai and Christian 1977, Smith 1988).

The distribution of vertical and horizontal stresses with depth, along the centre line of a model circular footing resting on a saturated normally consolidated clay, with a load intensity, $q/\sigma'_{vo} = 0.35, 0.77$, and 1.05 (q = applied pressure, σ'_{vo} = effective vertical consolidation pressure), as obtained from a nonlinear finite element analysis ((Das 1975) and (Das and Gangopadhyay 1978)), is shown in Fig. 5.33. On the same figure are plotted the stresses, obtained from elastic analysis and those obtained by measurement at $q/\sigma'_{vo} \approx 1$, using pressure cells. It can be seen that vertical stresses do not change much with load increments and elastic theory can predict the stresses quite well but horizontal stresses are significantly dependent on load increment. When the loading is small ($q/\sigma'_{vo} = 0.35$ in this case), the elastic theory may be capable of predicting horizontal stresses but at higher loads, non-linear analysis is necessary to predict horizontal stresses satisfactorily.

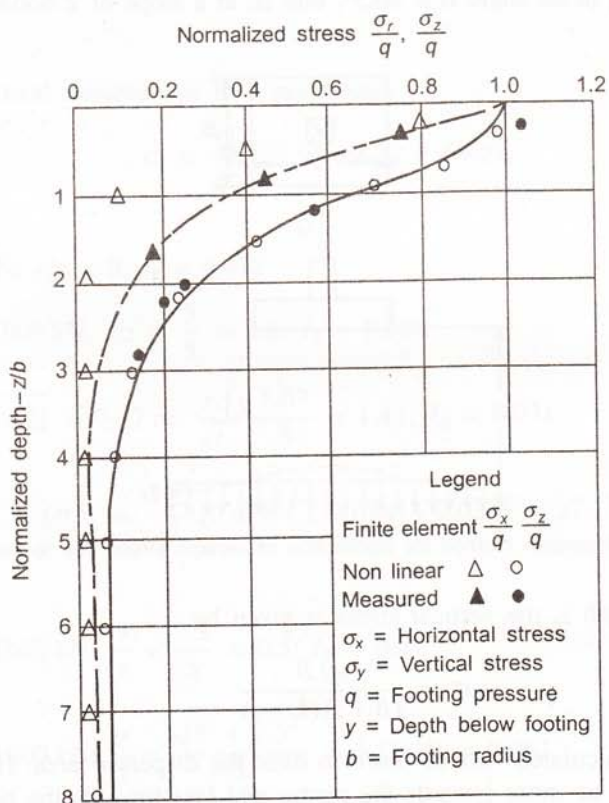


Fig. 5.33 Comparison of stresses obtained from linear and non-linear analysis (Das 1975).

Therefore, it appears that any deviation from the classical problem of homogeneous elasticity, either in terms of nonlinearity of stress-strain relationship or in terms of non-homogeneity of the medium will only have a marginal effect on the stress distribution so long as the medium is subjected to certain boundary stresses. The displacements will, of course, be significantly affected but from the foregoing it can be deduced that the settlement can be obtained with reasonable accuracy, by assuming the Boussinesq stress-distribution but taking account of the proper stress-strain relationship and/or non-homogeneity in calculating the strains. Also, as long as the pressure bulb due to a footing load is restricted within the upper layer of a soil deposit, the Boussinesq analysis should be reasonably valid, notwithstanding any non-homogeneity below that layer.

5.13 APPROXIMATE METHOD OF DETERMINING VERTICAL STRESS

The pressure on footing founded at or near the ground surface gets dispersed to a wider area at a depth. In the approximate method, the stress dispersion is assumed along lines through the edge of the footing at an angle $\alpha = 26.5^\circ$, that is, at a slope of 2 horizontal to 1 vertical, as shown in Fig. 5.34.

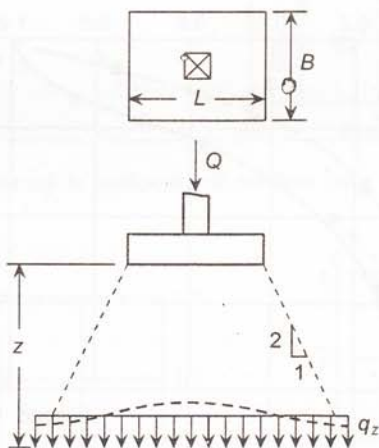


Fig. 5.34 2:1 dispersion method for distribution of vertical stress due to surface load.

Accordingly at any depth z , the vertical stress is given by,

$$\sigma_z = \frac{qLB}{(B+z)(L+z)} \quad (5.41)$$

The stress thus calculated will be uniform over the dispersed area. However, in actual practice, the stress will be more towards the centre and less towards the edges as shown by broken line in Fig. 5.34. The approximate method is not generally recommended for detailed design, although the method comes handy for rough calculations in the absence of necessary charts and tables.

Example 5.1

Figure 5.35 shows four vertical loads of 1000 kN each placed at the corners of a square of side 5 m. Determine the increase of vertical stress 5 m below

- each load
- midpoint between adjacent loads
- the centre of the rectangle

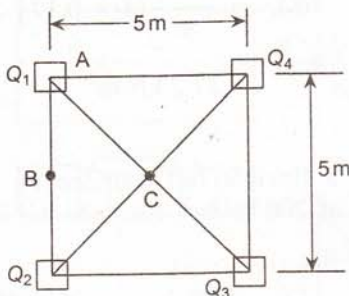


Fig. 5.35

Solution

From Fig 5.4, vertical stresses due to a point load

$$\sigma_z = \frac{Q}{z^2} I_B, \text{ where } I_B = f(r/z)$$

Point A

$$Q_1 = 1000 \text{ kN}; r/z = 0; I_B = 0.478$$

$$Q_2 = Q_4 = 1000 \text{ kN}, r/z = \frac{5}{5} = 1.0; I_B = 0.084$$

$$Q_3 = \sqrt{(5^2 + 5^2)} = 7.07 \text{ m}; \frac{r}{z} = \frac{7.07}{5} = 1.41; I_B = 0.031$$

$$\therefore (\sigma_z)_A = \frac{100}{5^2} [0.478 + 2(0.084) + 0.031] = 27.1 \text{ kN/m}^2$$

Point B

$$Q_1 = Q_2 = 1000 \text{ kN}; \frac{r}{z} = \frac{2.5}{5} = 0.5; I_B = 0.27$$

$$Q_3 = Q_4 = 1000 \text{ kN}; \frac{r}{z} = \frac{\sqrt{5^2 + 2.5^2}}{5} = 1.12; I_B = 0.062$$

$$\begin{aligned} \therefore (\sigma_z)_B &= \frac{100}{5^2} [2(0.27) + 2(0.062)] \\ &= 26.6 \text{ kN/m}^2 \end{aligned}$$

Point C

$$Q_1 = Q_2 = Q_3 = Q_4 = 1000 \text{ kN}$$

$$\frac{r}{z} = \frac{\sqrt{2.5^2 + 2.5^2}}{5} = 0.71; I_B = 0.17$$

$$\therefore (\sigma_z)_C = \frac{1000}{5^2} [4 \times 0.17]$$

$$= 27.2 \text{ kN/m}^2$$

Example 5.2

Figure 5.36 shows the plan of a flexible raft founded on the ground surface. The area supports a uniform vertical load of 200 kN/m^2 . Estimate the increase in vertical stress 15 m below point A.

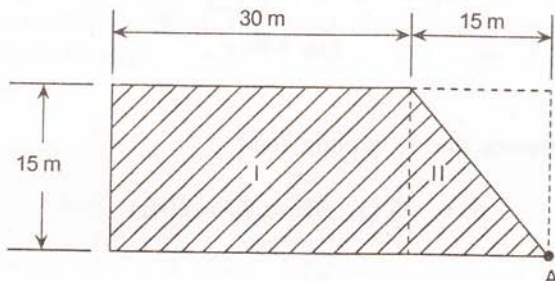


Fig. 5.36

Solution

Consider two rectangles (I + II) and II with the point A at the corner of each rectangle.

$$(\sigma_z)_A = q \left(I_{\sigma_{I+II}} - \frac{1}{2} I_{\sigma_{II}} \right)$$

Rectangle (I + II): $15 \text{ m} \times 45 \text{ m}$

$$m = \frac{45}{15} = 3.0; n = \frac{15}{15} = 1.0, I_{\sigma_{I+II}} = 0.201$$

Rectangle II: $15 \text{ m} \times 15 \text{ m}$

$$m = n = \frac{15}{15} = 1.0; I_{\sigma_{II}} = 0.174$$

$$\therefore (\sigma_z)_A = 200 [0.201 - \frac{1}{2} \times 0.174]$$

$$= 22.8 \text{ kN/m}^2$$

Example 5.3

Figure 5.37 shows a raft foundation ($10 \text{ m} \times 20 \text{ m}$) built 5 m from a tower. Determine the increase of stress 5, 10, 15, and 25 m below the tower and draw the stress distribution. (Take $q_n = 100 \text{ kN/m}^2$)

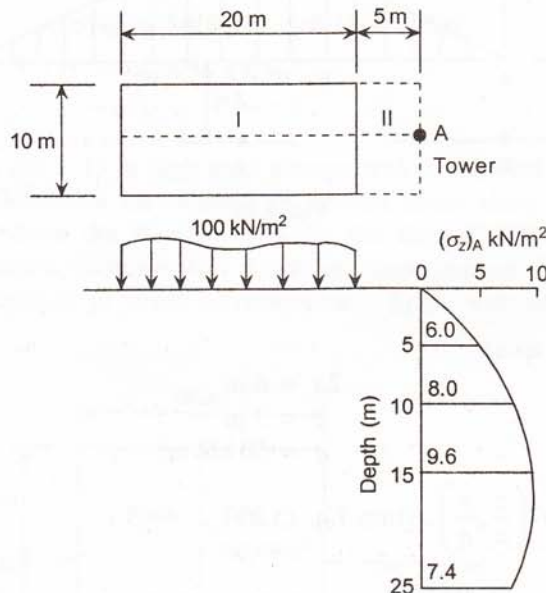


Fig. 5.37

Solution

Consider rectangles (I + II) and II with point A below each rectangle.

Rectangle (I + II): $25 \text{ m} \times 5 \text{ m}$

Rectangle II: $5 \text{ m} \times 5 \text{ m}$

Depth (m)	Influence factor		$I_\sigma = 2(I_{\sigma_{I+II}} - I_{\sigma_{II}})$ ($\sigma_z)_A = 100I_\sigma$			
	$I_{\sigma_{(I+II)}}$	$I_{\sigma_{(II)}}$			kN/m^2	
5 m	5	0.204	1.0	0.174	0.06	6.0
n	1		1.0			
10 m	2.5	0.136	0.5	0.096	0.08	8.0
n	0.5		0.5			
15 m	1.67	0.094	0.33	0.046	0.096	9.6
n	0.33		0.33			
25 m	1.0	0.054	0.2	0.017	0.074	7.4
n	0.2		0.2			

Example 5.4

Figure 5.38 shows the section of an earth dam. Determine the increase in vertical stress 3 m below points A and B.

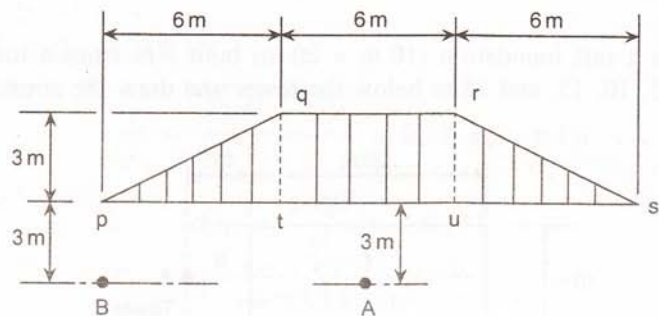


Fig. 5.38

Solution**Point A**

Stress due to strip load qrtut:

$$2a = 6 \text{ m}$$

$$z = 3 \text{ m}$$

$$q = 50 \text{ kN/m}^2$$

$$\sigma_z = q(I_\sigma) \text{ where } I_\sigma = f\left(\frac{z}{a}, \frac{x}{a}\right), \text{ from Eq. (5.23)}$$

$$\text{Here, } \frac{x}{a} = 0; \frac{z}{a} = \frac{3}{3} = 1.0; I_\sigma = 0.96$$

Stress due to triangular load, pqt

$$a = 6 \text{ m}$$

$$z = 3 \text{ m}$$

$$q = 50 \text{ kN/m}^2$$

$$\sigma_z = q(I_\sigma) \text{ where } I_\sigma = f\left(\frac{z}{a}, \frac{x}{a}\right), \text{ from Eq. (5.24)}$$

$$\text{Here, } \frac{x}{a} = \frac{9}{6} = 1.5; \frac{z}{a} = \frac{3}{6} = 0.5; I_\sigma = 0.06$$

$$\begin{aligned} \therefore (\sigma_z)_A &= 50[0.96 + 2(0.06)] \\ &= 54 \text{ kN/m}^2 \end{aligned}$$

Point B

Stress due to strip load: qrtut

$$\frac{x}{a} = \frac{9}{3} = 3.0; \frac{z}{a} = 1.0; I_\sigma = 0.003$$

Stress due to triangular load: pqt

$$\frac{x}{a} = 0; \frac{z}{a} = \frac{3}{6} = 0.5; I_\sigma = 0.13$$

Stress due to triangular load: rus

$$\frac{x}{a} = \frac{18}{6} = 3; \quad \frac{z}{a} = 0.5; \quad I_\sigma = 0.002$$

$$\therefore (\sigma_z)_B = 50(0.003 + 0.13 + 0.002) \\ = 6.75 \text{ kN/m}^2$$

Example 5.5

Figure 5.39 shows 20 m dia \times 15 m high steel storage tank is founded on RCC raft (500 mm thick) 5 m below GL. Determine the increase in vertical stress along the centre of the tank 10 m, 20 m and 30 m below the foundation when the tank is filled of water. Draw the distribution of vertical stress increase with depth and superimpose the same on the in-situ stresses to obtain the variation of stress increment ratio $\Delta p/p_0$ with depth. Take unit weight of soil = 18 kN/m³.

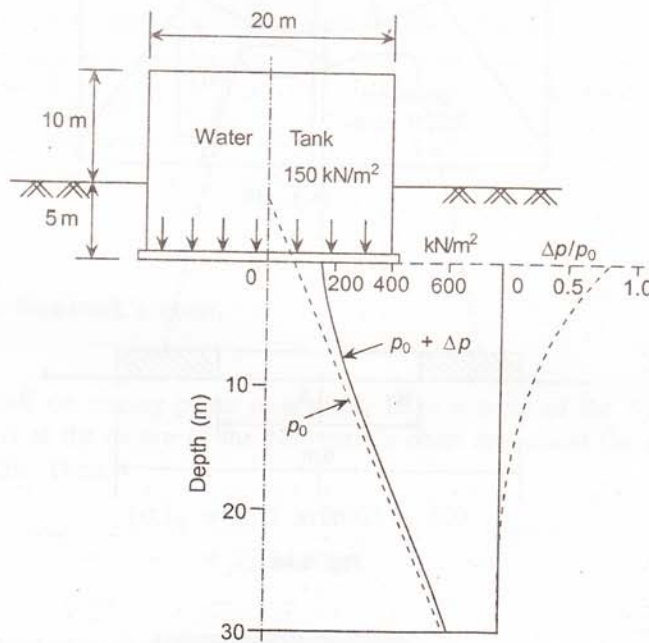


Fig. 5.39

Solution

$$\text{Water load} = 15 \times 10 = 150 \text{ kN/m}^2$$

$$\text{Self weight of foundation} = 0.5 \times 24 = 12 \text{ kN/m}^2$$

$$q_{\text{gross}} = 150 + 12 = 162 \text{ kN/m}^2$$

$$\text{Pressure reduced by excavation} = 18 \times 5 = 90 \text{ kN/m}^2$$

$$q_{\text{net}} = 162 - 90 = 72 \text{ kN/m}^2$$

Depth (m)	$\frac{r}{a}$	$\frac{z}{a}$	I_σ	$\Delta p = q_{\text{net}} I_\sigma$ (kN/m ²)	p_o (kN/m ²)	$\frac{\Delta p}{p_o}$
0	0	0	1.0	72.0	90	0.8
10	0	1.0	0.65	46.8	180	0.26
20	0	2.0	0.28	20.2	360	0.06
30	0	3.0	0.13	9.4	540	0.17
40	0	4.0	0.08	5.8	720	0.008

Example 5.6

A reinforced concrete tower is provided on a ring foundation of inner diameter 6 m and outer diameter 12 m, as shown in Fig. 5.40. If the foundation carries a distributed load of 150 kN/m², determine the vertical stress distribution at a depth of 6 m below the foundation. Use Newmark's chart.

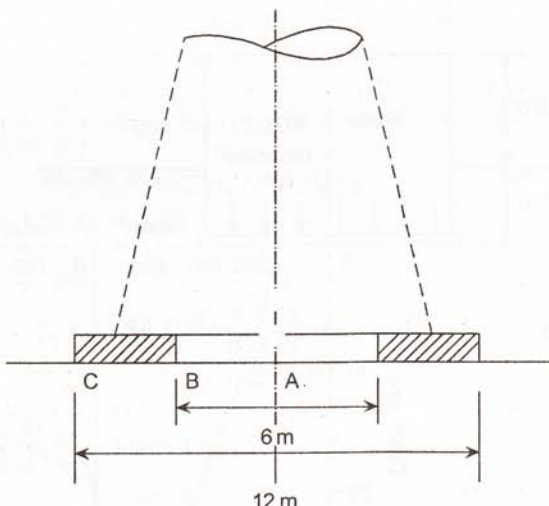


Fig. 5.40

Solution

Draw the plan of the foundation to scale, 3 m = the scale of the Newmark's chart to be used, as in Fig. 5.41. Then place points A, B, and C successively at the centre of the Newmark's chart and count the number of units enclosed in each case. Then,

$$\sigma_z = n(0.005) \times q_n$$

$$\text{Vertical stress below } A = 70 \times 0.005 \times 150 = 52.5 \text{ kN/m}^2$$

$$B = 60 \times 0.005 \times 150 = 45.0 \text{ kN/m}^2$$

$$C = 46 \times 0.005 \times 150 = 44.5 \text{ kN/m}^2$$

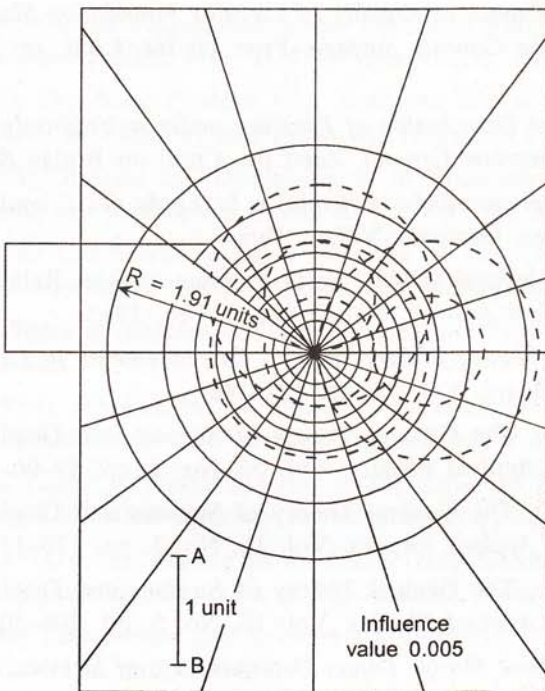


Fig. 5.41

Example 5.7

Solve Example 5.2 by Newmark's chart.

Solution

Draw the plan of the raft on tracing paper to a scale, 15 m = scale of the Newmark's chart, Fig. 5.40. Place point A at the centre of the Newmark's chart and count the number of units enclosed by the diagram. Then,

$$\begin{aligned}(\sigma_z)_A &= 23.5 \times 0.005 \times 200 \\&= 23.5 \text{ kN/m}^2\end{aligned}$$

REFERENCES

- Ahlvin, R.G. and H.H. Ulery (1962), *Tabulated Values for Determining the Complete Pattern of Stresses, Strains, and Deflections Beneath a Uniform Circular Load on a Homogeneous Half Space*, Highway Research Board Bulletin No. 342, p. 1.
- Biot, M.A. (1935), *The Effect of Certain Discontinuities on the Pressure Distribution in a Loaded Soil*, Physics, Vol. 6, No. 12, p. 367.
- Bishop, A.W. (1952), *The Stability of Earth Dams*, Ph.D. Thesis, University of London.

- Borowicka, H. (1936), *Influence of Rigidity of Circular Foundation Slab on the Distribution of Pressures over the Contact Surface*, Proc 1st Int. Conf. on S M & F E, Vol 2, pp. 144–149.
- Borowicka, H. (1938), *The Distribution of Pressure under a Uniformly Loaded Elastic Strip Resting on Elastic-isotropic Ground*, Zued Int. Conf. on Bridge & Str. Engs, Berlin.
- Boussinesq, J. (1985), *Application des Potential a L' Etude de L' equilibre et du Mouvement des Solides Elastiques*, Gauthiers Villars, Paris.
- Brooker, E.W. and H.O. Ireland (1965), Earth Pressure at Rest Related to Stress History, *Canadian Geotechnical Journal*, Vol. 2, No. 1, Feb. 1965.
- Burmister, D.M. (1943), *Theory of Stresses and Displacements in Layered Systems*, Proc. Highway Research Board, Vol. 22, pp. 127–148.
- Burmister, D.M. (1945 a), The General Theory of Stresses and Displacements in Layered Systems, *Journal of Applied Physics*, Vol. 16, No. 2, pp. 89–96.
- Burmister, D.M. (1945 b), The General Theory of Stresses and Displacements in Layered Systems, *Journal of Applied Physics*, Vol. 16, No. 3, pp. 126–127.
- Burmister, D.M. (1945 c), The General Theory of Stresses and Displacements in Layered Systems, *Journal of Applied Physics*, Vol. 16, No. 5, pp. 296–302.
- Carothers, S.D. (1920), *Plane Strain: Direct Determination of Stresses*, Proc . Royal Society Series A: Vol. 97, pp. 110–123.
- Das, B. (1997), *Advanced Soil Mechanics*, 2nd ed., Taylor and Francis, Washington, D.C.
- De Barros, S.T. (1966), *Deflection Factor Charts for Two and Three Layer Systems*, Highway Research Record No. 145, p. 83.
- Desai, C.S. and J.F. Abel (1972), *Introduction to Finite Element Methods*, Van Nostrand Reinhold, New York.
- Desai, C.S. and J.T. Christian (1977), *Numerical Methods in Geotechnical Engineering*, McGraw-Hill, New York.
- Das, S.C. (1975), *Predicted and Measured Values of Stress and Displacements Downloading and Construction under Circular Footings Resting on Saturated Clay Medium*, Ph.D. Thesis, Jadavpur University, Calcutta.
- Das, S.C. and C.R. Gangopadhyay (1978), *Undrained Stresses and Deformations under Footings as Clay*, Proc. ASCE, Vol. 104, GT 1, pp. 11–25.
- Fadum, R.E. (1948), *Influence Values for Estimating Stresses in Elastic Foundations*, Proc. 2nd ICSMFE, Vol. 3, p. 77.
- Fox (1948), *The Mean Elastic Settlement of a Uniformly Loaded Area at a Depth Below Ground Surface*, Proc. 2nd ICSMFE, Rotterdam, Vol. 1, p. 129.
- Gibson, R.E. (1967), Some Results Concerning Displacements and Stresses in Non-homogeneous Elastic Half Space, *Geotechnique*, Vol. 17, No. 1.
- Gibson, R.E. (1968), *Letter to Geotechnique*, Vol. 18, No. 2.

- Golecki, J. (1959), *On the Foundation of the Theory of Elasticity of Plane Incompressible Non-homogeneous Bodies*, Proc. IUTAM Symposium, Pergamon Press, London.
- Hruba, K. (1959), *The Basic Problem of a Nonlinear and a Nonhomogeneous Half Space, Nonhomogeneity in Elasticity and Plasticity*, Pergamon Press, London.
- Huang, Y.H. (1968), Stresses and Displacements in Nonlinear Soil Medium, *Journal ASCE Soil Mechanics and Foundation Division*, Vol. 94, SM 1.
- Jaky, J. (1944), *The Coefficient of Earth Pressure at Rest* (In Hungarian), Proc. 2nd Int. Conf. on Soil Mechanics and Foundation Engineering, Rotterdam, Vol. 2, pp. 16–20.
- Jones, A. (1962), *Table of Stresses in Three-layer Elastic Systems*, Highway Research Board Bulletin No. 342.
- Jurgenson, L. (1934), Application of Theories of Elasticity and Plasticity to Foundation Problems, *Journal Boston Soc. of Civil Engineering*, Vol. 21, No. 3.
- Kirk, J.M. (1966), *Tables of Radial Stresses in Top Layer of Three-layer Elastic Systems at Distance from Load Axis*, Highway Research Record No. 145.
- Korenev, B.G. (1957), *A Die Resting on an Elastic Half Space, the Modulus of Elasticity of which is an Exponential Function of Depth*, Dokl. Nank S.S.R., Vol. 112.
- Ladd (1977), *Stress Defamation and Strength Characteristics*, State-of-the art report, Proc. 7th ICSMFE, Vol. 2, pp. 421–494.
- Lekhnitskii, S.G. (1962), Radial Distribution of Stresses in a Wedge and in a Half Plane with Variable Modulus of Elasticity, *PMM*, Vol. 26, No. 1.
- Lemcof, M.M. (1961), *Stresses in Layered Elastic Solids*, Trans., ASCE, Vol. 126, p. 194.
- Love, A.E.H. (1928), *The Stress Produced in Semi-infinite Solid by Pressure on Part of the Boundary*, Phil. Trans. of Royal Society, Series A, Vol. 228, p. 377.
- Newmark, N.M. (1942), *Influence Charts for Computation of Stresses in Elastic Foundations*, Circular No. 24, Eng. Exp. Stn. Univ. of Illinois, USA.
- Plantema (1953), *Soil Pressure Measurements during Loading Tests on a Runway*, Proc. 3rd ICSMFE, Zurich, Vol. 1, p. 289.
- Pickett, G. (1938), *Stress Distribution in a Layered Soil with Some Rigid Boundaries*, Proc. Highway Research Board, Vol. 18, Part 2, 1938.
- Poulos, H.G. (1967), *Control of Leakage in the Triaxial Test*, Harvards Soil Mechanics Series No. 71, Cambridge, Mass.
- Peattie, K.R. (1962), *Stress and Strain Factors for Three-layer Systems*, Highway Research Board Bulletin No. 342.
- Schiffman, R.L. (1957), *Consolidation of Soil under Time-dependent Loading and Variable Permeability*, Proc. Highway Research Board, Vol. 37, pp. 584–617.
- Sherman, D.I. (1959), *On the Problem of Plane Strain in Nonhomogeneous Media, Nonhomogeneity in Elasticity and Plasticity*, Pergamon Press.
- Som, N. (1968), *The Effect of Stress Path on the Deformation and Consolidation of London Clays*, Ph.D. Thesis, University of London.

- Som, N. (1974), *Lateral Stresses during One-dimensional Consolidation of an Overconsolidated Clay*, Proc. 2nd S. E. Asian Conf. on Soil Mechanics and Foundation Engineering, Singapore, pp. 295-307.
- Terzaghi, K. (1943), *Theoretical Soil Mechanics*, John Wiley and Sons Inc.
- Turnbull, W.J., A. Maxwell, and R.G. Ahlvin (1961), *Stresses and Deflections in Homogeneous Soil Mass*, Proc. 5th ICSMFE, Paris, Vol. 2, p. 337.
- Uyeshita, K. and G.G. Meyerhof (1967), Deflections of Multilayered Soil System, *Journal ASCE SMFE*, Vol. 93, SM 5.
- Vesic, A.B. and R.D. Barksdale, (1963), *On Shear Strength of Sand at Very High Pressures*, ASTM STP No. 361, p. 301.
- Waterways Expt. Station, Vicksburg (1953, 1954), *Investigations of Pressures and Deflections for Flexible Pavements*, Report 3 (Sept. 1953), Report 4 (Dec. 1954).
- Zienkiewicz, O.C. (1977), *The Finite Element Method*, in *Engineering Science*, McGraw-Hill Book Co., London.

6

Bearing Capacity of Shallow Foundations

6.1 INTRODUCTION

The bearing capacity of foundation is the maximum load per unit area which the soil can support without failure. It depends on the shear strength of soil as well as on the type, size, depth, and shape of the foundation.

Figure 6.1 shows a typical load versus settlement relationship of a footing. As the footing load is increased, the settlement also increases. Initially the settlement increases almost linearly with load indicating elastic behaviour of the soil. Thereafter, the settlement increases more rapidly and then continues to increase even without any appreciable increase of load. The foundation is then said to have failed, that is, the soil has reached its capacity to bear superimposed load.

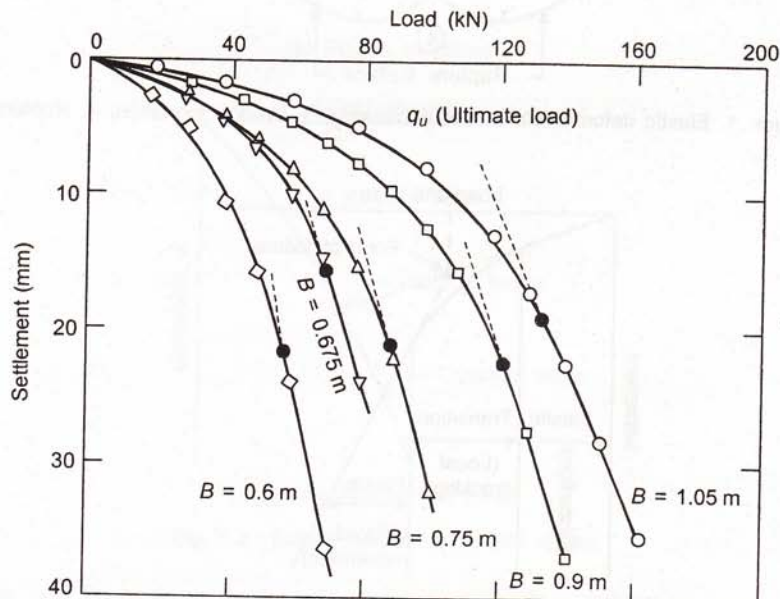


Fig. 6.1 Load versus settlement relationship of footing. (Test data from Das 1999)

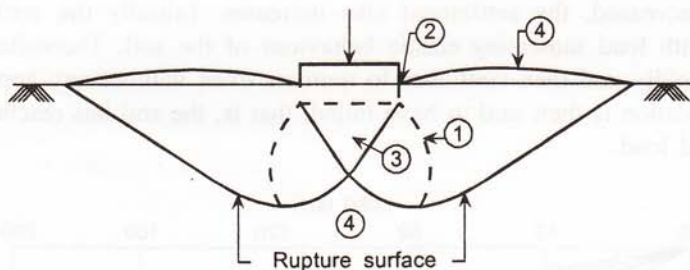
In order to make the bearing capacity analysis of a foundation it is necessary to know the actual mechanism of failure. There are different methods to analyze bearing capacity, each based on different assumptions on the mechanism of failure and mobilisation of shear strength of soil.

6.2 FAILURE MECHANISM

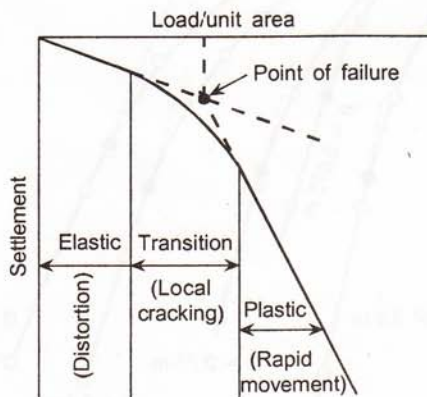
From model studies, it has been observed that there are possibly four stages of deformation in the soil leading ultimately to a bearing capacity failure. These include:

1. Elastic deformation or distortion
2. Local cracking around the perimeter of the loaded area
3. Formation of a wedge below the footing which moves downward, pushing the soil side ways.
4. Formation of a rupture surface which may extend upto the level of foundation. The footing then sinks rapidly into the soil followed by bulging or heaving at the top.

These stages are illustrated in Fig. 6.2(a) and the corresponding load-settlement curve is shown in Fig. 6.2(b) where a method of determining failure load is also indicated.



(a) Stages of failure: 1. Elastic deformation; 2. Local cracking; 3. Wedge formation; 4. Rupture surface.



(b) Load-settlement curve

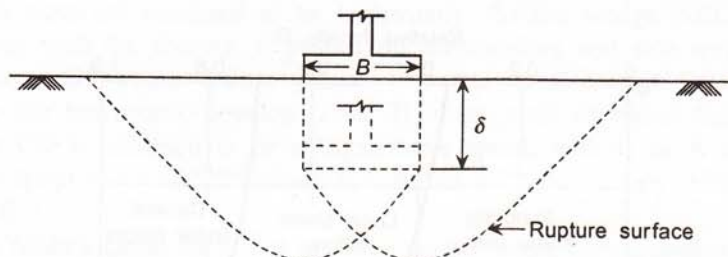
Fig. 6.2 Failure mechanism: General shear.

The load-settlement curve has three distinct parts:

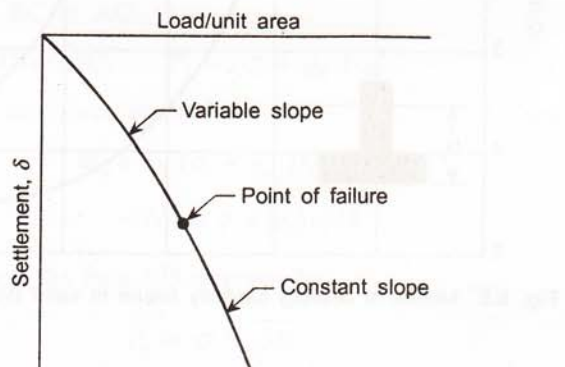
- Elastic*, where there is distortion of soil.
- Transition*, where there is local cracking.
- Plastic*, indicated by rapid movement.

This type of failure is called *General Shear Failure* where large settlement of footing is not required for the development of rupture surface. This is generally observed when the ratio of depth of footing to the width of footing is relatively small and the soil consists of medium to stiff clay or medium to dense sand.

In loose sand, much larger settlement would be required for the shear surface to develop upto the level of footing. The footing may be considered to have failed by excessive settlement before that stage is reached. This type of failure is known as *Local Shear Failure* and is illustrated in Fig. 6.3(a). The corresponding load-settlement curve is shown in Fig. 6.3(b). The point on the load-settlement curve where the slope becomes steep and almost constant is considered as the failure point. If the settlement corresponding to this point is more than a chosen critical value, say 10% of the width of the footing, then the load corresponding to that critical settlement is considered as the failure load.



(a) Stages of failure



(b) Load-settlement curve

Fig. 6.3 Failure mechanism: Local shear.

When the soil is predominantly soft and cohesive, the settlement increases at a very rapid rate and reaches the critical value even before the rupture surface is fully developed. This type of failure is known as *punching shear failure*, refer Fig. 6.4.

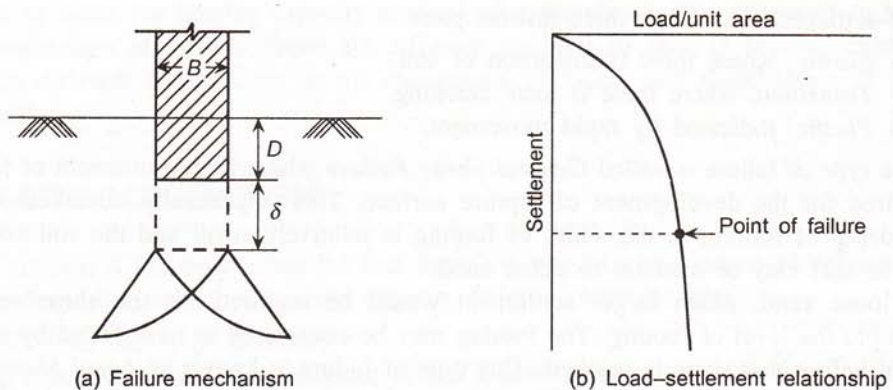


Fig. 6.4 Punching shear failure.

Vesic (1973) gives the range of relative density of granular soil for punching shear, local shear, and general shear failure, depicted in Fig. 6.5.

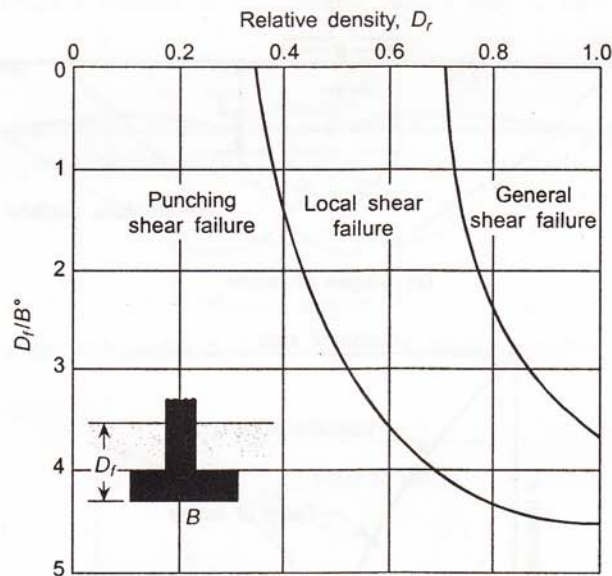


Fig. 6.5 Modes of bearing capacity failure in sand (Vesic, 1973).

6.2.1 Prandtl's Analysis

A method for analysis of bearing capacity, considering an apparently realistic mechanism of failure was first suggested by Prandtl in his plastic equilibrium theory (Terzaghi, 1943). According to Prandtl, the failure mass consists of three zones, with the failure surface given by a logarithmic spiral. Figure 6.6 shows Prandtl's bearing capacity analysis.

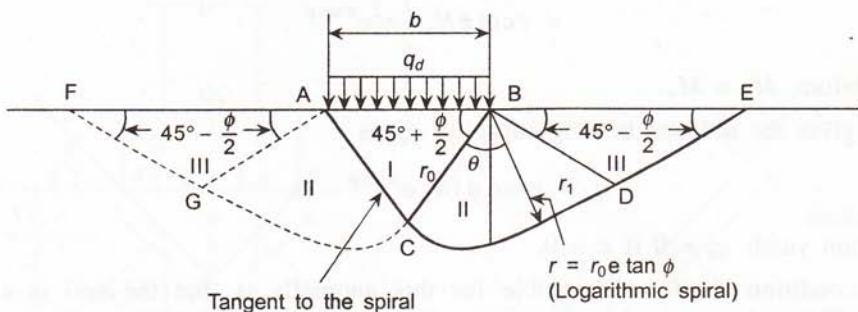


Fig. 6.6 Prandtl's bearing capacity analysis: failure surface and zones of failure.

When the applied footing pressure reaches the ultimate bearing pressure, the soil fails along a surface ACDE or BCGF. The failure mass consists of three zones. Zone I, immediately below the footing is under active pressure where failure surfaces AC and BC develop, inclined at $(45^\circ + \phi/2)$ to horizontal. The soil is assumed to be weightless, and the stresses in this zone are assumed to be hydrostatic. As the wedge ABC tends to move downward along with the footing, it pushes the surrounding soil side ways. Passive state develops in zone III where failure planes FG, AG or BD, and DE, all inclined at $(45^\circ - \phi/2)$ to the horizontal, develop. Zone II is the zone of radial failure planes. The surface CG or CD is assumed to be a logarithmic spiral, with B or A as the pole. The equation of the spiral is $r = r_0 e^{\theta \tan \phi}$ where $r_0 = BC$ or AC , and r is any radius BX at a spiral angle $CBX = \theta$.

From the Mohr's circle for $c - \phi$ soil, the normal stress corresponding to the cohesion intercept, is $\sigma_i = c \cot \phi$. This is termed as *initial stress*, which acts normally to BC and AC (assumed hydrostatic pressure in zone I). Also the applied pressure, q_d is assumed to be transferred normally on to BC or AC.

Thus, the force on BC or AC, $P_I = (\sigma_i + q_d) r_0$.

The disturbing moment of this force about B is

$$\begin{aligned} M_d &= r_0 (\sigma_i + q_d) r_0 / 2 \\ &= (c \cot \phi + q_d) r_0^2 / 2 \end{aligned} \quad (6.1)$$

The passive resistance, P_p on the face BD is given by

$$P_p = \sigma_i N_\phi \overline{BD}$$

where, $N_\phi = \tan^2(45^\circ + \phi/2)$

This is because σ_i , due to cohesion alone, is transmitted by the wedge BDE. The resisting moment M_y is given by its moment about B as,

$$M_y = \frac{P_p BD}{2} = \frac{\sigma_i N_\phi (BD)^2}{2}$$

$$= c \cot \phi N_\phi \frac{1}{2} r_0^2 e^{\pi \tan \phi} \quad (6.2)$$

For equilibrium, $M_d = M_y$.

This gives the ultimate bearing capacity, q_d , as

$$q_d = c \cot \phi (N_\phi e^{\pi \tan \phi} - 1) \quad (6.3)$$

This equation yields $q_d = 0$ if $c = 0$.

The condition chiefly responsible for this anomaly is that the soil is considered weightless. This was corrected by Reissner (1924) and Terzaghi (1943) as

$$q_d = c \cot \phi + \left(\frac{1}{2} \gamma B \sqrt{N_\phi} \right) (N_\phi e^{\pi \tan \phi} - 1) \quad (6.4)$$

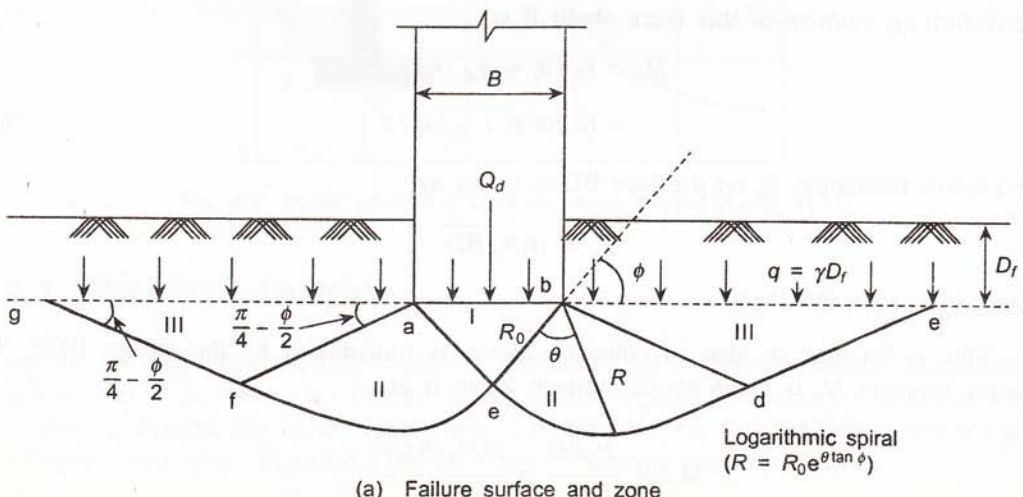
For soil with $\phi = 0$, the logarithmic spiral becomes a circle, and Prandtl's Eq. (6.3) or (6.4) gives on application of L'Hospital's rule,

$$q_d = (\pi + 2)c = 5.14c \quad (6.5)$$

It may be noted that Prandtl's expression is independent of the width of the footing. Also the assumed shape of the failure surface does not resemble the actual failure surface because of the compressibility of soil, roughness of contact surface and other factors.

6.2.2 Terzaghi's Analysis

Terzaghi (1943) considered the roughness of the footing and also the weight of the soil above the horizontal plane through the base of the footing, and modified the expression derived by Prandtl. The corresponding failure surface and failure mass are shown in Fig. 6.7.



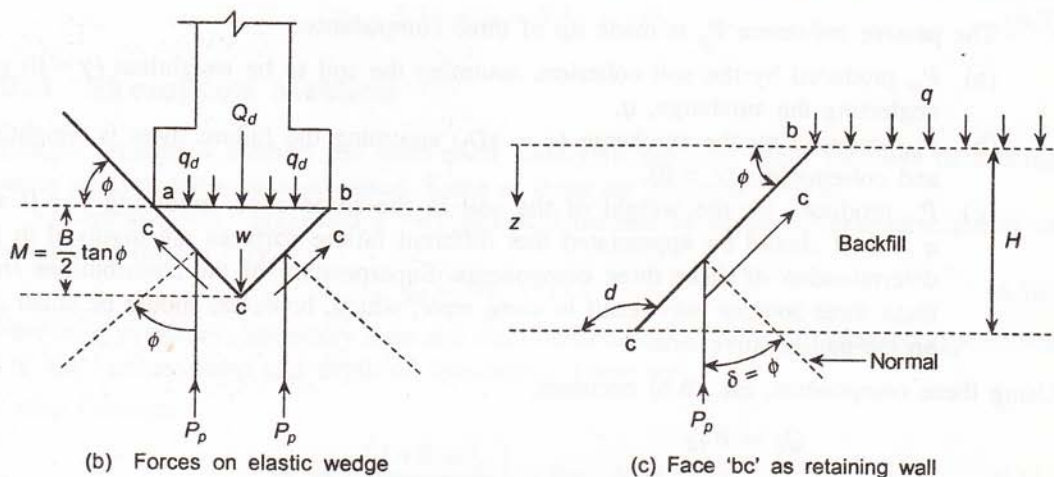


Fig. 6.7 Terzaghi's bearing capacity analysis.

The soil mass above the failure surface consists of three zones:

Zone I: Due to the friction and adhesion between the soil and the base of the footing, this zone cannot spread laterally. It moves downward as an elastic wedge and the soil in this zone behaves as if it is a part of the footing. The two sides of the wedge ac and bc make angle ϕ with the horizontal.

Zone II: The zones aef and bed are zones of radial shear. The soil in this zone is pushed into zone III.

Zone III: These are two passive Rankine zones. The boundaries of these zones make angles $(45^\circ - \phi/2)$ with the horizontal.

As the footing sinks into the ground, the faces ac and bc of the wedge abc push the soil to the sides. When plastic equilibrium is reached, the forces acting on the wedge abc are the ones shown in Fig. 6.6. The forces are

- The ultimate footing load $Q_d = Bq_d$
- The weight of the wedge, $W = (1/4)\gamma B^2 \tan \phi$
- The passive resistance P_p acting on the faces ac and bc. Since the soil shears along these planes, and the shearing is between soil and soil, P_p is inclined at an angle ϕ to the normal. Since ac and bc are inclined at ϕ to the horizontal, P_p acts vertically.
- The cohesive force on the faces ac and bc: $C_a = cB/(2\cos \phi)$ where c = unit cohesion.

For equilibrium,

$$Q_d + \frac{1}{4}\gamma B^2 \tan \phi - 2P_p - Bctan\phi = 0$$

or,

$$Q_d = 2P_p = Bctan\phi - \frac{1}{4}\gamma B^2 \tan \phi \quad (6.6)$$

An expression for P_p may be obtained by considering the face bc as a retaining wall.

The passive resistance P_p is made up of three components:

- P_{pc} produced by the soil cohesion, assuming the soil to be weightless ($\gamma = 0$) and neglecting the surcharge, q .
- P_{pq} produced by the surcharge ($q = \gamma D_f$) assuming the failure mass is weightless and cohesionless ($c = 0$).
- $P_{p\gamma}$ produced by the weight of the soil in the shear zone, assuming $c = 0$ and $q = 0$. It should be appreciated that different failure surfaces are involved in the determination of these three components. Superposition of the contributions from these three sources may result in some error, which, however, should be small and on the conservative side.

Using these components, Eq. (6.6) becomes,

$$\begin{aligned} Q_d &= Bq_d \\ &= 2(P_{pc} + P_{pq} + P_{p\gamma}) + Bc \tan \phi - \frac{1}{4}\gamma B^2 \tan \phi \end{aligned} \quad (6.7)$$

Let $2P_{pc} + Bc \tan \phi = BcN_c$

$$2P_{pq} = BqN_q$$

$$2P_{p\gamma} - \frac{1}{4}\gamma B^2 \tan \phi = B \frac{1}{2}\gamma BN_\gamma$$

Eq. (6.7) can now be written as

$$q_d = cN_c + qN_q + 0.5\gamma BN_\gamma \quad (6.8)$$

Eq. (6.8) is the Terzaghi's bearing capacity equation for a strip footing corresponding to general shear failure. N_c , N_q , and N_γ are dimensionless bearing capacity factors which depend on ϕ only.

The values of Terzaghi's bearing capacity factors for general shear failure given in Table 6.1.

Table 6.1 Terzaghi's bearing capacity factors for general shear failure

Q	N_c	N_q	N_γ
0	5.7	1.0	0.10
5	7.0	1.6	0.14
10	9.5	2.7	0.7
15	13.0	4.5	2.0
20	17.0	7.5	4.8
25	24.0	13.0	9.8
30	37.0	23.0	20.0
35	58.0	42.0	43.0
40	98.0	77.0	98.0

For footings on saturated cohesive soil, critical condition for stability generally occurs at end of construction. Here, undrained condition exists, for which $\phi_u = 0$. Corresponding values of bearing capacity factors (refer Eq. 6.8) are $N_c = 5.7$, $N_q = 1$ and $N_\gamma = 0$.

Thus,

$$q_d = 5.7c + q = 5.7c + \gamma D_f \quad (6.9)$$

6.2.3 Skempton Method

Although Terzaghi's method has been used widely in practice, other methods of bearing capacity analysis have been proposed. Some of these are presented below:

Skempton (1951) suggested a very practical method of obtaining bearing capacity of footings on saturated clay.

$$q_d = cN_c + \gamma D_f \quad (6.10)$$

On the basis of theory, laboratory tests and field observations, Skempton obtained expressions for N_c for various shape and depth of foundation. These are:

For strip footings:

$$N_c = 5 \left(\frac{1 + 0.2D_f}{B} \right), \quad \text{for } N_c \leq 7.5 \quad (6.11)$$

For rectangular, square or circular footings:

$$N_c = 6 \left(1 + 0.2 \frac{B}{L} \right) \left(1 + 0.2 \frac{D_f}{B} \right), \quad \text{for } N_c \leq 9 \quad (6.12)$$

where, D_f = depth of footing

B = width (or diameter) of footing

L = Length of footing

6.2.4 Meyerhof's Method

Meyerhof (1951) suggested a method of analysis in which the failure surface would extend upto the ground surface, unlike that of Terzaghi's analysis, in which failure surface was considered to extend upto the base level of the footing. The failure surface and the zones of shear considered by Meyerhof are shown in Fig. 6.8.

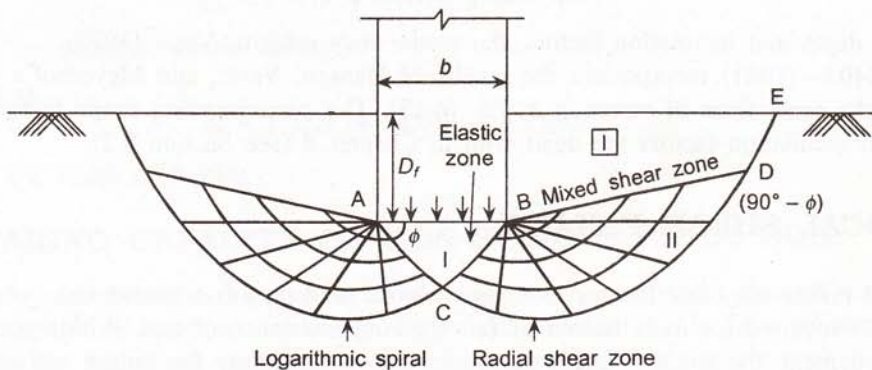


Fig. 6.8 Meyerhof's bearing capacity analysis.

Meyerhof's bearing capacity equation for strip footing is similar in form to that of Terzaghi, but the values of N_c , N_q , and N_γ are different. This method generally over estimates bearing capacity for sandy soil, because footings may fail from settlement consideration much before the failure surface reaches the ground surface. However, for clay soil the method gives quite good results.

6.2.5 Hansen's Method

Brinch Hansen (1957, 1970) proposed a general expression for bearing capacity considering effects of shape and depth of footing and inclination of applied load:

$$q_d = cN_c s_c d_c i_c + qN_q s_q d_q i_q + 0.5\gamma BN_\gamma s_\gamma d_\gamma i_\gamma \quad (6.13)$$

where s_c , s_q , and s_γ are empirical shape factors.

d_c , d_q and d_γ are empirical depth factors.

i_c , i_q , and i_γ are empirical inclination factors.

The recommendations of Hansen for N_c and N_q are identical to those of Meyerhof, and are the result of those of Prandtl (1921) and Reissner (1924).

These are :

$$\begin{aligned} N_c &= (N_q - 1)\cot \phi \\ N_q &= (e^{\pi \tan \phi}) \tan^2(45^\circ + \phi/2) \\ N_\gamma &= 1.5(N_q - 1) \tan \phi \end{aligned} \quad (6.14)$$

6.2.6 Vesic's method

The failure surface considered by Vesic is similar to that of Terzaghi's with the exception that the zone I below the footing is in active Rankine state, with inclined faces of the wedge at $(45^\circ + \phi/2)$ to the horizontal. The bearing capacity equation is the same as Eq. (6.13). The factors N_c and N_q are identical to those of Meyerhof and Hansen. N_γ , given by Vesic, is a simplified form of that given by Caquot and Kerisel (1948).

$$N_\gamma = 2(N_q + 1)\tan \phi \quad (6.15)$$

For shape, depth and inclination factors, the reader may refer to Vesic (1973).

I.S. 6403—(1981) incorporates the results of Hansen, Vesic, and Meyerhof's analyses and gives the same form of equation as Eq. (6.13). The corresponding shape factors, depth factors, and inclination factors are dealt with in Chapter 8 (see Section 8.2).

6.3 LOCAL SHEAR FAILURE

Local shear failure may develop for footings on loose sand or soft cohesive soil, where large settlement is required for mobilization of full shearing resistance of soil. Within permissible limit of settlement, the shear strength parameters mobilized along the failure surface are c_m and ϕ_m . Terzaghi proposed that for local shear failure, c_m and ϕ_m should be used in the

bearing capacity equation and factors N'_c , N'_q , and N'_γ should be determined on the basis of ϕ_m instead of ϕ . Terzaghi empirically suggested that

$$\phi_m = (2/3)\phi \quad \text{and} \quad c_m = (2/3)c$$

Thus, the bearing capacity equation for local shear failure becomes,

$$q_d = (2/3)cN'_c + qN'_q + 0.5\gamma BN'_\gamma \quad (6.16)$$

where N'_c , N'_q , and N'_γ are bearing capacity factors for local shear failure depicted in Fig. 6.9.

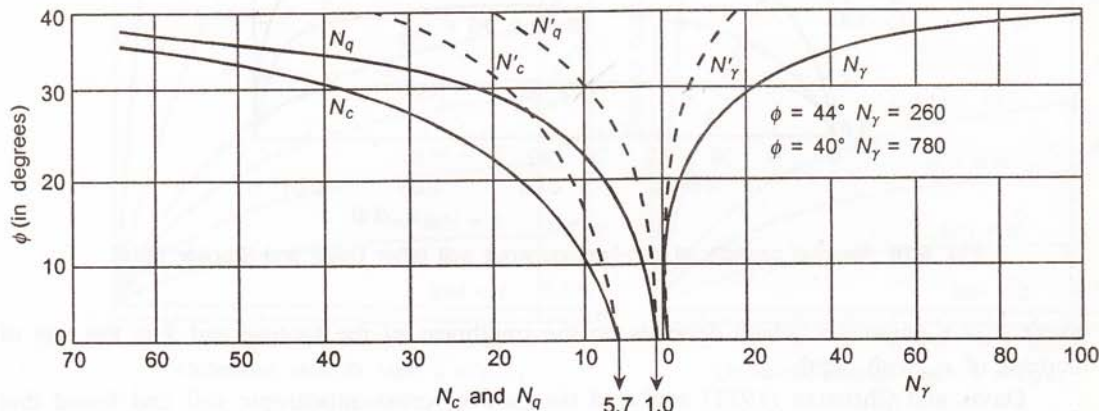


Fig. 6.9 Terzaghi's bearing capacity failure for general and local shear.

6.4 SQUARE AND CIRCULAR FOOTINGS

Equation (6.8) is valid for plane strain failure condition, as may occur in the case of strip footings. For square or circular footings, plastic zones would be three dimensional. So plane strain analysis is not strictly applicable. On the basis of experimental and field evidences, Terzaghi suggested the following modifications for circular and square footings.

Circular footing

$$q_d = 1.3cN_c + \gamma D_f N_q + 0.3\gamma DN_\gamma \quad (6.17)$$

where D is the diameter of the footing.

Square footing

$$q_d = 1.3cN_c + \gamma D_f N_q + 0.4\gamma BN_\gamma \quad (6.18)$$

where B is the width of footing.

6.5 BEARING CAPACITY OF NON-HOMOGENEOUS SOIL

Soft normally consolidated clays often show increase of undrained shear strength with depth because of increasing overburden pressure. Davis and Brooker (1973) gave solutions for a strip footing for undrained shear strength of the soil increasing linearly with depth, as illustrated in Fig. 6.10. The net ultimate bearing capacity is given by,

$$q_{ult} = A \left[(2 + \pi) c_{uo} + \lambda \frac{B}{4} \right] \quad (6.19)$$

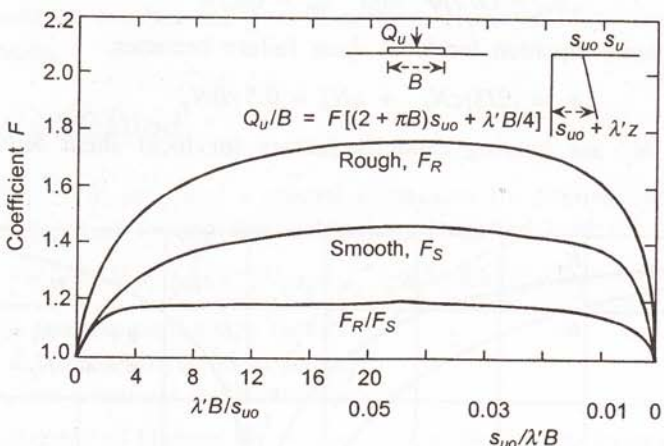


Fig. 6.10 Bearing capacity of non-homogeneous soil (after Davis and Brooker 1973).

where A is a parameter which depends on the roughness of the footing and λ is the rate of increase of c_u with depth.

Davis and Christian (1971) analyzed the case of cross-anisotropic soil and found that the value of c_u may be taken with sufficient accuracy, as

$$c_u = 0.9 \left(\frac{c_{uv} + c_{uh}}{2} \right) \quad (6.20)$$

where c_{uv} and c_{uh} are the undrained strength of the soil in the vertical and horizontal direction respectively. Good prediction of bearing capacity of model footings in Boston blue clay was obtained by using Eq. (6.20).

Vesic (1975) made detailed theoretical analysis of two-layer soil system, shown in Fig. 6.11, with the bearing stratum either softer or stiffer than the underlying stratum. In the first case, failure is partly by lateral plastic flow whereas in the second situation, failure is caused by punching shear. The net ultimate bearing capacity of the footing is given by,

$$q_{ult} = c_1 N_m \quad (6.21)$$

where N_m is a modified bearing capacity factor which depends on the ratio of shear strength of the two strata and the thickness of the bearing stratum and is given as

$$N_m = \frac{kN_c^*(N_c^* + \beta - 1)[(k + 1)N_c^{*2} + (1 + k\beta)N_c^* + \beta - 1]}{[k(k + 1)N_c^* + k + \beta - 1][(N_c^* + \beta)N_c^* + \beta - 1] - (kN_c^* + \beta - 1)(N_c^* + 1)} \quad (6.22)$$

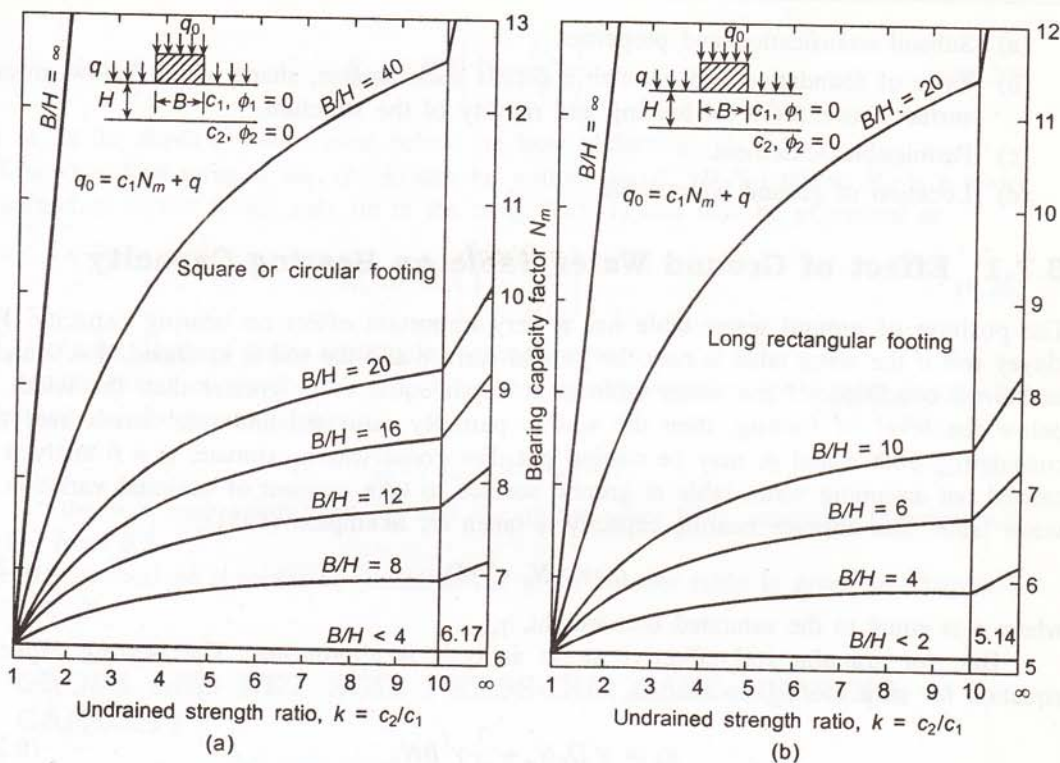


Fig. 6.11 Bearing capacity of stratified soil (after Vesic 1975).

With the development of non-linear finite element techniques, it is now possible to carry out rigorous analysis to determine the bearing capacity of footing for non-ideal field situations. Simple cases of bilinear stress-strain model, elastoplastic model or piecewise linear representation of the stress-strain behaviour have been adopted to obtain good prediction of the load-deformation behaviour of footings (D'Appolonia and Lambe 1970).

6.6 LIMITATIONS OF THEORETICAL ANALYSIS

Accurate prediction of bearing capacity by theoretical analysis often becomes difficult due to various reasons. This departure from accuracy may be because

- Correct estimation of in-situ soil properties are not always possible.
- Bearing capacity factors are sensitive to ϕ , which may change even during the process of failure.
- The unit weight of soil in the failure zones also changes during failure.
- The true shape of rupture surface is difficult to determine.

6.7 FACTORS AFFECTING BEARING CAPACITY

Bearing capacity depends on a number of factors. Some of the important factors are listed here.

- (a) Subsoil stratification and properties.
- (b) Type of foundation and geometric details such as size, shape, depth below ground surface, eccentricity of loading and rigidity of the structure.
- (c) Permissible settlement.
- (d) Location of ground water table.

6.7.1 Effect of Ground Water Table on Bearing Capacity

The position of ground water table has a very important effect on bearing capacity. For clayey soil if the water table is near the ground surface and the soil is saturated, $\phi = 0$ under undrained condition. If the water table is at depth equal to or greater than the width, B below the level of footing, then the soil is partially saturated and total stress analysis, considering both c and ϕ , may be carried out. For conservative estimate, $\phi = 0$ analysis is carried out assuming water table at ground surface to take account of seasonal variation in water table. The ultimate bearing capacity is taken as, Skempton (1951),

$$q_d = cN_c + \gamma D_f \quad (6.23)$$

where γ is equal to the saturated unit weight, γ_{sat} .

But, for granular soil effective stress analysis is appropriate. The bearing capacity equation for strip footing on sand is,

$$q_d = \gamma' D_f N_q + \frac{1}{2} \gamma' B N_\gamma \quad (6.24)$$

where γ' is the effective unit weight and N_q and N_γ depend on ϕ' . Here, γ' depends on the position of water table, as depicted in Fig. 6.12.

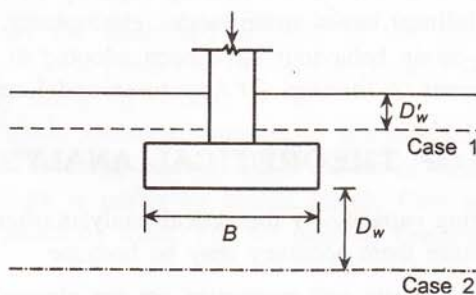


Fig. 6.12 Effect of ground water table.

For the strip footing shown in Fig. 6.12, the depth of failure surface does not extend beyond a depth equal to the width of the footing B below the footing base. If the water table is at or beyond this depth, it will have no effect on bearing capacity. If the water table is at the base of the footing or above, then in the second term of Eq. (6.24) $\gamma' = \gamma'_{\text{sub}}$, which is about half the value of γ_{sat} . The second term of Eq. (6.24) can now be written as $(1/2)R_w \gamma B N_\gamma$ where R_w is a water table correction which may vary from 0.5 to 1 and can be expressed as

$$R_w = 0.5 \left(1 + \frac{D_w}{B} \right) \quad (6.25)$$

where D_w is the depth of water table below the base of footing.

Likewise, first term of Eq. (6.24) can be written as $(R'_w \gamma D_f N_q)$ where R'_w is a water table correction factor, which may lie in the range (0.5–1) and may be expressed as

$$R'_w = 0.5 \left(1 + \frac{D'_w}{D_f} \right) \quad (6.26)$$

where D'_w is the depth of water table below ground surface.

Thus, to take effect of water table, the bearing capacity equation for a strip footing on granular soil may be expressed as:

$$q_d = R'_w \gamma D_f N_q + 0.5 R_w \gamma B N_\gamma \quad (6.27)$$

where γ is the bulk unit weight, and R_w , and R'_w are the water table correction factors which may vary from 0.5–1.

A practical method of considering the effect of ground water table is given in Chapter 8 (Section 8.2.3)

6.8 GROSS AND NET SOIL PRESSURE: SAFE BEARING CAPACITY

The total pressure transmitted to the subsoil by a foundation is the *gross soil pressure*, and the maximum gross pressure at which the soil fails is known as the *ultimate gross bearing capacity*. At the level of foundation, which is at a depth D_f below the ground surface, the overburden pressure is γD_f . The soil at this level was under this pressure prior to the application of footing load. The pressure transmitted by the foundation in excess of the overburden pressure is the *net bearing pressure*. The maximum net pressure at which the foundation fails is known as *ultimate net bearing capacity*. *Safe bearing capacity* is the maximum intensity of pressure which the soil can support without the risk of shear failure. This is obtained by dividing the ultimate bearing capacity by a factor of safety. Since the soil is originally subjected to the overburden pressure γD_f , there is no need to apply a factor of safety to the component of gross bearing capacity which is due to γD_f .

Therefore,

$$q_g (\text{all}) = \frac{q_{\text{ult}(n)}}{F_s} + \gamma D_f$$

It may be noted that there is a difference between safe bearing capacity and allowable bearing pressure. The allowable bearing pressure is the maximum net pressure that can be applied on the soil without the risk of shear failure or settlement beyond permissible limits.

6.9 BEARING CAPACITY FROM FIELD TESTS

For granular soils, estimation of field value of ϕ from laboratory test is extremely difficult. It is more convenient to estimate ϕ from results of penetration tests, for example, N value

from SPT, N_c value from dynamic cone penetration test, or q_c from static cone penetration test. Methods are also available to compute bearing capacity directly from penetration test results. Some of these methods are as follows:

1. *Using charts given by Peck, Hansen, and Thornburn (1976):*

Figure 6.13 is a plot of bearing capacity factors, N_q and N_y against ϕ as well as N value (corrected). Considerations of both general and local shear failures are incorporated in the chart. This chart can be used directly for N_q and N_y (according to Terzaghi's method) for use in bearing capacity equation, Eq. (6.8).

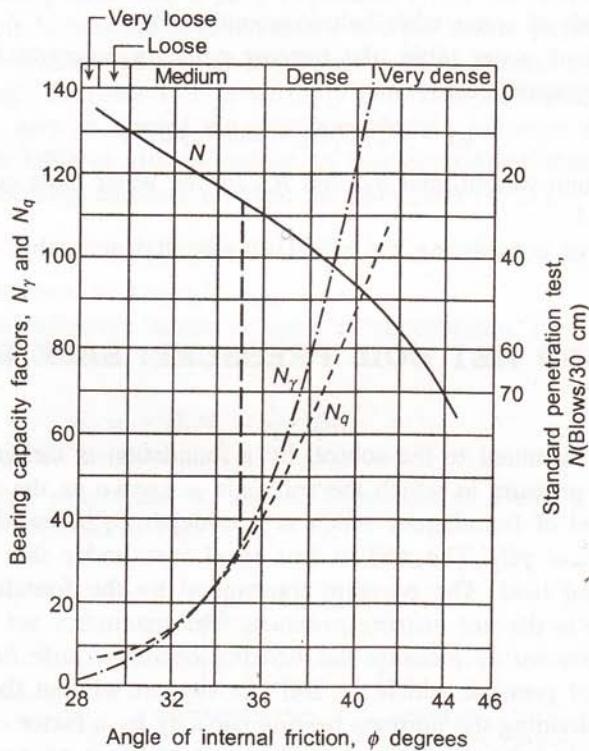


Fig. 6.13 Bearing capacity of footings based on 'N' value.

2. *Teng's Formulae:*

Using the concept of Peck, Hansen, and Thornburn, Teng (1962) developed the following expression for calculating net ultimate bearing capacity on granular soil. For strip footing,

$$q_{nd} = \frac{1}{60} [3N^2 BW'_y + 5(100 + N^2) D_f W'_q] \quad (6.28)$$

For square or circular footings,

$$q_{nd} = \frac{1}{30} [N^2 BW'_y + 3(100 + N^2) D_f W'_q] \quad (6.29)$$

where q_{nd} = net ultimate bearing capacity in t/m^2 or kN/m^2 .

N = average N value corrected for overburden pressure.

D_f = depth of footing in metres; If $D_f > B$, take $D_f = B$.

W'_q and W'_{γ} = correction factors for water table.

3. Static cone test:

IS:6403—1981 gives a method of determining net ultimate bearing capacity of strip footings on cohesionless soil using static cone resistance, q_c . The chart is presented in Fig. 6.14. q_c values at different depth are obtained for selected locations at the site. The field values are corrected for the dead weight of the sounding rod. Then the average q_c value is obtained for each of the locations by averaging the values between the base of the footing and depth below the base 1.5–2 times the width of the footing. The smallest of the average values is used in Fig. 6.11 to find bearing capacity factors N_q and N_{γ} , which may be used for computing the bearing capacity.

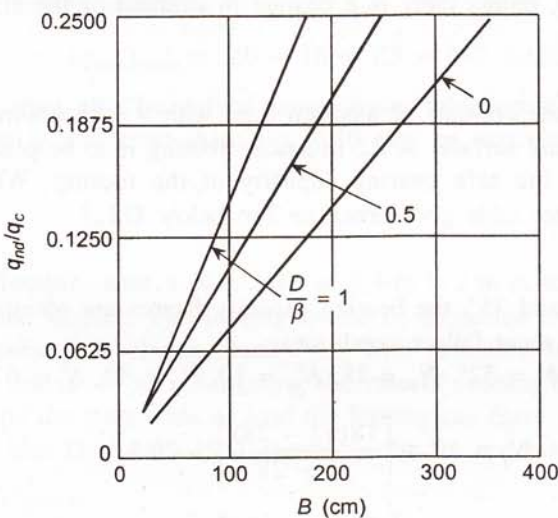


Fig. 6.14 Bearing capacity from static cone test.

Example 6.1

A square footing of width 2 m rests at a depth of 1 m at a site where the subsoil consists of soft to medium clay down a depth of 8 m below ground level, which is underlain by a dense coarse sand deposit. The water table is at 1.5 m below G.L. The clay has $c_u = 30 \text{ kN/m}^2$, $\phi = 0$ and $\gamma = 19 \text{ kN/m}^3$.

Determine the net load the footing can safely carry with a factor of safety of 3 against shear failure. What will be the safe load if the water table rises to the ground surface?

Solution

Since the thickness of clay layer beneath the level of footing base is more than the width of the footing, the bearing capacity will be governed by upper layer of clay.

According to Skempton's formula

$$(q_{\text{ult}})_{\text{net}} = c_u N_c \quad \text{Here, } N_c = 6(1 + 0.2 D_f/B)$$

$$= 30 \times 6.6 \text{ kN/m}^2 \quad = 6 \left(1 + 0.2 \left(\frac{1}{2} \right) \right)$$

$$= 6.6$$

$$\therefore (q_{\text{safe}})_{\text{net}} = \frac{30 \times 6.6}{2.5} \quad (Fs = 2.5)$$

$$= 80 \text{ kN/m}^2$$

$$\therefore \text{Net safe carrying capacity of the footing} = 80 \times 2 \times 2$$

$$= 320 \text{ kN}$$

Since this is a total stress analysis, there will be no change in the safe load if the water table rises to the ground surface, unless there is a change in strength of the clay.

Example 6.2

The subsoil at a building site consists of medium sand with $\gamma = 18 \text{ kN/m}^3$, $c' = 0$, $\phi' = 32^\circ$ and water table at the ground surface. A 2.5 m square footing is to be placed at 1.5 m below ground surface. Compute the safe bearing capacity of the footing. What would be safe bearing pressure if the water table goes down to 3 m below G.L.?

Solution

Since ϕ' lies between 28° and 35° , the bearing capacity factors are obtained by interpolation between local and general shear failure conditions.

Referring to Fig. 6.7, for $\phi' = 32^\circ$, $N_q = 28$, $N'_q = 10$, $N_\gamma = 30$, $N'_\gamma = 6$

we get,

$$N_q = 10 + \left[\frac{18(32 - 28)}{35 - 28} \right] = 20.3$$

and

$$N_\gamma = 6 + \left[\frac{24(32 - 28)}{35 - 28} \right] = 19.7$$

Case I (water table at G.L.)

Using Eq. (6.27) modified for square footing, ultimate gross bearing capacity

$$(q_{\text{ult}})_{\text{gross}} = \gamma'D_f N_q + 0.4\gamma'BN_\gamma$$

$$= 8.0 \times 1.5 \times 20.3 + 0.4 \times 8.0 \times 2.5 \times 19.7$$

$$= 243.6 + 157.6 = 401.2 \text{ kN/m}^2$$

and ultimate net bearing capacity,

$$(q_{\text{ult}})_{\text{net}} = (q_{\text{ult}})_{\text{gross}} - \gamma D_f$$

$$= 401.2 - 18 \times 1.5 = 384.2 \text{ kN/m}^2$$

Safe net bearing capacity,

$$(q_{\text{safe}})_{\text{net}} = 384.2/2.5 = 152 \text{ kN/m}^2 \quad (Fs = 2.5)$$

and gross bearing capacity,

$$(q_{\text{safe}})_{\text{gross}} = 152 + 18 \times 1.5 = 179 \text{ kN/m}^2$$

Case II (Water table at 3 m below G.L., that is, at a depth greater than width footing)

$$\begin{aligned}(q_{\text{ult}})_{\text{gross}} &= 18 \times 1.5 \times 20.3 + 0.4(14 \times 2.5)19.7 \\ &= 548.1 + 275.8 = 823.9 \text{ kN/m}^2\end{aligned}$$

$$(q_{\text{ult}})_{\text{net}} = 823.9 - 18 \times 1.5 = 796.9 \text{ kN/m}^2$$

∴ safe net bearing capacity,

$$(q_{\text{safe}})_{\text{net}} = 796.9/2.5 = 319 \approx 320 \text{ kN/m}^2$$

and safe gross bearing capacity,

$$(q_{\text{safe}})_{\text{gross}} = 320 + 18 \times 1.5 = 347 \approx 350 \text{ kN/m}^2$$

(This problem may also be solved using water table correction factors W'_q and W'_{γ} with marginal change in the result. Also Fig. 6.10 may be used for obtaining relevant N_q and N_{γ} values.)

Example 6.3

A rectangular footing, with a plan area of $1.4 \text{ m} \times 2 \text{ m}$ is to be placed at a depth of 2 m below the ground surface. The footing would be subjected to a load inclined at 10° to the vertical. The subsoil is clayey, sandy silt with saturated unit weight of 18 kN/m^3 , and $c' = 10 \text{ kN/m}^2$ and $\phi' = 30^\circ$. Assuming the rate of loading is such that drained condition prevails, compute the magnitude of load the footing can carry if the water table is at the base of the footing. Use IS: 6403—1981 recommendations and take $Fs = 3$.

Equation (6.13) gives,

$$q_{nd} = cN_c s_c d_c i_c + q(N_q - 1)s_q d_q i_q + 0.5\gamma B N_{\gamma} s_{\gamma} d_{\gamma} i_{\gamma} W'$$

Here $c = c' = 10 \text{ kN/m}^2$, $\phi = \phi' = 30^\circ$

$$N_q = (e^{\pi \tan \phi}) \tan^2(45^\circ + \phi/2) = 18.38$$

$$N_c = (N_q - 1) \cot \phi = 17.38 \cot 30^\circ = 30.10$$

$$N_{\gamma} = 2(N_q + 1) \tan \phi = 22.37$$

$$s_c = 1 + 0.2B/L = 1.14$$

$$s_q = 1 + 0.2B/L = 1.14$$

$$s_{\gamma} = 1 - 0.4B/L = 0.72$$

$$d_c = 1 + 0.2D_f/B \tan(45^\circ + \phi/2) = 1 + 0.2 \times 2/1.4 \times 1.732 = 1.5$$

$$d_q = d_\gamma = 1 + 0.1D_f \tan(45^\circ + \phi/2) = 1 + 0.35/1.4 = 1.25$$

$$i_c = i_q = (1 - \alpha/90)^2 = 0.79$$

$$i_\gamma = 0.44$$

$$W' = 0.5$$

Hence,

$$\begin{aligned} q_{nd} &= (10 \times 30.1 \times 1.14 \times 1.5 \times 0.79) + (18 \times 2 \times (18.38 - 1) \times 1.14 \times 1.25 \times 0.79) \\ &\quad + (0.5 \times 18 \times 1.4 \times 22.37 \times 0.72 \times 1.25 \times 0.44 \times 0.5) \\ &= 406.6 + 704.4 + 55.8 = 1166.8 \text{ kN.} \end{aligned}$$

$$\therefore (q_{\text{net}})_{\text{safe}} = 1166.8/3 = 388.9 \approx 380 \text{ kN/m}^2$$

$$\text{Hence, safe load} = 380 \times 1.4 \times 2 = 1064 \approx 1060 \text{ kN}$$

Example 6.4

What will be the safe load in Example 6.3 if undrained condition prevails? Take $c_u = 30 \text{ kN/m}^2$, $\phi_u = 0$, $N_c = 5.14$, $N_q = 1$, and $N_\gamma = 0$.

Solution

$$\begin{aligned} q_{nd} &= c_u N_c s_c d_c i_c \\ &= 30 \times 5.14 \times 1.14 \times 1.5 \times 0.79 \\ &= 208.3 \text{ kN/m}^2 \end{aligned}$$

$$\therefore (q_{\text{net}})_{\text{safe}} = 208.3/3 = 69.4 \approx 70 \text{ kN/m}^2$$

$$\therefore \text{Safe load} = 70 \times 1.4 \times 2 = 196 \text{ kN} \approx 200 \text{ kN}$$

REFERENCES

- Brinch Hansen, J. (1961), *A General Formula For Bearing Capacity*, Danish Geotechnical Institute, Bulletin No. 11, Copenhagen.
- Brinch Hansen, J. (1970), *A Revised and Extended Formula for Bearing Capacity*, Danish Geotechnical Institute, Bulletin No. 28, Copenhagen.
- Davis and Brooker (1973), The Effect of Increasing Strength with Depth on the Bearing Capacity of Clays, *Geotechnique*, Vol. 23, pp. 551–563.
- D'Appolonia, D.J. and T.W. Lambe (1970), Method of Predicting Initial Settlement, *Journal Soil Mechanics and Foundation Division*, ASCE, Vol. 96, pp. 523–544.
- IS 6403 (1981), *Code of Practice for Determination of Bearing Capacity of Shallow Foundations*, Bureau of Indian Standards, New Delhi.
- Meyerhof, G.G. (1951), The Ultimate Bearing Capacity of Foundations, *Geotechnique*, Vol. 2, pp. 301–332.

- Peck, R.B., W.E. Hansen, and W.H. Thornburn (1962), *Foundation Engineering*, 2nd Edition, John Wiley & Sons, New York.
- Prandtl, L. (1921), Über die Eindringungs Festigkeiten von Schneiden, *Zeitschrift für Angewandte Mathematik und Mechanik*, Vol. 1, No. 1, pp. 15–22.
- Reissner (1924), *Zuns Erdruck-problem*, Proc. First Int. Congress on Applied Mechanics, Dept. pp. 295–311.
- Skempton, A.W. (1951), *The Bearing Capacity of Clays*, Building Research Congress, England.
- Terzaghi, K. (1951), *Theoretical Soil Mechanics*, John Wiley, New York.
- Vesic, A.S. (1973), Analysis of Ultimate Loads of Shallow Foundations, *Journal of Soil Mechanics and Foundation Division ASCE*, Vol. 99, No. S M 1, pp. 45–73.
- Vesic, A.S. (1975), Bearing Capacity of Shallow Foundations, Chapter 3 of *Foundation Engineering Handbook*, Van Nostrand Reinhold Co., New York.